CHARACTERIZATION OF A UNIQUE SULFOXIDE SYNTHASE FOUND IN PATHOGENIC TRYPANOSOMES

Gabriel Tshwahla Makgotloduwa Mashabela

Thesis Presented for the Degree of
DOCTOR OF PHILOSOPHY

Department of Clinical Laboratory Sciences
UNIVERSITY OF CAPE TOWN
AUGUST 2013

Supervisors: Associate Prof: D.J Steenkamp and Associate Prof: D. Gammon

Declaration:

I, Gabriel Tshwahla Makgotloduwa Mashabela, hereby grant the University of Cape Town free licence to reproduce this thesis in whole or in part, for the purpose of research.

I declare that this dissertation is based on my original work, both in concept and execution, and that apart from the normal guidance from my supervisor, I have received no assistance, except where acknowledgements indicate otherwise. I also declare that all sources that I have used have been indicated and acknowledged by means of complete references.

Signature:…….

Date:…….

Acknowledgements:

I would like to thank everyone who helped to make this thesis successful, and here I would like to mention just a few:

This thesis would not have been possible without the help, support and patience of my supervisors, Associate Professor Daniel Steenkamp and Associate Professor David Gammon, for which my mere expression of thanks does not suffice.

I am indebted to Professor Florian Seebeck for his kindness, great inspiration and encouragement during the last phase of this research.

I am grateful to Kenneth Kirk of the Institute of Diabetes, and Digestive and Kidney Diseases, National Institutes of Health, DHHS, Bethesda, for the generous gift of 2-fluorohistidine and 5-fluorohistidines compounds.

Special gratitude goes to my mother for her never ending love, support and encouragement. Thank you Pheladi for all the sacrifices and difficulties you had to endure to see me through the university.

I would also like to thank my sisters, Makibane, Molefe, Lebato, Makgwale, Ramogothlo and Digwai, for their prayers, friendship and unequivocal support throughout. My fiancée Dimakatso and my daughter Tsheamo, thank you for being such a wonderful source of inspiration, consolation and encouragement.

I would like to thank my friend Sebisi Kgaphola for his kindness, friendship, generosity and support throughout my studies.

To all former members of Biochemistry of Pathogens group, Dr Mohlopheni Marakalala, Dr Vuyo Mavumengwana and Dr Monique Williams, thank you guys for all your assistance, encouragement and mostly for the insightful discussions we had.

I am so grateful for the fruitful discussions I had with my current and former fellow postgraduate students in the laboratory of Associate Professor David Gammon, Department of chemistry, University of Cape Town.

To my fellow postgraduate students in the laboratory of Professor Florian Seebeck, Department of chemistry, University of Basel, thank you so much for promoting such a stimulating and welcoming academic and social environment.

I would like to acknowledge the academic and technical support of the University of Cape Town and its staff, particularly Postgraduate Administration staff and all staff in the division of Chemical Pathology and Department of Chemistry.

I am so grateful for the financial support provided by the University of Cape Town, National Research Foundation of South Africa, Medical Research Foundation of South Africa and Swiss government Scholarship of Excellence.

'To God be the Glory..!'

Abstract:

Ovothiol is a 3-methyl-5-mercaptohistidine that was first discovered in sea urchin eggs. It is a proficient one electron donor that is characterized by low thiol pK_{SH} and high redox potential. Ovothiols have been isolated from pathogenic trypanosomes that cause human tropical diseases such as Chagas disease, Leishmaniasis and Sleeping sickness. The physiological function of ovothiol is currently unknown. Here, we report characterization of 5-histidyl cysteine sulfoxide synthase (OvoA), the first enzyme in ovothiol biosynthesis, which mediates an unusual oxidative transsulfuration reaction at the L-histidine C-5 position using L-cysteine as sulfur donor. OvoA was found to be characterized by L-cysteine and L-histidine K_M values of 339 ± 22 μM and 347 ± 27 μM respectively. The enzyme was found to be most active at pH 7.5 with acidic pK_a of 6.8 and alkaline pK_a of 8.0. Sulfur acceptor specificity studies revealed that OvoA converts histamine and D-histidine about 7 and 20 times less efficiently respectively, than L-histidine. Ascorbate and isoascorbate were found to increase OvoA activity by over a 100 fold. OvoA was found to convert 2-fluorohistidine into 2-fluorohistidyl cysteine sulfoxide at a similar rate to L-histidine despite the high electron deficiency of 2-fluorohistidine. The mechanism of action of OvoA was found not to be limited by proton transfer as judged by the observed low solvent isotope effect of just 1.2. The compound 5-fluorohistidine inhibited OvoA activity by 80%. In a related study, 5-fluorohistidine inhibited ergothioneine production by *Mycobacterium smegmatis* by 40%. 5-chlorohistidine inhibited both OvoA activity and ergothioneine biosynthesis by 30%. Understanding the mechanisms of ovothiol and ergothioneine biosyntheses and the effect of 5-fluorohistidine in these pathways may assist in finding inhibitor molecules that can be developed into drugs against bacterial and trypanosomal pathogens.

Abbreviations:

AdoMetDC	adenosylmethionine decarboxylase
AIDS	acquired immune deficiency syndrome
ATP	adenosine triphosphate
BAN	2-bromo-2'-acetonaphthone
BBB	blood brain barrier
Boc-	tert-butyloxycarbonyl-
BSO	buthionine sulfoximine
CL	cutaneous Leishmaniasis
Da	dalton
DAST	diethylaminosulfur trifluoride
DCM	dichloromethane
DFMO	α-difluoromethylornithine
DHFR	dihydrofolate reductase
DMF	dimethylformamide
DMSO	dimethyl sulfoxide
DNA	deoxyribonucleic acid
ELISA	enzyme-linked immunosorbent assay
ESI-MS	electron-spray ionization mass spectrometry
Fe(II)	divalent iron metal
Fe-SOD	iron containing super oxide dismutase
G3PDH	glycerol-3-phosphate dehydrogenase
GPDH	glyceraldehyde-3-phosphate dehydrogenase
H_2O_2	hydrogen peroxide
HAT	human African trypanosomiasis
HPLC	high-performance liquid chromatography
HRM	high resolution mass
IPTG	isopropyl-β-D-thiogalactopyranoside
k_{cat}	turnover number
k_{cat}/K_M	specificity constant

K_M	Michaelis constant
LDL	low-density lipoproteins
LPG	lipophosphoglycan
min	minute
ml	millilitre
mM	millimolar
Mn- SOD	manganese containing super oxide dismutase
NMR	nuclear magnetic resonance
NO	nitric oxide
ODC	ornithine decarboxylase
ONOO-	peroxynitrites
PCR	polymerase chain reaction
PFK	phosphofructokinase
PGPA	p-glycoprotein-like protein A
PKC	protein kinase C
Redox	reduction-oxidation
RNA	ribonucleic acid
RNI	reactive nitrogen intermediate
ROI	reactive oxygen intermediate
ROS	reactive oxygen species
SDS-PAGE	sodium dodecyl sulphate polyacrylamide gel
SOD	super oxide dismutase
TCA cycle	tricarboxylic acid cycle
TEA	triethylamine
TFA	trifluoroacetic acid
THF	tetrahydrofuran
TLC	thin layer chromatography
TSH2	trypanothione
VL	visceral Leishmaniasis
Vmax	maximum rate of reaction
VSGs	variant surface glycoproteins
WHO	world health organization

Zn2+	divalent zinc cation
Zn-SOD	zinc containing superoxide dismutase

List of figures:

List of Schemes:

List of tables:

Brief Contents:

Detailed Contents:

CHAPTER 1:
GENERAL INTRODUCTION

1. **Trypanosomatids**

1.1. History of the Order Kinetoplastida

The *Kinetoplastida* are a Class in the Phylum *Euglenozoa* that comprise Orders *Trypanosoma* and *Bodonida*. These flagellate protozoa are characterized by the presence of a kinetoplast, a DNA containing body present in the single mitochondrion. A kinetoplast consists of a network of maxi- and mini-circle DNAs, which are responsible for posttranscriptional editing, and are located in the single mitochondrion near the basal body of the flagellum (Stuart *et al.*, 2008). The order *Trypanosoma* is of particular importance to humans, because its members cause a variety of diseases in human and animals in different countries. The Genera, *Leishmania* and *Trypanosoma* are parasites that cause human diseases such as Leishmaniasis, human African trypanosomiasis (HAT) (also referred to as sleeping sickness) and American trypanosomiasis (Chagas disease). Their parasitism can either be monogenic, involving a single host or digenic where there is alternation between two hosts, most commonly an insect vector and a mammal.

Trypanosomatids are digenic parasites and thought to have originated from their monogenic ancestors at least 250 million years ago through adaptation in animals (Lake *et al.*, 1988). It is widely believed that *Leishmania* and *Trypanosoma* have a common ancestor. While lack of fossil records makes it difficult to obtain reliable evolutionary information about these protozoa, application of modern molecular evolutionary methods and other historical incidences put the estimated time of divergence between *Leishmania* and *Trypanosoma* between 80 and 140 million years ago (Lake *et al.*, 1988). The divergence is believed to have preceded the divergence of the American species, *T. cruzi* and the African, *T. brucei*, which is thought to have happened shortly before splitting of Gondwanaland about 80 million years ago (Lake *et al.*, 1988).

1.2. History and Discovery of Trypanosomatids diseases

Leishmaniasis: Leishmaniasis is one of the most ancient human parasitic diseases reported in both Old and New Worlds. Different forms of the disease have been described: Cutaneous Leishmaniasis (CL), a skin disease characterized by sores and scars has long been known as oriental sores in the Old World (reviewed in Cox, 2002). One of its clearer descriptions was found on tablets in the library of the Assyrian King Ashurbanipal dated back to the 7th century BC. Some of these descriptions are thought to have originated from earlier texts dating as far back as 1500 to 2500 BC. In the Indian subcontinent, the visceral leishmaniasis (VL) (also known as Kala-azar, meaning *Black fever*) was first discovered in 1824 in Jessore (reviewed in Cox, 2002).

Evidence for the existence of Cutaneous and Mucocutaneous Leishmaniasis in the New World was obtained from pre-Inca potteries found in Ecuador and Peru (reviewed in Cox, 2002). The potteries, dated as far back as first century AD, had representations of facial deformities and skin lesions, which clearly matched the lesions of Cutaneous Leishmaniasis sufferers. Although it can be traced back hundreds of years, the earliest clinical descriptions of Cutaneous Leishmaniasis were made by Alexander Russell in 1756 after examination of a Turkish patient. On his note was written:

"*After it is cicatrised, it leaves an ugly scar…….It affects the natives when they are children, and generally appears in the face, though they also have some lesions on their extremities……., but they seldom affect the same person above once*."

Despite the fact that the disease had been known for such a long time the parasites that cause leishmaniasis were discovered only in 1903 (Ross, 1903). However, due to many different observations reported by early scientists in the late 19th century, there is still a controversy as to whom the initial discovery of the parasite responsible for Cutaneous Leishmaniasis should be attributed. In contrast, it is universally accepted that Scottish army doctor, William Leishman, and Charles Donovan, the Professor of Physiology at Madras University, independently discovered the parasite that causes Visceral Leishmaniasis in 1903. Hence, in their honour, Ross named the parasite, *Leishmania donovani* bearing both their names.

About 30 species of Leishmania infect mammals and about 20 of these are responsible for different forms of Leishmaniasis in humans. The parasites use female sand-flies as their transmission vector and about 30 of 500 known phlebotomine species have been positively identified as vectors of the disease. In the New World the disease is transmitted by *Lutzomyia* genera while in the Old world Leishmania transmission is via *Phlebotomus* genera.

Chagas Disease: Chagas' disease is a human tropical disease predominantly found in Latin America. The existence of Chagas disease could be dated back to 2000 BC after isolation of DNA of *T. cruzi* in the heart and oesophagus of Peruvian and Chilian mummies (Rothammer *et al.,* 1985 and Guhl *et al.*, 1997). But it was not until 1909 that the discovery of *T. cruzi* as the causative agent was made by Carlos Chagas. The parasites, contained in the faeces of the triatomine bugs (large blood sucking insects that occur mainly in Latin America) are transmitted to humans when the bug feeds on its human prey. Domestic animals serve as reservoirs (Rothammer *et al.,* 1985).

Sleeping sickness/ Human African trypanosomiasis (HAT): Due to a lack of fossils for the causative agents of HAT, it has become difficult to speculate on the origin of the disease. An early historic report of sleeping sickness was that of the death of a Malian emperor in 1374 AD from a disease description of which matched that of modern sleeping sickness (Williams, 1996). Two subspecies of *T. brucei* cause different clinical infections of Human African trypanosomiasis in different African geographical locations (Steverding 2008). In West Africa, T. brucei *gambiense* causes the chronic form of the disease while in East Africa *T.b. rhodesiense* is responsible for the acute form. In some central African regions, such as Uganda, however, both species have been isolated and co-infection has also been reported (Stich *et al.*, 2002). Both parasites are transmitted by female tsetse flies of the genus *Glossina*. Domestic and game animals are reservoirs of the parasites. The animal form of the disease, nagana, is caused by infection with *T. b. brucei* subspecies which are not pathogenic to humans (Stich *et al.*, 2002).

1.3. Epidemiology of Trypanosomal Diseases

Different diseases caused by kinetoplastida affect many people in different countries. They occur mostly in geographical locations where the insect vectors are found (table 1.1) (Stuart *et al.*, 2008).

Leishmaniasis: Leishmaniasis affects about 350 million people in 88 countries where it is known to be endemic. The reported infection rate stands between 1- 1.5 million for cutaneous Leishmaniasis (CL) and 500 000 visceral Leishmaniasis (VL) per year with overall infection figures standing at about 12 million people. VL is responsible for about 50 000 deaths a year and is regarded as the second-largest parasitic killer in the world after malaria, (Desjeux *et al.*, 2001).

Chagas disease: Chagas' disease is endemic in 21 Latin American countries, putting the lives of 100 million people in danger. There are about 200 000 new cases every year, leaving a total of about 18 million people infected. The death rate resulting from Chagas disease is approximated to be 21 000 deaths per year.

Sleeping sickness: Sleeping sickness is almost exclusively found in Africa in the regions where the Tsetse flies, the transmission vector occur. The disease affects approximately 60 million people living in 36 African countries located south of Sahara and north of the Kalahari Desert. Despite a successful programme in the 1970's, which almost eradicated Human African Trypanosomiasis, there has been a steady re-emergence of the disease in the new millennium (WHO, 2006). It is now estimated that over 46 000 people die every year from the disease, which has an annual infection rate of 300 000 new cases (Mathers *et al.*, 2007 and WHO, 2006).

Table 1.1: Table showing diseases caused by kinetoplastidae parasites (unmodified from Stuart et al., 2008)

	HAT/Seesping sickness	Chagas disease	The leaishmaniasis
Principal disease forms or stages	Early (hemolymphatic) stage, late (CNS) stage	Acute phase, indeterminant phase, chronic phase (cardiac and digestive forms)	Viceral leishmaniasis (VL), mucocutaneous leishmaniasis (MCL), cutaneous leishmaniasis (CL)
Causative organism	*T.b. gambiense, T.b. rhodesiense*	*T. cruzi*	about 21 *Leishmania* species., e.g., *L. donovani* (VL), *L. braziliensis* (MCL, L. major (CL)
Host cell/tissue	Extracellular, in blood, lymph, cerebral spinal fluid, and intercellular spaces	Intracellular, in cytoplasm of heart, smooth muscle, gut, CNS, and adipose tissue cells	Intracellular, in phagolysosomes of macrophages
Vectors of medical importance	Tsetse flies (about 20 *Glossina* species) (*palpalis* group, *T.b. gambiense*; *morsitans* group, *T.b. rhodesiense*)	Reduviid bugs (about 12 to 138 *Triatominae* species) (*Triatoma*, *Rhodnius*, and *Panstrongylus* species	Phebotomine sandflies (about 70 species) (*Phlebotimus* species in Old World, and *Lutzomyia* species in New World
Transmission	Infected fly bite, congenital (rare), blood trasfusion (rare)	Contamination by feces of infected bugs (e.g., bite site, in mucous membranes, in food or drink), blood trasnfusion, conjenital, organ trasplantation (rare)	Infected fly bite
Geographical distribution	Sub-Saharan Africa (about 20 countries)	South and Central America (19 countries)	South and Central America, Europe, Africa, Asia (88 endemic countries)
Population at risk	50 million	100 million	350 million
Infected	70 000 - 80 000	8 - 11 million	12 million
Health burden (DALYs)	1.5 million	0.7 million	2.1 million
Deaths (per annum)	about 30 000	14 000	51 000 (VL)
Prevention and control measures	Active surveilance of at risk population, drug treatment of infected patients, tsetse fly traps, residual insecticides, sterile insect technique, tsetse habitat destruction to inhibit reinvasion	Treatment of homes with residual insecticides, blood donor screening, drug treatment for acute, early indeterminate and conjenital cases, better housing (plastered walls and metal roof replacing adobe-walled, thatch-roofed dwellings)	Surveilance and treatment of VL cases, resevoir (dog) control (VL); treatment of homes with residual insecticides; insecticide-treated bed nets, fabrics, and dog collars; live vaccination (CL)

1.4. Diagnosis

The oldest and most commonly used detection method to date involves visualization of the live parasites. Aspirates from appropriate organs are fixed, stained and visualized under the light microscope. Although this method provides very reliable results, it has

many limitations, relating to low parasite concentrations during chronic infections and the early stages of infection (Kennedy, 2008). This method also fails to differentiate early infection from late infection, making treatment difficult, especially for Sleeping sickness, where drugs for the early stage are not effective in the late stage and the drugs for late stage are associated with a high level of toxicity (Kennedy, 2006).

To deal with low parasite concentrations in the blood, the parasites are cultured in appropriate media and then visualized under a microscope. However, this method cannot be applied in field tests due to the slow growth of the parasites in culture (Sundar and Rai, 2002).

Indirect tests which rely on production of antibodies have a long history and some of them are still in use today (Rosenblatt, 2009). The principle of these tests relies on the presence of antibodies produced by infected persons, which selectively bind to trypanosome antigens and results in blood agglutination. Various agglutination tests have been used successfully in Chagas disease, Sleeping sickness and Leishmaniasis (Rosenblatt, 2009). Although these tests are sensitive, they suffer from poor selectivity as similar antibodies are raised in response to other pathogens (López-Antuñano *et al.*, 2000). Moreover, the antibodies remain in the blood of cured patients for a number of years which will then give false positive results (Sundar and Rai, 2002). As a result, more work is needed to improve the specificity and sensitivity of these methods. For example, the use of a parasite specific antigen (rK39 antigen) led to development of a more sensitive and specific ELISA test kit for Leishmaniasis. The rK39 ELISA tests kits are currently commercialized and have significantly improved diagnosis of Leishmaniasis (Sundar and Rai, 2002).

Development of molecular assays that rely on the polymerase chain reaction (PCR) has provided more reliable and sensitive diagnostic results. In this procedure, repetitive sections of kinetoplast DNA are amplified and analyzed. Due to its high specificity and sensitivity, PCR tests are mostly recommended for cure confirmation in treated patients. However, these methods require skilled personnel and are very expensive, which then limit their application as a sole diagnostic tool for field tests. PCR based tests are

therefore recommended when all other tests have failed or when a confirmation is required (Rosenblatt, 2009).

1.5. Current chemotherapy against trypanosomal diseases

The first real work on the treatment of trypanosomes started can be dated back to the work done by Paul Ehrlich on arsenicals and dyes. Although some drugs were quickly developed afterwards, most of them are no longer currently in use due to high levels of cytotoxicity (Frézard *et al.*, 2009).

Leishmaniasis: Pentavalent antimonials, meglumine antimonate and sodium stibogluconate, have been used as the first line drugs for treatment of Leishmaniasis since the 1940s. The drugs are given parenterally daily for 20-30 days (Frézard *et al.*, 2009). The drugs are believed to disrupt the parasite's energy production pathway as their main mode of action while other researchers have also linked the drugs with interference of the parasite's antioxidant pathway by reacting with trypanothione (Singh, 2006).. Despite their anti-parasitic effect, the drugs have adverse side effects including diarrhoea, vomiting nausea, skin rashes and cardiotoxicity (Singh, 2006). In the recent past there has been a wide spread development of resistance against pentavalent antimonials in many countries. Antimonial resistance in Leishmaniasis is associated with drug efflux as resistant strains were found to express high levels of ABC transporter proteins and that inhibition of ABC transporters abolished resistance to antimonials (Basu *et al.*, 2008)

Pentamidine and amphotericin are the second line drugs against strains resistant to antimonials while miltefosine, the first orally administered drug, has recently been introduced for treatment of Leishmania strains resistant to antimonials (Soto *et al.*, 2004).

Sleeping sickness: Treatment of Sleeping sickness can be divided into two categories, the early stage and late stage drugs. In the early stage the parasites are present mostly in the haemolymphatic system and the liver. The two drugs, suramin and pentamidine are used in the early stage of sleeping sickness (Nok, 2003). Suramin is a poly-sulfonated naphthylamine and very water soluble. It is thought to bind strongly to low-density

lipoproteins (LDL) thereby starving the parasite of the essential cholesterol. However, suramin's ionic structure has proven to be a disadvantage as it limits its penetration of the blood brain barrier. Hence, suramin is only used in the early stage of the disease before the parasites enters the brain (Nok, 2003). Pentamidine, an aromatic diamidine, was introduced in the 1940s to treat the early stage of *T. b. gambiense* Sleeping sickness (Luorie, 1942). Pentamidine does not cross the blood brain barrier (BBB) in reasonable concentrations to attain drug levels necessary for cure, and for that reason it is only used for treatment of the early stage. Although it is not fully understood why pentamidine is not effective against *T. b. rhodesiense*, it is thought that the high reproduction rate of *T. rhodesiense* leads to a rapid invasion of the central nervous system before the early stage of infection can be cleared by the drug. Pentamidine's mode of action is not known. However recent studies associate reaction of the drug with ubiquitin (Nguewa *et al.,* 2005). Field resistance to both pentamidine and suramin has never been reported while laboratory resistance of up to 300 fold can be induced. The induced resistance in both drugs is associated with rapid drug efflux (Nok, 2003).

The late stage sleeping sickness begins when the parasites which had been in the human body pass through the blood brain barrier (BBB) into the central nervous system. Therefore, only drugs which are able to cross the BBB in the right quantities can be used to treat the late stage sleeping sickness. Melarsoprol and eflornithine are currently in use to treat patients with late stage sleeping sickness (Blum and Burri, 2002). Treatment with melarsoprol, however, may result in severe encephalopathy with up to 10% mortality in treated patients (Pepin and Milord, 1994). Severe side effects associated with melarsoprol are believed to occur as a result of binding to disulfide bonds of proteins. Although the mode of action of melarsoprol is still under investigation, the new reports link it to binding to thiol containing enzymes like glycerol-3-phosphate dehydrogenase (G_3PDH) (Nok, 2003). The high mortality rate and adverse side effects of melarsoprol led to introduction of eflornithine as alternative drug. Despite its effectiveness, eflornithine is too expensive to be administered in poor African countries where it is needed most. Its other disadvantage is that eflornithine is not effective against *T. b. rhodesiense* (Iten *et al.*, 1995). These and other factors make it imperative to search for more efficient drugs against sleeping sickness.

Chagas disease: Current chemotherapy for Chagas disease consists of two drugs; Benznidazole and Nifurtimox. Benznidazole, an azole derivative, is very effective against the acute phase of Chagas disease with over 80% parasitological cure. Although the mode of action of Benznidazole is poorly understood, it is believed to involve covalent modification of macromolecules such as lipids, DNA and proteins through its nitro-reduction intermediates generated through reduction by nitro-reductases (Coura and de Castro, 2002). Nifurtimox, a 5-nitrofuran is an orally administered drug given to Chagas disease patients, 8-10 mg/Kg/day for 1-2 months. The mode of action of nifurtimox involves generation of nitro anion radicals, which in the presence of oxygen leads to generation of reactive intermediates that are responsible for eradication of the parasites (Coura and de Castro, 2002). However, the nitro radicals generated during the metabolism of the drug have also been implicated in the adverse side effects associated with administration of nifurtimox (Urbinal and Docampo, 2003). Both drugs have shown poor efficacy in treating patients with the chronic form of the disease. As a result, some South American countries such as Brazil, Argentina, Chile and Uruguay stopped commercialization of nifurtimox in the 1980s (Urbinal and Docampo, 2003). On the positive side, a nifurtimox- melarsoprol combination is being investigated as potential alternative chemotherapy for treatment of the second stage of sleeping sickness with positive results (Bisser *et al.*, 2007). With benznidazole being the only effective drug against the acute Chagas disease, there is a dire need for development of new chemotherapeutic agents to treat Chagas disease.

1.6. Unique metabolic pathways of trypanosomatids as potential drug targets

Successful development of new effective chemotherapies against trypanosomal diseases would need to take into account factors such as drug targets and modes of action, low side effects etc. It is therefore important that potential drug targets be found and validated. The obvious targets should be proteins or enzymes which are not only unique to the parasites but also significant for survival of the parasites. Some of the recently discovered potential drug targets are briefly discussed here.

1.6.1. Sterol synthesis

Unlike animals which produce cholesterol to maintain membrane integrity, trypanosomatids and fungi synthesize unique sterols such as ergosterol (*T. cruzi*) and ergostane (Leishmania) as the final products of the sterol biosynthetic pathway (figure 1.1). The absence of ergosterol in animals makes the enzymes involved in the ergosterol biosynthetic pathway suitable drug targets (Urbina *et al.*, 2002). Amphotericin B, developed as an antifungal drug, was found to be very effective in the treatment of Sleeping sickness. It is believed to bind to the ergosterol, resulting in the formation of pores, which leads to cell death as ions (K^+ and Na^+) leak out of the cell. Amphotericin B however seems to have multiple binding sites, which leads to undesirable side effects (Urbina *et al.*, 2003). Other inhibitors of ergosterol biosynthetic enzymes have been explored as potential drugs against Chagas disease. Thus, antifungals, ketoconazole and itraconazole (Roberts *et al.*, 2003) and triazoles, posaconazole and UR-9825 all known for their interference with ergosterol biosynthesis have been tested for anti-trypanosomal activity with positive outcomes. Treatment with UR-9825 and posaconazole results in diminished proliferation of epimastigotes and amastigotes coincident with the depletion of sterols, while in animal studies the drug resulted in 50% cure rate of mice infected with *T. cruzi* strains that were resistant to Nifurtimox, benznidazole and ketoconazole (Roberts *et al.*, 2003).

Leishmania species produce ergostane rather than ergosterol (figure 1.1). Due to structural similarities with ergosterol, biosynthesis of ergostane can also be interrupted by inhibitors of ergosterol biosynthesis, ketoconazole and itraconazole. As such these drugs have also been tried successfully against Leishmania (Roberts *et al.*, 2003).

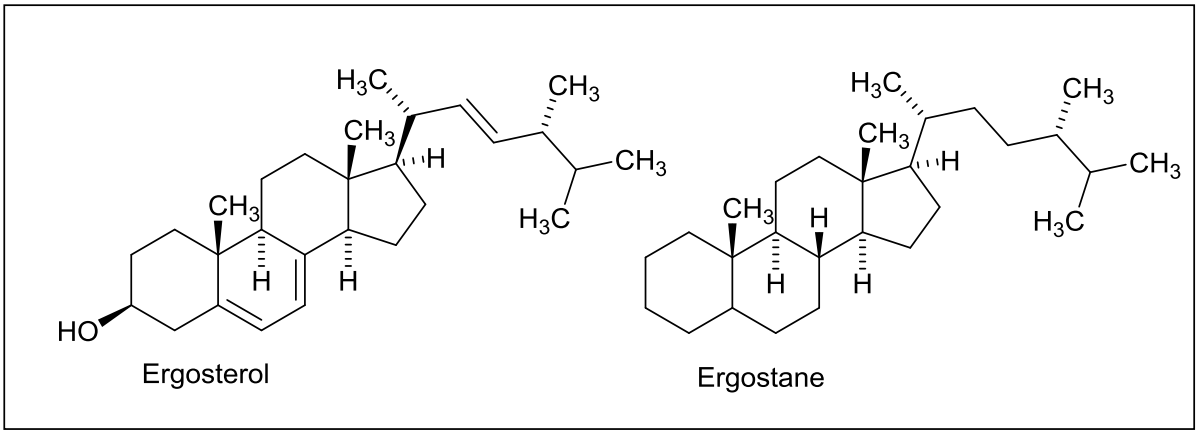

Figure 1.1: Chemical structures of ergosterol and ergostane.

However treatment of blood parasites with anti-sterols tends to be ineffective in parasites which possess mechanisms whereby they can assimilate sterol from the host cells (Roberts *et al.*, 2003). That is the case with *T. brucei* species which, even with ergosterol biosynthesis completely inhibited, assimilate cholesterol from the host serum lipoproteins and as such cannot be treated with Amphotericin B and the antifungals, ketoconazole and itraconazole (Balaña-Fouce *et al.*, 1998, and Roberts *et al.*, 2003).

1.6.2. Glycosomal enzymes

Trypanosomatid parasites like all other living organisms require energy for their normal metabolism. But unlike their mammalian hosts, trypanosomatids do not have a functional TCA cycle or mitochondrial respiratory chain and rely entirely on glycolysis for ATP supply (Michels *et al.*, 2006). The parasites have fully functional glycolysis with all ten required glycolytic enzymes. However it is the organization of the glycolytic enzymes that sparked interest among researchers. Seven of the glycolytic enzymes that convert glucose to 3-phosphoglycerate are located in specialized peroxidase-like organelles called glycosomes (Michels *et al.*, 2006). That is different from other organisms where glycolysis is completely cytosolic with all enzymes located in the cytosol. This organization and the distant divergence of trypanosomatids from mammals have endowed trypanosomal enzymes with unique characteristics (Nowicki, 2008).

Although the amino acid similarities for most glycolytic enzymes amongst the trypanosomatid family ranged between 80 and 95%, some striking differences were observed when such enzymes were compared with their mammalian counterparts, showing similarities of only about 20 to 47% (Nowicki, 2008). One of the mostly studied glycolytic enzymes in *T. brucei* is phosphofructokinase (PFK) which mediates the synthesis of fructose-1, 6-bisphosphate from fructose 6-phosphate using ATP as phospho donor. It is a tetrameric enzyme which is also located in the glycosome. It shares only about 20% sequence homology with its human isoenzymes suggesting that the enzyme can be selectively inhibited. In a recent study, the PFK selective inhibitors showed strong potency against *T. brucei* and *Leishmania parasites* (Guido *et al.*, 2008).

Another important glycolytic enzyme is glyceraldehyde-3-phosphate dehydrogenase (GAPDH) structure of which is highly conserved among trypanosomal family members (90% similarity) (Guido *et al.*, 2008). GAPDH catalyzes the oxidative phosphorylation of D-glyceraldehyde-3-phosphate into 1,3-bisphosphoglycerate. Trypanosomal GAPDH possesses only 45% amino acid similarity with the mammalian GAPDH form and provides unique structural features exploitable for drug development. A striking example is that of an inhibitor of GAPDH, 2'-deoxy-2'-(3-methoxybenzamido) adenosine, which could selectively inhibit the GADPH of *T. brucei* and *L.mexicana* while showing marginal inhibition of the human enzyme (Callens and Hannaert, 1995). Molecular docking and other advanced techniques are currently used to find selective inhibitors of trypanosomal GAPDH (Guido *et al.*, 2008).

1.6.3. Purine salvage pathway

Unlike their mammalian host, trypanosomatids cannot synthesize purines *de novo* and therefore are solely reliant on purine salvage pathways for nucleotide biosynthesis. As such, enzymes involved in this pathway present good drug targets (El Kouni, 2003). Of particular importance in this pathway is that trypanosomatids use a single enzyme, Hypoxanthine-guanine phosphoribosyltransferase (HGPRT), to convert bases to ribonucleotide. Recent molecular docking studies revealed significant differences between trypanosomal and mammalian HGPRT and proved that selective inhibition of

the trypanosomal HGPRT is possible (Zuccotto, 1999). Therefore a search for HGPRT inhibitors is becoming a crucial goal to achieving new drugs against the parasites.

1.6.4. Special hydrolases

Cruzain is a member of the papain C1 family of cysteine proteases and is a primary cysteine protease in *T. cruzi*. It is essential for the survival of *T. cruzi*, because of its involvement in crucial reactions such as differentiation and intracellular replication (Hart *et al.*, 1993). Unlike mammalian enzymes, which are located in the lysosome, cruzain is cytosolic in *T. cruzi* (McKerrow *et al.*, 1999). The different sub-cellular location and observed lack of redundancy make cruzain an attractive drug target. Recent studies have confirmed eradication of *T. cruzi* parasite from infected J744 macrophages (mammalian culture) after treatment with specific reversible and irreversible inhibitors of cruzain, with acyloxymethyl ketone inhibitors and aryloxymethyl ketone inhibitors showing potential for new drugs against Chagas disease (Brak *et al.*, 2008).

DNA topology is an important process during cell division and gene expression. The alteration of cellular DNA is catalyzed by topoisomerase II. The function of topoisomerase II is to cut both strands of double stranded DNA and allow tangling or de-entanglement of DNA. It is a crucial enzyme for replication as it enables separation of newly formed daughter strands. This is a crucial enzyme to target for the development of anti-trypanosomal drugs because of extra kDNA located in the kinetoplast. Inhibition of trypanosomal topoisomerases II resulted in inhibition of both differentiation and proliferation in the parasites causing major damage to nucleus and kinetoplast. Other potential drug targets are enzymes involved in folate biosynthesis. Dihydrofolate reductase (DHFR), the enzyme involved in reduction of dihydrofolate to tetrahydrofolate, has been successfully targeted for drug development in other ailments such as cancer, malaria and bacterial infections (Coura and de Castro, 2002). Although previously less attention was focused on trypanosomal DHFR, recent studies have reported high activity of selective inhibitors of trypanosomal DHFR against trypanosomatids (Khabnadideh *et al.*, 2005).

1.6.5. Oxidative metabolism: The role of low molecular thiols

Like all aerobic organisms, trypanosomes are subjected to reactive oxygen and nitrogen species, which need to be detoxified. Mammalian parasites are subjected to even higher amounts of oxidant species produced as result of the mammalian immune response (Droge, 2002). Unlike their mammalian counterparts, trypanosomatids lack catalase and glutathione peroxidase, the two important enzymes involved in detoxification of reactive oxygen species in mammals. Instead trypanosomatids possess a different detoxification pathway in which superoxides are converted into hydrogen peroxide by iron containing superoxide dismutase (Fe-SOD), instead of Mn- or Zn-SODs found in mammals (Scheme 1.1). Fe-SOD has been proven to be important for survival of the parasites in the mammalian hosts. *T. chagasi* mutants generated through deletion of one gene resulted in hypersensivity of the mutants to peroxides (Plewes *et al*, 2003). Fe-SOD overexpression in *T. cruzi* was found to result in increased benznidazole resistance (Temperton *et al*, 1998). That is because benznidazole is believed to produce high amounts of superoxides which will then be reduced by highly expressed Fe-SOD.

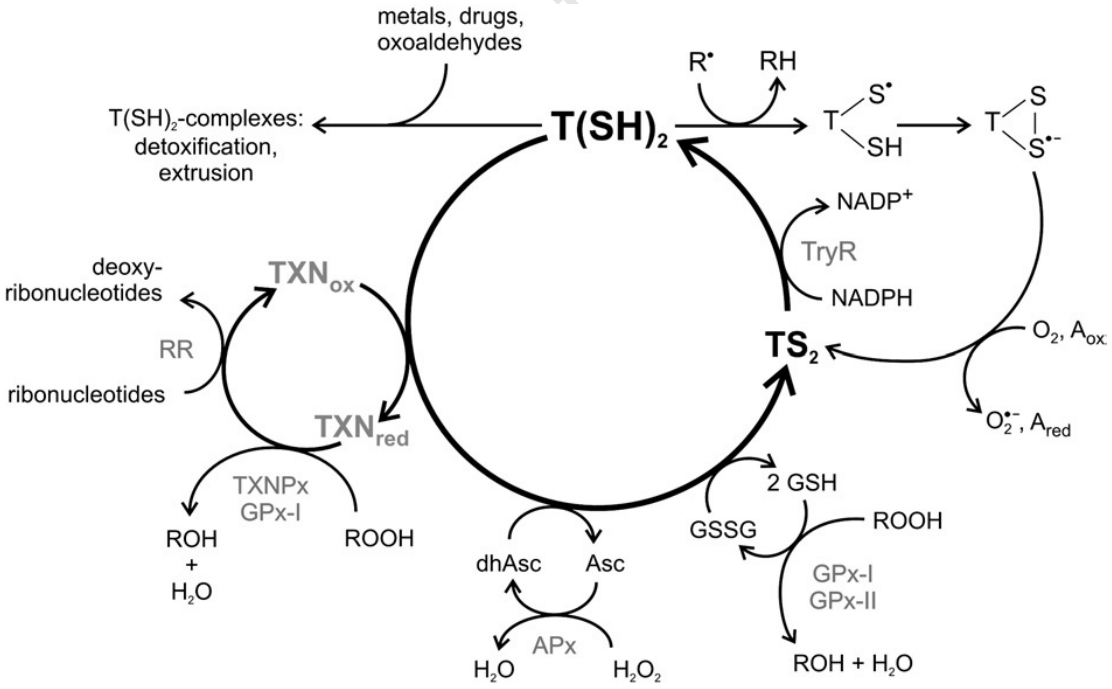

Scheme 1.1: Trypanothione dependent detoxification system (Irigoín, 2008).

In the absence of efficient enzymatic detoxification system, trypanosomes have evolved an efficient non-enzymatic oxidant detoxification system comprising of ascorbate-dehydroascorbate and low molecular thiols, glutathione, glutathionylspermidine, trypanothione, and ovothiol to play similar role (Irigoín, 2008) (scheme 1.1)

1.7. Trypanothione

Trypanothione is an aliphatic dithiol synthesized from conjugation of two molecules of glutathione to one molecule of polyamine spermidine in two ATP requiring steps, mediated differently within trypanosomatids genera (Comini, 2003) (scheme 1.2). Conjugation of a glutathione molecule to spermidine, results in the formation of glutathionylspermidine, an intermediate which itself serves as an antioxidant. Conjugation of the second glutathione to glutathionylspermidine results in trypanothione (Scheme 1.2). In *T. brucei* and *T. cruzi* both steps are catalyzed by a single enzyme, trypanothione synthetase, and each step requires an ATP molecule (Comini, 2003 and Oza, 2002). In contrast, two distinct enzymes are required to catalyze the two steps in *C. fasciculata* (Smith, 1992). Glutathionylspermidine synthetase catalyses the first step to form glutathionylspermidine and trypanothione synthetase catalyses the second step to make glutathione.

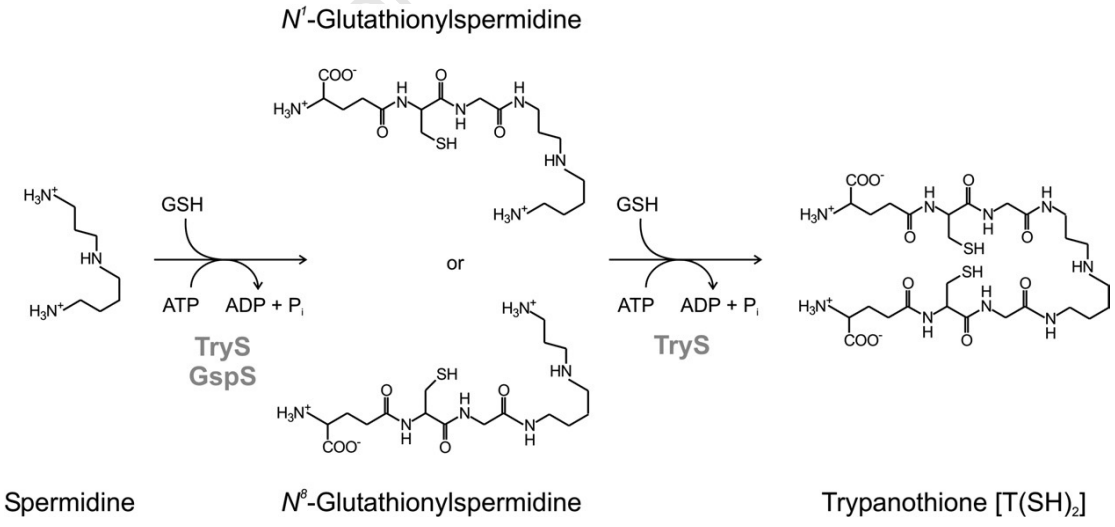

Scheme 1.2: Trypanothione biosynthetic pathway (Irigoín, 2008).

Trypanothione biosynthesis is not limited to trypanosomatids as other organisms such as *Entamoeba histolytica* and *Euglena gracilis* were also reported to produce trypanothione (Montrichard *et al*, 1999). The role of trypanothione in these organisms is, however, yet to be established.

1.7.1. Functions of trypanothione in trypanosomatids

Trypanothione plays a central role in redox regulation in trypanosomatids by being directly involved in the detoxification of reactive oxygen species (ROS). Trypanothione can be seen as replacing glutathione in trypanosomatids and is a better antioxidant than glutathione. With a thiol pK_a value of 7.4 compared to 8.6 for glutathione, trypanothione is more reactive in thiol disulfide exchange reactions than glutathione at physiological pH (Mountiez *et al.*, 1994).

In vitro studies have shown trypanothione as a spontaneous reductant of glutathione disulfides, ovothiol disulfides, thioredoxin, and is also expected to perform similar functions *in vivo*. It has also been found to be an efficient reductant of radiation induced radicals and peroxynitrite (Mountiez *et al.*, 1994).

Other studies have linked trypanothione to the resistance of *Leishmania* to trivalent arsenics and antimonials. Trypanothione is thought to bind to the drugs and form adducts which are then sequestrated out of the cell through a P-glycoprotein-like protein A (PGPA). Indeed the PGPA overexpression was observed in multidrug resistant parasites (Goyeneche-Patino *et al.*, 2008).

Perhaps of particular importance in trypanosomatids is the fact that trypanothione serves as an electron donor for the reduction of tryparedoxins. The trypanothione-tryparedoxin system probably accounts entirely for the ability of trypanosomatids to deal with oxidative stress (Krauth-Siegel and Comini, 2008).

1.7.2. Enzymes of trypanothione metabolism as potential drug targets

The absence of trypanothione metabolism in mammalian hosts, its major contribution towards redox metabolism in trypanosomatids and the susceptibility of trypanosomatids to oxidative stress make enzymes involved in trypanothione metabolism attractive drug targets. The evidence for sensitivity of the parasites to oxidative stress was provided by a study done using a potent inhibitor of glutathione biosynthesis, buthionine sulfoximine (BSO). In that study it was found that treatment with BSO resulted in prolonged survival of or even cure of mice infected with African trypanosomes (Arrick *et al.*, 1981). BSO treatment was also found to reverse nifurtimox and benznidazole resistance by African trypanosome (Faundez *et al.*, 2005). Treatment with BSO results in diminished glutathione which would lead to low levels of trypanothione and ultimately impaired capacity to detoxify oxidants such as reactive oxygen and reactive nitrogen species. However, BSO cannot be used as a drug against trypanosomes since it does not differentiate between mammalian and parasite enzymes (Huynh *et al.*, 2003).

1.7.2.1. Polyamine biosynthesis

Spermidine is a polyamine on which two molecules of glutathione are linked to form trypanothione. Its biosynthesis is similar in parasite and their mammalian hosts. Spermidine is synthesized by conjugation of putrescine and decarboxylated S-adenosylmethionine in an enzymatic reaction catalyzed by spermidine synthase (Tabor and Tabor, 1984). No structural differences have been found between parasite and mammalian spermidine synthases and both enzymes were found to be very stable. As a result, the parasite's spermidine synthase is not attractive drug target.

However, putrescine and decarboxylated S-adenosylmethionine are themselves synthesized separately in the reactions catalyzed by ornithine decarboxylase (ODC) and S-adenosylmethionine decarboxylase (AdoMetDC), respectively. Although both parasites and their mammalian hosts possess ODC, the parasite enzyme displays significant differences exploitable for development of selective inhibitors. Unlike the mammalian

enzyme, parasite ODC lacks the C-terminal degradation signal, resulting in decreased enzyme turnover (Ghoda *et al.*, 1990). This is a crucial factor because the inactivated mammalian enzyme is quickly replenished unlike parasite enzyme because rapid enzyme degradation in a cell is balanced by rapid synthesis. This is the basis for the trypanostatic activity of α-difluoromethylornithine (DFMO) (Ghoda *et al.*, 1990).

Because *T. brucei* has diminished putrescine uptake it cannot replenish the polyamine shortage through putrescine uptake from the host blood (Heby *et al*, 2003) and therefore, treatment with DFMO leads to diminished levels of polyamines and trypanothione in *T. brucei* and *Leishmania* species. Hence, DFMO is currently used as drug to treat Sleeping sickness caused by *T. b. gambiense*. *T. cruzi* lacks ODC and cannot synthesize putrescine *de novo* and therefore all ODC inhibitors are ineffective against *T. cruzi* (Carrillo *et al.*, 1999). *T. cruzi* transports polyamine quite efficiently across the membrane, making it difficult to use polyamine synthetic pathway as target for drug development against these parasites. However, inhibitors of polyamine transporters should provide good drug candidates, considering that the parasites lack ODC to make putrescine. *Leishmania* species known to have high resistance to polyamine biosynthetic inhibitors were found to overproduce ODC, AdoMetDC or Spermidine synthase (Heby *et al.*, 2003).

Studies on development of selective inhibitors of parasites' S-adenosylmethionine decarboxylase are also producing promising results (Heby *et al.*, 2007).

1.7.2.2. Trypanothione synthetase

Validation of trypanothione synthetase as a drug target was first reported in 2003 by Comini *et al*. Using double-stranded RNA interference they knocked out the trypanothione synthetase gene, resulting in diminished trypanothione and glutathionylspermidine levels, proliferation arrest and impaired viability in the *T. brucei* mutants. The mutants also showed high sensitivity to the natural oxidants like H_2O_2 and *ter*t- butyl hydroperoxide (Comini *et al.,* 2003). The results of Comini's group were later confirmed by Wyllie *et al* (2009) using a different system. This group preferred gene

replacement by homologous recombination over RNA interference. Mutants of trypanothione synthetase single-gene knockdown by gene replacement displayed similar effects reported by Comini *et al* (2003). Using the same technique the researchers developed a mutant that overexpressed trypanothione synthetase to make a clear comparative study. Both mutants were treated with the selective trypanothione synthetase inhibitor, DDU 86439 (N-(3-(dimethylamino)propyl)-2-(3-(3-fluorophenyl)-1H-indazol-1-yl)acetamide). The mutants that overexpressed the enzyme tolerated the compound while the gene knockdown mutants were killed by the compound. Although more work is still needed on this subject, it is clear that trypanothione synthetase makes an attractive drug target (Wyllie *et al.*, 2009).

1.7.2.3. Trypanothione reductase

The parasites' trypanothione reductase and the host glutathione reductase belong to the same family of flavoprotein-disulfide oxidoreductases. However, the mutual exclusiveness between the two with regard to the disulfide substrates (Shames *et al.*, 1986) means selective inhibition of the parasite's enzyme is possible.

1.8. Ovothiols

Ovothiols are 3-methyl-5-mercaptohistidines derivatives first isolated from sea urchin eggs where they were initially thought of as cofactors for cyanide-insensitive NAD(P)H oxidase of ovoperoxidase (Tuner *et al.*, 1985 and 1986) . Three types of ovothiols exist; denoted Ovothiol A, B, and C, and they differ only in the degree of methylation at the α-amino group of histidine. Ovothiol A does not have a methyl group, whereas ovothiol B contains one methyl group and ovothiol C two methyl groups (Turner *et al.*, 1987). High amounts of ovothiols were found in trypanosomes where they are believed to protect the parasites against oxidants.

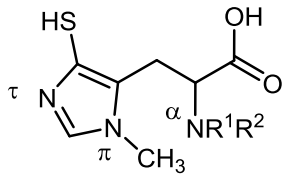

	R^1	R^2
ovothiol A	H	H
ovothiol B	CH_3	H
ovothiol C	CH_3	CH_3

Figure 1.2: Chemical structures of ovothiol

1.8.1. Properties of ovothiols

Ovothiols are aromatic thiols as opposed to the aliphatic thiols of glutathione and trypanothione. Their aromatic nature confers desirable properties to ovothiols such as resistance to oxidation by Fe^{3+}. Unlike glutathione which has a pK_a of 8.65 (Holler and Hopkins, 1990), ovothiol A has pK_{SH} of 1.42 (Weaver and Rabenstein, 1995), meaning they exist under physiological conditions as imidazolium thiolate zwitterions. The thiolates are stronger nucleophiles than thiols, and as such are more reactive towards electrophiles than thiols (Holler and Hopkins, 1988). Ovothiols were found to be very efficient as one-electron donors showing a second order rate of reduction of cytochrome C compared to insignificant reduction by glutathione under similar conditions (Holler and Hopkins, 1988). The thiolate not only makes ovothiols efficient as a one-electron donor, but also as good radical scavengers. The one-electron donating potential of ovothiols is comparable to that of ascorbic acid and Trolox C. Ovothiol aromatic radicals were also found to be more stable towards oxygen reduction than glutathione thiyl radicals (Holler and Hopkins, 1990). That is an important factor because higher radical stability means low radical propagation.

Although they react slowly with oxygen, ovothiols react spontaneously with hydrogen peroxides. Ovothiols were found to inhibit pyrogallol oxidation 50 times faster than glutathione, meaning they can decompose hydrogen peroxide 50 times faster than glutathione (Holler and Hopkins, 1990). *In vitro* studies showed ovothiol analogues as scavengers of superoxides and linoleate peroxyl radicals, a property which is believed to be shared by ovothiols *in vivo* (Hand *et al.*, 2005).

1.8.2. Proposed biological role of ovothiols

The discovery of ovothiol emanated from observation of a cofactor that confers cyanide-resistant peroxidase activity to ovoperoxidase in sea urchin eggs, and that the factor existed in millimolar concentrations (3 to 6.8 mM) (Turner *et al.*, 1986). Isolation and characterization led to the identification of the cofactor as 3-methyl α-N,N-dimethyl-5-mercaptohistidine (ovothiol C). Fertilization in sea urchin eggs is followed by development of the fertilization envelope, which is believed to protect the egg from multiple sperm invasion. The process is characterized by massive consumption of oxygen and production of corresponding hydrogen peroxide (Foerder and Shapiro, 1977). Hydrogen peroxide production from oxygen is catalysed by NADPH dependent oxidase. The produced hydrogen peroxide is then used as an oxidant in forming the fertilization envelop. The envelope forms by cross-linking tyrosine residues of the adjacent proteins utilizing hydrogen peroxide in a reaction catalysed by ovoperoxidase. Although this is a well regulated process taking place near the plasma membrane, diffusion of the hydrogen peroxide into the egg may be very toxic (Shapiro, 1991). In the absence of the glutathione peroxidase system which is normally used for detoxification of peroxides in mammalian cells, sea urchin eggs utilize ovothiols for decomposition of hydrogen peroxides that may dissolve into the eggs during envelope formation. Although there is coexistence of glutathione and ovothiols in urchin eggs, ovothiols have been found to be 50-fold superior as hydrogen scavengers as compared to glutathione (Bailly *et al.*, 2000).

Discovery of ovothiols in other different organisms has led to the assumption that its physiological role could be wider than that of an antioxidant. For example, the

Steenkamp group have shown that ovothiols convert long-lived S-nitrosoglutathione and S-nitrosotrypanothione to short-lived $NO^{\bullet}$ and the free thiols, which then reduce ovothiol disulfide back to reduced ovothiols (Vogt and Steenkamp, 2003). Ovothiol disulfides have been isolated from a unicellular green alga, *Dunaliella salina*, where it was thought to act as a reductant of the chloroplast ATP synthase complex (Selman-Reimer *et al.*, 1991). The identification of ovothiols as male pheromones for the marine polychaete *Platynereis dumeriliihas,* has also been reported (Röhl *et al.*, 1999).

1.8.3. The prevalence of ovothiol in trypanosomatids

Although Turner *et al* 1986, it was Steenkamp who in 1993 discovered the presence of ovothiol A in *C. fasciculata*, a non-human insect parasite (Steenkamp, 1993 and Steenkamp and Spies, 1994). Subsequent studies led to further isolation of ovothiols from all life cycle stages of trypanosomatid parasites. Ovothiols were later isolated in millimolar concentrations from the insect forms of all tested *Leishmania* species and in some cases the ovothiol content was even higher than that of trypanothione (table1.2) (Ariyanayagam and Alan H. Fairlamb, 2001). High amounts of ovothiols observed in the amastigotes are believed to protect the parasites against harsh oxidative stress produced by the host immune response. However, the amounts of ovothiol were found to be low in all bloodstream parasites (table 1.2). Generally ovothiols were found in higher amounts in intracellular parasites (*Leishmania* and *T. cruzi*) than in intercellular parasites (*T. brucei*) although the reason is not known (table1.2) (Ariyanayagam and Alan H. Fairlamb, 2001). Studies in *M. smegmatis* found that ergothionine is 26-fold increased in MSH deficient mutants and is also excreted into the medium (Ta *et al,* 2011and Sao Emai *et al,* 2013). Similar studies in trypanosomatids have not been done but would be relevant

Like all thiol antioxidants, ovothiols are oxidized to form disulfides through reaction with oxidants. Most reduced thiols, such as glutathione in mammals and trypanothione in trypanosomes, are regenerated from their disulfides through enzymatic reactions with their specific reductases. However, no ovothiol disulfide reductase has been identified as

yet, and based on *in vitro* studies the oxidized ovothiols are thought to be reduced by trypanothione *in vivo* (Weaver and Rabenstein, 1995).

Table 1.2: Ovothiol in different life-cycle stages of trypanosomatid parasites. Values were expressed as a percentage of total thiols (Ariyanayagam and Fairlamb, 2001).

Organism	Life cycle stage	Ovothiol (%)	Trypanothione (%)
L. donovani	Promastigote	35	43
	Amastigote	<3	76
L. major	Promastigote	58	25
	Amastigote	58	25
T. cruzi	Epimastigote	7	76
	Trypomastigote	28	55
T. brucei	Procyclic trypomatigote	4	67
	Bloodstream trypomastigote	<1	32

Although the physiological role of ovothiols in trypanosoma98tids is not yet fully known, it could be assumed from the *in vitro* studies to be that of antioxidants (Holler and Hopkins, 1990, and Vogt and Steenkamp, 2003). High ovothiol concentrations observed in the human infective parasites in the insect forms (table 1.2) could be seen as preparing the parasites for human invasion. In *L. major*, promastigotes and amastigotes have the same ovothiol levels. It is not known whether this is a property that distinguishes Leishmania spp responsible for cutaneous Leishmaniasis from those causing visceral forms of the disease. Inhibition of the ovothiol biosynthetic pathway will therefore shed some light on physiological functions of ovothiol, and its redox potential makes it an efficient antioxidant.

1.8.4. Biosynthesis of Ovothiols

Biosynthesis of ovothiols starts with formation of S-(5'-L-histidyl)-L-cysteine sulfoxide (**3**) from conjugation of cysteine and histidine in an enzymatic reaction catalyzed by sulfoxide synthase (Vogt *et al.*, 2001) (Scheme 1.3). The only previous report that

described the formation of such a unique imidazolyl sulfoxide had been that of Ishikawa *et al* (1974). These workers described the conjugation of a cysteine sulphur to C-2 of hercynine as a step in the biosynthesis of ergothioneine. Formation of the sulfoxide proceeded with retention of the histidine double bond at the site of substitution in a redox reaction in which oxygen served as the final electron acceptor. The mechanism for 5-histidyl cysteine sulfoxide formation is yet to be understood. In the second step, 5-histidyl cysteine sulfoxide undergoes lysis to form 5-mercaptohistidine and pyruvic acid in a reaction mediated by cysteine sulfoxide lyase. An *in vitro* study showed that the lyase reaction requires pyridoxal phosphate (Vogt *et al.*, 2001). Very recently the group of Seebeck identified two enzymes that catalyze the biosynthesis of ovothiol, designating them OvoA and OvoB for the synthase activity that catalyzes formation of 5-histidyl cysteine sulfoxide and the lyase which converts 5-histidyl cysteine sulfoxide in to 5-mercaptohistidine, respectively. OvoA was found to have a C-terminal methyl tranferase domain which is believed to be responsible for the last methylation step (scheme 1.3).

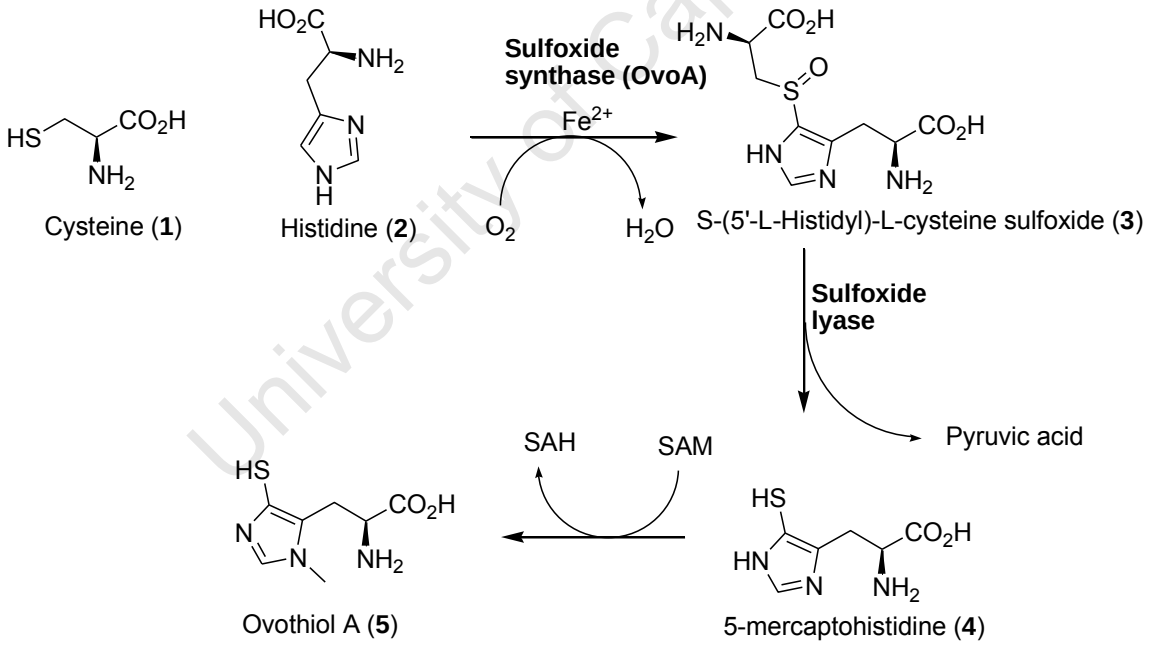

Scheme 1.3: Ovothiol biosynthetic pathway

Understanding the mechanism of ovothiol biosynthesis will provide a platform for designing inhibitors which eventually will shed light on the physiological role of

ovothiols in human pathogens, such as trypanosomes. The uniqueness of the ovothiol biosynthetic pathway would make OvoA and OvoB good targets for selective inhibition.

Some hypotheses have been made on the mechanism of the transsulfuration mediated by OvoA and EgtB. For example, one study suggested that ferrous peroxysulfur (i.e., FeOOS) oxidises histidine to form a $HisN_{\delta}(-H)^{\bullet}$ which then attacks the bound iron to form the sulfoxide product (Bushnell *et al.,* 2012). Ishikawa and his co-workers showed that the thioether β-amino-β-carboxyethylergothionine can be utilized as an intermediate (Ishikawa *et al.*, 1974), suggesting that sulfoxide formation in ergothioneine biosynthesis may be occuring via a thioether intermediate even though the thioether intermediate was never isolated from the reaction mixture. Due to the lack of the corresponding thioether, Steenkamp and his co-workers could not study the involvement of thioether as a potential precursor for sulfoxide synthesis in ovothiols A biosynthesis (Steenkamp, 2002).

In this study, a sulfoxide synthase (OvoA) from the bacterium, *E. tasmaniensis* was characterized with respect to substrate specificity, Michaelis-Menten constants, solvent isotope effect and inhibition by histidine analogues. Where the required histidine analogues were not available commercially, they were either obtained from researchers who had reported their preparation, or were synthesized from readily available precursors. Data from evaluation of activity of some of these analogues contributed evidence towards a proposed mechanism of the transsulfuration reaction, while that from other analogues revealed the role played by the amino acid moiety on the location of sulfur transfer on imidazole ring of sulfur acceptors.

AIM AND OBJECTIVES

The aim of this project was to provide insights on the mechanism of the oxidative transsulfuration step mediated by sulfoxide synthase, by characterizing the activity of OvoA (sulfoxide synthase) from *E. tasmaniensis* with chemically synthesized and commercially available histidine analogues. A better understanding of mechanisms of enzymes involved in the biosynthesis of ovothiol and ergothioneine would then inform the design and development of specific inhibitor molecules that can be later investigated as drugs against trypanosomal and bacterial human pathogens.

The main objectives of this project were:

1. Design and synthesis of histidine analogues that can act as inhibitors and/or alternative substrates of 5-histidyl cysteine sulfoxide synthase (OvoA).
2. Optimization of the OvoA assay
3. Characterization of sulfoxide synthase kinetic constants
4. Evaluation of histidine derivatives as inhibitors and/or alternative substrates of OvoA.

CHAPTER 2:

DESIGN AND CHEMICAL SYNTHESIS OF HISTIDINE ANALOGUES AS POTENTIAL INHIBITORS AND ALTERNATIVE SUBSTRATES OF SULFOXIDE SYNTHASE (OVOA)

2.1. Overview

Despite identification of the intermediates (Vogt *et al.,* 2001) and the enzymes (Braunshausen and Seebeck, 2011) involved in ovothiol biosynthesis, the mechanism that leads to formation of S-(5'-L-histidyl-L-cysteine sulfoxide, **3** (here referred to as 5-histidyl cysteine sulfoxide) (Scheme 1.3) in the first step of the pathway remains poorly understood. The reaction involves oxidative transsulfuration of histidine, while retaining the double bond on the histidine moiety, using cysteine as the sulfur donor. This is a unique biological reaction for which there has only been one literature precedent: in ergothioneine. In ergothioneine biosynthesis, a sulfoxide intermediate is formed from conjugation of γ-glutamylcysteine to the C-2 of hercynine in a reaction mediated by EgtB, a homologous sulfoxide synthase found in mycobacteria (Braunshausen and Seebeck, 2011).

OvoA and EgtB are iron-dependent enzymes, involved in activating the oxygen molecule to oxidize their respective substrates. The mechanism underlying sulfur transfer in ovothiol and ergothioneine biosynthesis is still unclear, and in particular the oxidation of the sulfur on the product because such a modification is not carried through into the subsequent steps. Therefore more work is required to elucidate the unique mechanism of sulfoxide synthesis mediated by these two enzymes. Three mechanisms were proposed as plausible alternatives for the oxidative transsulfuration step (Braunshausen and Seebeck, 2011). Initial characterization revealed OvoA as a promiscuous enzyme when it comes to the selection of sulfur acceptors. Even though the enzyme used only cysteine as sulfur donor it utilized α-N-methylhistidine and α-N,N-dimethylhistidine derivatives as sulfur acceptors (Braunshausen and Seebeck, 2011).

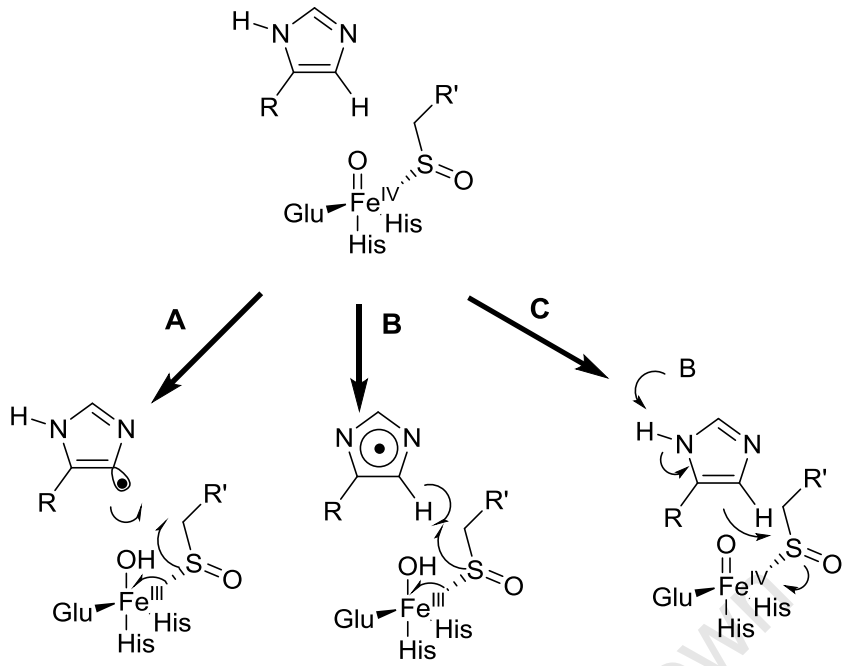

Scheme 2.1: Proposed plausible mechanisms of the transsulfuration reaction of OvoA: C-S bond formation is initiated by (A) formation of a histidyl sp^2 radical, (B) formation of a histidyl π- radical, and (C) electrophilic attack of the iron-coordinated cysteine sulfoxide on histidine (Braunshausen and Seebeck, 2011).

To exploit the loose selection of sulfur acceptors, more histidine derivatives were envisaged as possible alternative substrates and/or inhibitors of OvoA. Histidine analogues with halogens at the imidazole ring might be potential subversive substrates in a reaction that follows mechanism **C** in scheme 2.1, with 5-fluorohistidine in particular having promise because of the strong C-F bond which will be difficult to break in an S_N2' nucleophic elimination. Iodine and bromine are good leaving groups, sometimes even as radicals, a characteristic which makes them good candidates to study mechanisms A and B. Other derivatives bearing alkyl groups (e.g. methyl) on the imidazole ring would also be of interest to study the OvoA mechanism.

Here we report successful synthesis of 5-chloro, 5-bromo and 5-iodo-histidine using a succinimide based reagent. Fluorinating agents such as selectfluor, Diethylaminosulfur trifluoride (DAST) and N-fluorobenzenesulfonimide were used in an attempt to obtain 2- or 5-fluorohistidine, but without success. Synthesis of histidine analogues with alkylation at positions 1 and 3 is also reported. Histidine derivatives that could be used to prepare C-5 functionalized histidine analogues were also synthesized.

2.2. Objective

Histidine derivatives were invasaged as good candidate for use as either OvoA inhibitor and or affinity ligands for purification of the enzyme from the host cell. Histidine derivatives some containing halogen and other having different amino acid functional groups were designed and synthesed.

2.2.1. Synthesis of imidazole-halogenated histidines as sulfoxide synthase (OvoA) inhibitors. Set (A)

Halogens are often used to study reactions where a loss of hydride is proposed. Fluorine in particularly is more suitable as hydrogen replacement as it provides a much stronger C-F bond without significantly increasing the size of the molecule. Therefore, objectives of this work were to synthesize and evaluate the effect of 5-halogenated histidines (figure 2.1) as potential inhibitors or alternative substrates of sulfoxide synthase (OvoA).

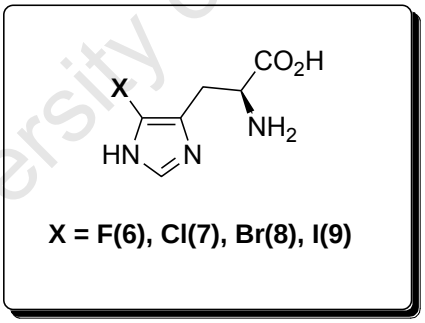

Figure 2.1: 5-halohistidines as potential sulfoxide synthase (OvoA) inhibitors and/or substrates.

2.2.2. Synthesis of other histidine derivatives. Set (B)

Histidine analogues in figure 2.2 were synthesized, with the objective that they could be used as alternative substrates of OvoA and as potential affinity ligands which could be used for the purification of novel sulfoxide synthases (OvoA) from host organisms. The last step in the biosynthesis of ovothiol A is the methylation of 4-mercaptohistidine at N-3 of the imidazole ring. It would therefore be important to investigate if 3-methylhistidine (**15**) and 1-methylhistidine (**14**) are substrates of the sulfoxide synthase step, because it will suggest an alternative biosynthetic route to ovothiol. Other histidine analogues **16** and **17** bearing modifications on α-amino were also envisaged as potential affinity ligands for the purification of the sulfoxide synthase (figure 2.2).

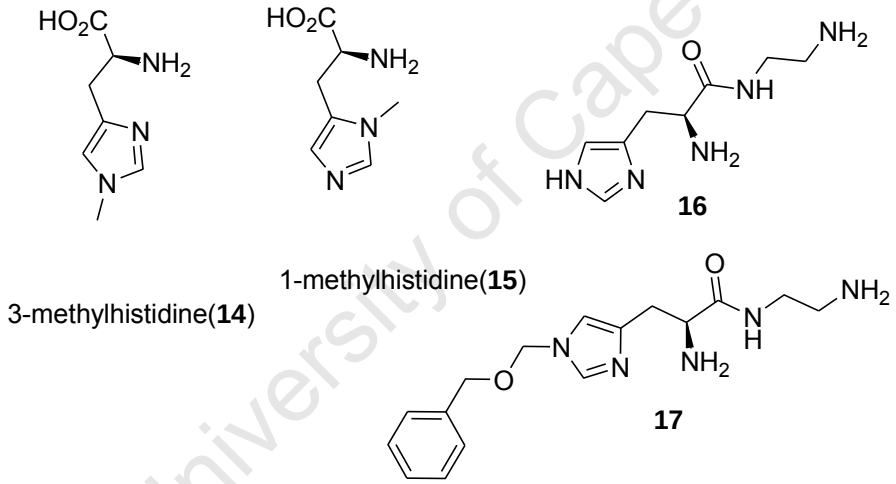

Figure 2.2: N-Alkylated histidine derivatives as sulfoxide synthase (OvoA) inhibitors

2.2.3. Synthesis of 5-alkylated histidines as potential inhibitors of sulphur oxidation step (Set C)

Alkylated histidine derivatives listed in figure 2.3 were targeted as potential inhibitors of OvoA and OvoB, based on structural similarities of these compounds with 5-histidyl cysteine sulfoxide, the product of OvoA and substrate for OvoB (figure 2.3).

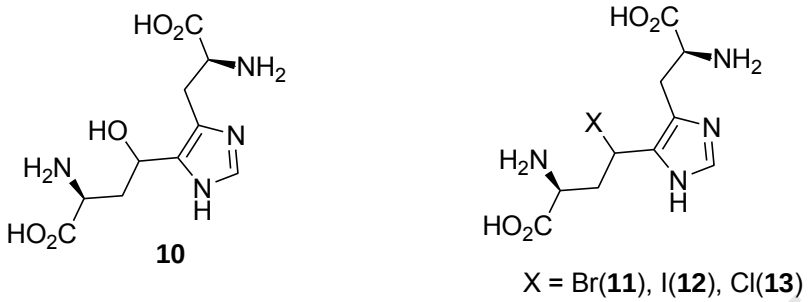

Figure 2.3: Analogues of 5-histidyl cysteine sulfoxide as potential inhibitors or alternative substrates of sulfoxide synthase.

2. 3. RESULTS AND DISCUSSION

2.3.1. Synthesis of ring N-alkylated histidine derivatives as sulfoxide synthase alternative substrates. (Set C)

The first step in the biosynthesis of ovothiol is the formation of S-(5'-L-histidyl-L-cysteine sulfoxide, **3**, scheme 1.3 (here referred to as 5-histidyl cysteine sulfoxide). Availability of histidine derivatives would therefore provide useful analogues for characterization of the enzyme involved. The methyl group was thought to be the best candidate for this purpose for two main reasons: (a) the methyl group is present in the final product (ovothiol) of this biosynthetic pathway (therefore 3-methyl-histidine would be evaluated as potential natural substrate), (b) the methyl group is the smallest and least sterically-demanding alkylating agent. Moreover, as a result of imidazole tautomerization it would also be interesting to evaluate whether the position of the alkyl group (or N-H) on the imidazole ring played a role in ovothiol biosynthesis.

Synthesis of N(1)-methylhistidine (**14**) and N(1)-methylhistamine (**38**) required prior protection of both the 3-nitrogen and the α-amino group (Jain and Cohen, 1996; Narayanan *et al.,* 2001). Reaction of N,N'-carbonyldiimidazole with **35a** (Scheme 2.2), obtained by methylation of histidine, or **35b** in refluxing acetonitrile afforded cyclic ureas **36a** and **36b** respectively. Alkylation of **36a** and **36b** with methyl iodide at reflux afforded quaternary iodide salts **37a** and **37b** which upon deprotection in dilute hydrochloric acid provided the desired N-alkylated derivatives **14** and **38** in 72% and 77% overall yields respectively (Scheme 2.2).

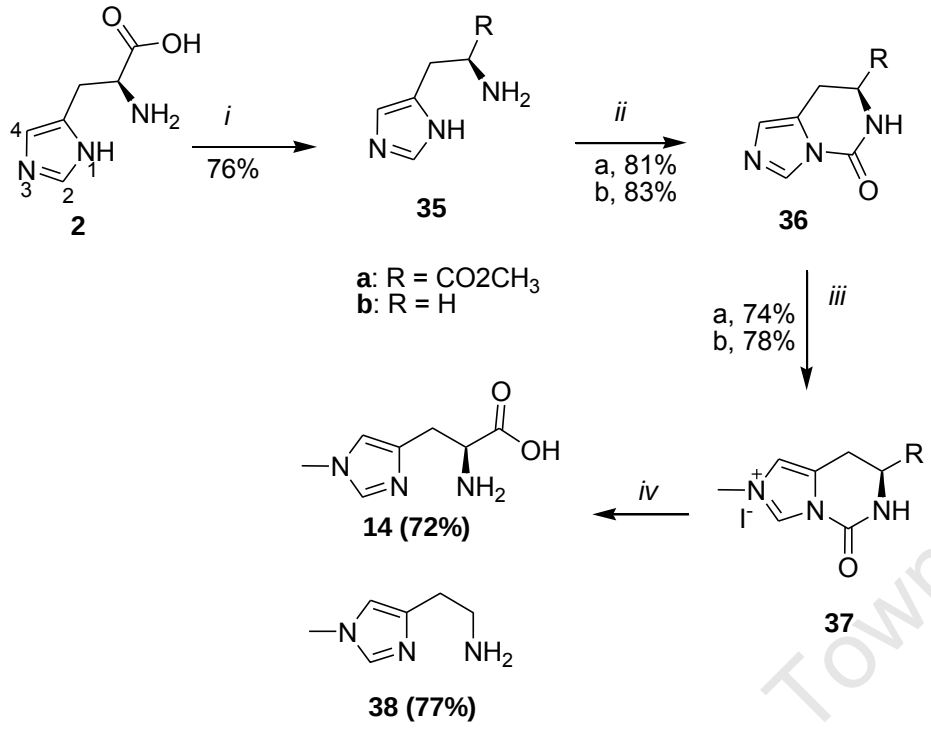

Scheme 2.2: Synthesis of N(1)-methyl-histidine and N(1)-methyl-histamine: *Reagents and conditions:* i) Thionyl chloride, MeOH, reflux, 16 h; ii) N,N'-carbonyldiimidazole, CH_3CN, reflux, 18 h; iii) MeI, CH_3CN, reflux, 18 h, iv) 6 N HCl, 70^oC, 20 h.

Identification of final products was based on appearance of the N-methyl group protons at δ 3.65 in the ^1H NMR spectra, which were in agreement with the literature values (Jain and Cohen, 1996). It was interesting to note that the acylation at the N(3) did not reduce the nucleophilicity of the N(1) enough to prevent alkylation step iii (Scheme 2.2).

Similarly, synthesis of N(3)-methylhistidine and N(3)-methylhistamine required prior protection of 3-nitrogen and the α-amino group (Chivikas and Hodges, 1987). The cyclic ureas **36a** and **36b** (Scheme 2.3) proved ideal starting materials and were alkylated with an alkylating group which could be selectively removed at the end of the reaction. Thus, **36a** and **36b** were reacted with 2-bromo-2'-acetonaphthone (BAN) in refluxing acetonitrile to give compounds **39a** in 71% yield and **39b** in 74% yield. The ^1H NMR spectra of **39a** and **39b** each displayed overlapping signals in the aromatic region of the spectrum integrating for seven protons, and a signal at δ 6.27 ppm for the two N(1)-CH_2 protons, clearly indicating the presence of the BAN group (see experimental section).

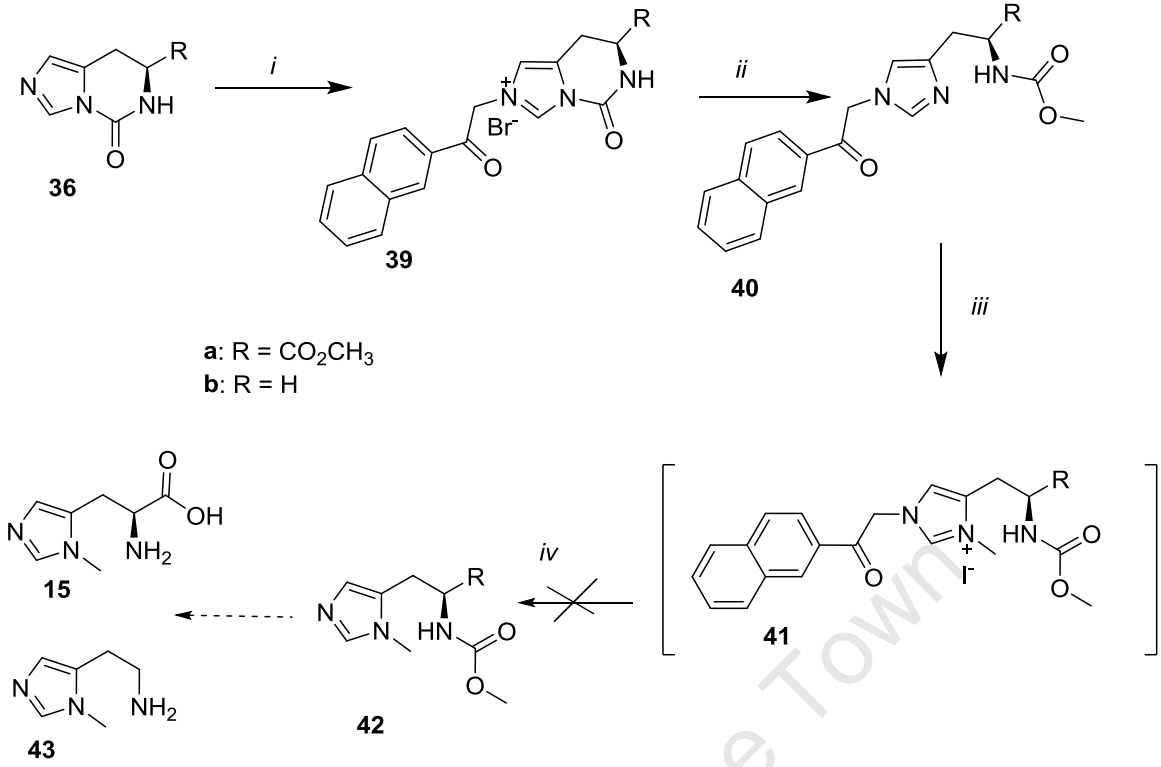

Scheme 2.3: Synthesis of N(3)-methyl-histidine (15) and N(3)-methyl-histamine (43): *Reagents and conditions:* i) 2-Bromo-2'-acetonaphthone, CH_3CN, reflux, 18 h; ii) MeOH, DIEA, reflux, 16 h; iii) MeI, CH_3CN, reflux, 24 h; iv) Zn, HOAc-MeOH (1:1), sonicate, 3 h.

Quaternary salts **39a** and **39b** on treatment with N,N-diisopropylethylamine in methanol at reflux afforded fully protected histidine and histamine derivatives **40a** and **40b** respectively, in good yields. Appearance of the singlet at δ 3.70 ppm in the ^{1}H NMR spectra of the compound confirmed the presence of the methyl ester. Alkylation of compounds **40a** and **40b** with methyl iodide in refluxing acetonitrile for 24 hours, led to the formation of the quaternary salts **41a** and **41b**. Consumption of the starting material and formation of the new product with lower R_f value (monitored by tlc) was enough to show that the quaternary salts were formed. However, because of their highly hygroscopic nature it was recommended not to isolate the compounds **41a** and **41b** (Chivikas and Hodges, 1987). The crude quaternary salts were therefore dissolved in acetonitrile, and the resultant solution was added drop wise to vigorously stirring dry ethyl ether. The resultant solution was immediately treated with glacial acetic acid/methanol (1:1) and zinc dust under ultra-sonication conditions as previously

described (Chivikas and Hodges, 1987). However, when the reaction mixture was examined by tlc, it showed multiple products which proved difficult to separate by column chromatography. Repeated efforts to obtain **42a** and **42b** were not successful.

After unsuccessful preparation of N(3)-methylhistidine, attention was then shifted to obtaining a different N(3)-alkylated histidine, **45** (scheme 2.4). Compound **45** was easily synthesized in excellent yield from commercially available starting material, **44**, by acid cleavage of the Boc protecting group in 20% TFA/DCM (Sprout *et al* 2005). The absence of the up field signals for the t-butyl protons in the ^{1}H NMR spectrum confirmed the complete removal of the Boc group.

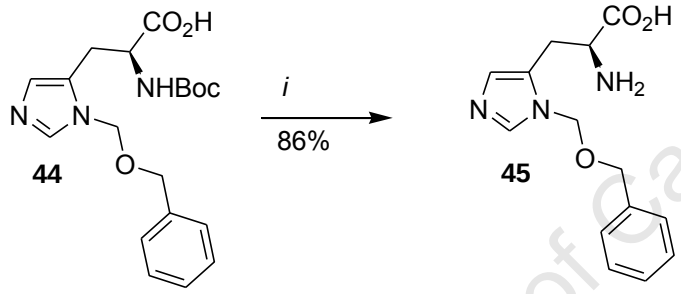

Scheme 2.4: Synthesis of 2-amino-3-(1-((benzyloxy)methyl)-1H-imidazol-5-yl)propanoic acid: *Reagents and conditions*: i) 20% TFA/DCM, rt, 2 h.

2.3.2. Synthesis of ring halogenated histidine derivatives as potential sulfoxide synthase inhibitors

Synthesis of ring halogenated histidine and histamine derivatives can be achieved by a number of methods. However, most procedures utilize unprotected starting materials and harsh, acidic conditions, with large excesses of halogenating reagents, resulting in low yields and many side products, possibly due to the participation of the free α-amino group. Therefore, a method reported by Jain and co-workers was preferred since it

required prior protection of the α-amine by labile protecting groups, which could be removed under mild conditions to obtain the product in high yields (Jain *et al.*, 1998). Protected histidine **46** was chosen as the starting material because of its commercial availability and the 5-halohistidines **7, 8** and **9** were duly obtained in 54-68% overall yields (Scheme 2.5).

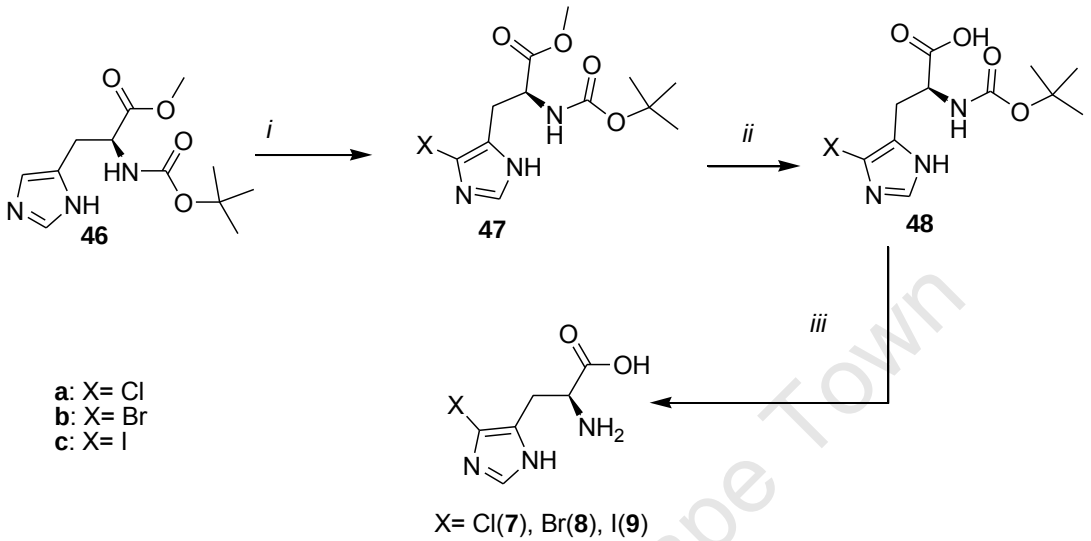

Scheme 2.5: Synthesis of ring halogenated histidines: *Reagents and conditions*: i) N-halo(Br, Cl, I)-succinimide, CH_3CN, N_2, dark, rt, 2 h; ii) LiOH, MeOH, rt, 2 h; iii) TFA (20% in CH_2Cl_2), CH_2Cl_2, rt, 2 h.

Electrophilic halogenation of **46** with 1 molar equivalent of N-halosuccinimide gave 5-halohistidine derivatives **47** in moderate to good yield. Unprotected histidine has ^{1}H NMR signals at δ 6.8 and δ 7.6 ppm for H-5 and H-2 respectively, and since electrophilic halogenation is not restricted to the C-5 position, identification of the 5-halohistidine product was confirmed by disappearance of the signal at δ 6.8 in the ^{1}H NMR spectrum. The 2,4-dihalohistidine derivatives were also isolated in 8-30% yield and were easily identified by the absence of both H-2 and H-5 signals in the ^{1}H NMR spectrum. The regio-selectivity of halogenation at C-5 was found to be in the order: Cl > Br > I with the 2,4-diiodohistidine derivative isolated in higher yield than the 2,5-dichloro- and 2,5-dibromohistidine derivatives (8% and 18%, respectively). A similar phenomenon has been previously observed (Jain *et al.*, 1998).

Hydrolysis of the methyl ester with LiOH using a method described by Boger and Yohannes (1988) gave Boc-protected derivatives, which were not isolated but subjected immediately to treatment with 20% (v/v) TFA in DCM, followed by removal of the cations using an ion-exchange column (Dowex 50W, H^+, 100 mesh) to afford the 5-halohistidines (Jain *et al.*, 1998). The absence of signals for the methoxy and *t*-butyl protons at δ 3.61 ppm and δ 1.42 ppm respectively was an indication of complete deprotection. The two-step deprotection sequence reported here was preferred to the acid hydrolysis reported by Jain *et al.* because the acid hydrolysis required 72 hours while the two-step sequence needed just 5 hours to obtain the product. In some cases the acid hydrolysis was also reported to lead to regiospecific electrophilic dehalogenation at C-5 (Jain *et al.*, 1998).

Fluorohistidines could however not be synthesized by the same method due to the unavailability of 4-fluorosuccinimide. Instead, alternative strategies using different fluorinating agents were employed, such as selectfluor, diethylaminosulfur trifluoride and N-fluorobenzenesulfonimide. However these attempts failed to produce the desired fluorohistidines (data not shown).

2.3.3. Synthesis of affinity ligands for potential use in the purification of sulfoxide synthase (OvoA).

Compounds **17** and **16** were identified as potential affinity ligands for sulfoxide synthase (OvoA) purification, based on their chemical similarities with histidine substrate, and the incorporation of an amine-terminated linker for coupling to a solid support. These target compounds, without modification on the α-amino group, were synthesized from a suitably protected N(α),N(3)-protected starting material, **44**, (scheme 2.6).

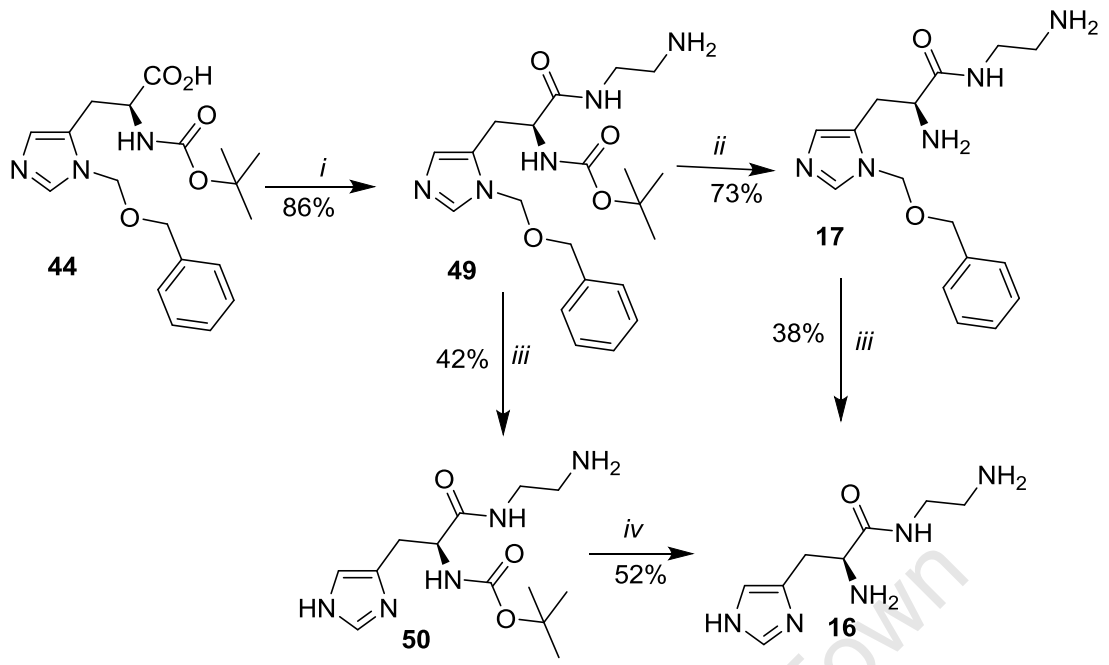

Scheme 2.6: Synthesis of histidine ethylenediamine: *Reagents and conditions*: i) N, N'-carbonyldiimidazole, ethylenediamine, THF, -10°C to rt, 2.5 h; ii and iv) 20% (v/v) TFA/DCM, rt, 2 h; iii) Formic acid, Hydrazine hydrate, Pd-C, MeOH, 24 h.

Synthesis of the target compounds began with reaction of commercially available protected histidine **44** with N, N'-carbonyldiimidazole to form an activated carboxyl group, which was then reacted with excess ethylenediamine to form amide **49** in excellent yield (Tolbert and Wong, 2000). Compound **49** had a low R_f value compared to the starting material and a positive reaction with ninhydrin indicated the presence of a more hydrophilic primary amine group on the compound. The ^{1}H NMR of **49** displayed multiplets at δ 3.17 ppm integrating for two protons, and δ 3.09 ppm also integrating for two protons, consistent with the presence of the N-(2-aminoethyl)-amido group. Acid cleavage of **49** in 20% TFA/DCM at room temperature afforded **17** in good yield (Jain *et al.*, 1998). The absence of the *tert*-butyl group singlet at δ 1.41 ppm in the ^{1}H NMR spectrum and δ 28 ppm in the ^{13}C NMR spectrum of **17** was a confirmation of the successful removal of the Boc group from **49**.

Alternatively, hydrogenolysis of **49** over Pd/C in methanol at room temperature with formate serving as hydrogen donor, gave **50** in 42% yield (Gowda and Mahesh, 2002).

Analysis of **50** by ^{1}H NMR spectrum showed the absence of the aromatic protons in the benzyl group which provided enough evidence for the successful synthesis of **50**. Removal of the Boc protecting group from **50** gave the target compound **16** in 52% yield. Compound **16** could also be synthesized from **17** by hydrogenolytic cleavage of the Bom-protective group over Pd-C as in the formation of **50** from **49** as described above.

2.3.4. Synthesis of 5-histidyl cysteine sulfoxide analogues as affinity ligands

Purification of sulfoxide synthase (OvoA) by affinity chromatography using the analogues of the 5-histidyl cysteine sulfoxide (the product of the sulfoxide synthase catalysed reaction) would allow characterization of the novel enzyme. The 5-histidyl cysteine sulfoxide analogues bearing different functionality at the histidine C-5 position (figure 2.4) were envisaged as potential ligands for sulfoxide synthase purification.

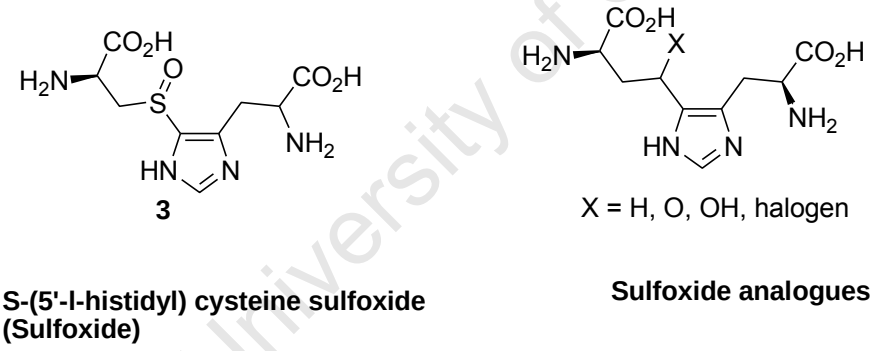

Figure 2.4: Structural analogues of 5'-histidyl cysteine sulfoxide

Thus, the synthesis of the 5-histidyl cysteine sulfoxide analogues in figure 2.3 was envisaged to start from coupling of a suitably protected and activated histidine (Nucleophile) and suitably protected homoserine aldehyde (Electrophile) as outlined in the retrosynthetic analysis in scheme 2.7 below.

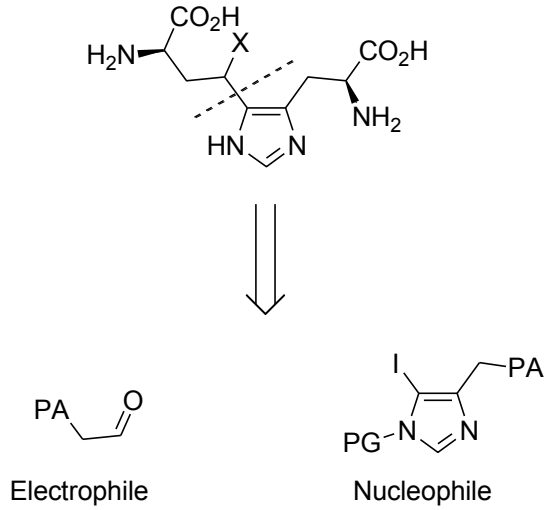

Scheme 2.7: Retrosynthetic analysis of 5-histidyl cysteine sulfoxide structural analogues

A metal-halogen exchange reaction was investigated in order to prepare the histidine derivative for the coupling step. Groziak and Wei have successfully synthesized 5-formylated imidazole (**55**) derivatives using a metal-halogen exchange reaction (Groziak and Wei, 1991) and these conditions were thus used to carry out the synthesis of 5-formylated imidazole **55** as a model study for the histidine functionalization experiments. Substituted imidazole **53** (scheme 2.8) was synthesized in two steps from **51** in good overall yield by iodination followed by N-protection. Compound **53** was then reacted with nBuLi in THF at -78^{o}C to form the lithiated species **54**, which after rapid quenching with DMF gave the formylated product **55** in 60% yield (Groziak and Wei, 1991).

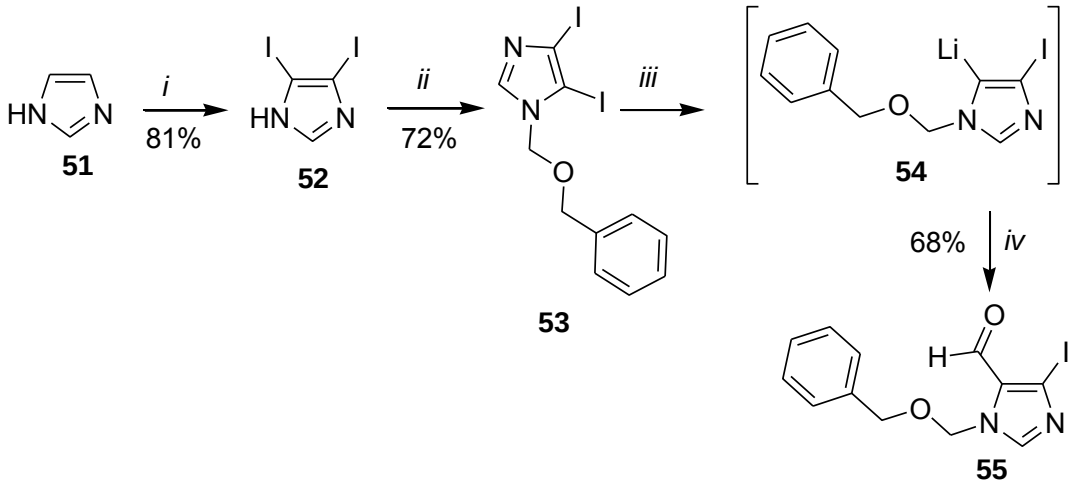

Scheme 2.8: Synthesis of formylated imidazole using metal-halogen exchange reaction: *Reagents and conditions:* i) 0.04 N NaOH, I_2, Hexane, 0^{o}C -rt, 18 h (a); ii) DCM, K_2CO_3, BomCl, rt, 16 h; iii) nBuLi, DMF, THF, -78^{o}C, 10 min; iv) H_2O, -78^{o}C–rt, 2 h.

The ^{1}H NMR of the formylated product displayed a diagnostic aldehyde proton at δ 9.740, which was in agreement with the literature value (Groziak and Wei, 1991).

Encouraged by these positive results, the application of a similar metal-halogen exchange reaction was attempted in order to substitute the C-5 position of histidine. From our retrosynthetic analysis in scheme 2.7, protected 5- iodohistidine **57** (scheme 2.9) was anticipated to provide a good starting material for the coupling step. The 5-formyl derivative **58** would then provide a good intermediate for the subsequent steps leading up to the target compounds.

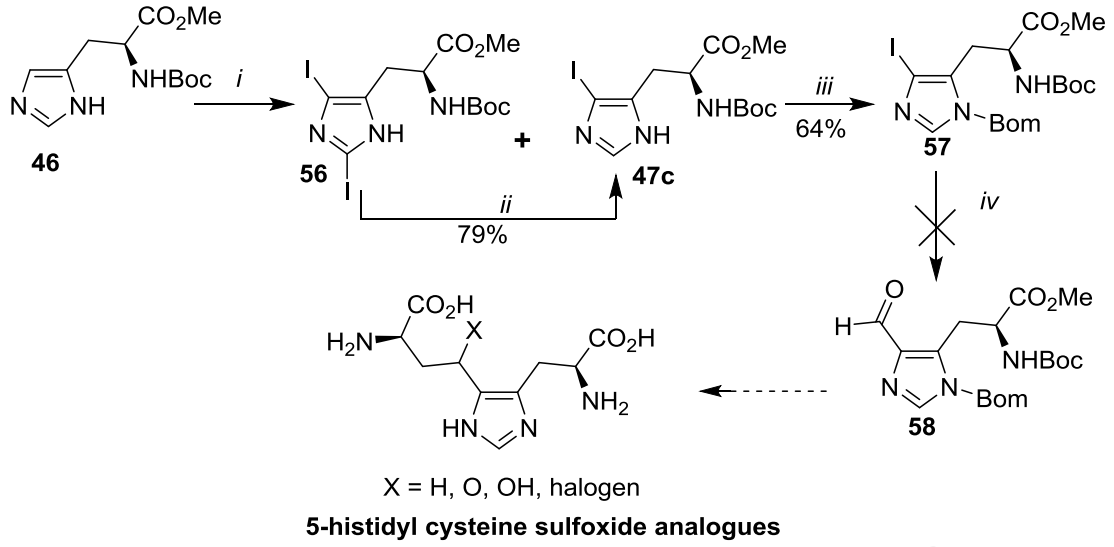

Scheme 2.9: Attempted synthesis of 5-functionalized histidines using metal-halogen exchange: *Reagents and conditions*: i) NIS, CH_3CN, rt, N_2, dark, 2 h; ii) NaH, thiophenol, isopropanol, 35°C, 30 min; iii) BomCl, Et_3N, DCM, rt, 24 h; iv) nBuLi, DMF, THF, -78°C, 10 min.

Iodination of commercially available histidine derivative **46** using 1.5 equivalents of NIS in acetonitrile provided the desired tert-butyl 1-(methoxycarbonyl)-2-(4-iodo-1H-imidazol-5-yl)ethylcarbamate **47c** in 36% yield together with the 2,5-diiodo derivative **56** derivative in 58% yield (Jain *et al.*, 1998). The latter could however be converted to the mono-iodinated derivative **47c** in good yield through regio-specific deiodination at C-2 using sodium thiophenolate (Iddon *et al.*, 1987). The appearance of the signal for H-2 at δ 7.59 in the ^{1}H NMR spectrum was evidence for the presence of **47c**. Treatment of **47c** with benzyloxymethyl chloride (BomCl) in dichloromethane in the presence of triethylamine afforded **57** in good yield. Protected iodide **57** was then reacted with 1.1 equivalents of n-butyl lithium (BuLi) before addition of DMF. The TLC of the reaction mixture showed multiple overlapping spots, indicating multiple products which became difficult to separate. Because of the apparent substrate instability in the presence of nBuLi it became apparent that a more stable substrate was required for the lithium mediated coupling step. As a result the focus was turned to investigation of the possibility of protecting both the carboxyl and primary amino groups in histidine, converting them into more stable oxazolidine or oxazoline derivatives.

2.3.4.1. Synthesis of the electrophile for the lithium mediated C-C coupling reaction

tert-Butyl 4-(formylmethyl)-2,2-dimethyloxazolidine-3-carboxylate **63** (Scheme 2.11) was identified as a suitable aldehyde (electrophile partner) for the lithium mediated coupling at the histidine C-5 position. Following a literature review, it was noted that **63** could be easily synthesized from an aspartic acid derivative (Paintner *et al*, 2005). Thus, the commercially available, selectively benzylated aspartic acid, **58**, was treated with methyl iodide in DCM to form methyl ester **59** in excellent yield (scheme 2.10). The reaction product did not require further purification and analysis by ^{1}H NMR showed a diagnostic methoxy signal at δ 3.69.

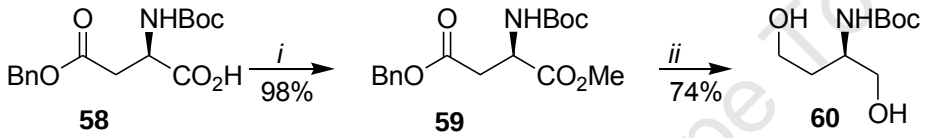

Scheme 2.10: Synthesis of N-Boc-protected 2-amino-1,4-propane-diol. *Reagents and conditions:* i) MeI, K_2CO_3, DCM, rt, 16 h; ii) $NaBH_4$, MeOH/THF, 50^{o}C, 20 min.

Reduction of **59** with five equivalents of $NaBH_4$ in a mixture of MeOH and THF at reflux, afforded the diol **60** in good yield (Hou *et al*, 2001). Appearance of signals in the ^{1}H NMR spectrum for two sets of coupled ethylene protons together with the absence of signals for the aromatic and methoxy groups provided evidence for complete reduction of **59** to form **60**. However, reduction with commonly used ester reducing agent, $LiAH_4$, afforded the same product but in very low yield. This could be due to the higher reactivity of $LiAH_4$ which results in removal of the Boc protecting group. Treatment of **60** with 2.2-dimethoxypropane at 40°C in the presence of a catalytic amount of para-toluenesulfonic acid resulted in formation of the cyclic oxazolidine derivatives **61** and **62** in 42% and 19% yield respectively (Scheme 2.11). The ^{1}H NMR spectrum of the latter compound displayed a broad peak at δ 5.14 for N-H, which supported the assignment of the structure whereas the absence of the N-H peak in the ^{1}H NMR spectrum of **61** confirmed the participation of the α-nitrogen in the ring closure. Furthermore,

comparison of the ^{13}C NMR spectra of **61** and **62** showed that the α-C in **61** (δ 58.69) resonated significantly further downfield to that in **62** (δ 48.61), consistent with chemical shifts of C-4 in five membered oxazolidine rings. Swern oxidation of **61** gave tert-butyl 4-(formylmethyl)-2,2-dimethyloxazolidine-3-carboxylate **63** in good yield. The diagnostic signal for the aldehyde proton at δ 9.79 in the ^{1}H NMR spectrum of **63** was noted (Paintner *et al*, 2005).

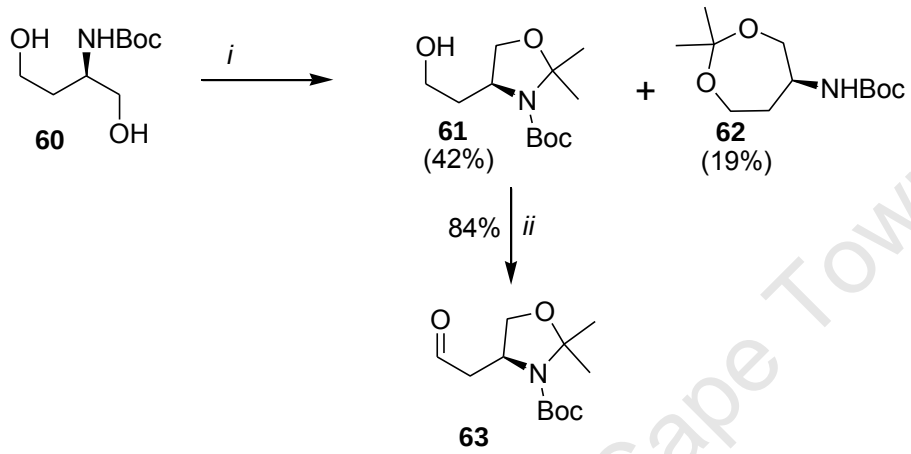

Scheme 2.11: Synthesis of the electrophile for the lithium mediated C-C coupling reaction: *Reagents and conditions:* i) 2,2-dimethoxypropane, TsOH (cat), rt, N_2, 18 h; ii) DMSO, Et_3N, oxalyl chloride, DCM, -78°C – rt, 3 h.

2.3.4.2. Synthesis of the nucleophile for the lithium mediated C-C coupling reaction

2.3.4.2.1. Synthesis of oxazolidine based nucleophile

Compound **46** (Scheme 2.12) which is commercially available was chosen as the starting material for the synthesis of suitably protected histidine, **67** (Scheme 2.13), needed for coupling. Thus, treatement of **46** with $NaBH_4$ in a mixture of MeOH and THF at 50°C provided Boc-protected α-amino alcohol **64** in good yield (Kumar *et al*, 2002). Halogenation of the resulting alcohol **64** using NIS in acetonitrile afforded a mixture of mono-iodo and di-iodo derivatives **65a** and **65b** in 30% and 42% yields, respectively

(Jain *et al*, 1998). The di-iodo compound was regioselectively deiodinated at C-2 to give **65b** in 71% yield by reaction with sodium thiophenolate in isopropyl alcohol (Iddon *et al*, 1987). ^{1}H NMR spectra of **65b** showed a signal at δ 7.56 for H-2 on the imidazole ring.

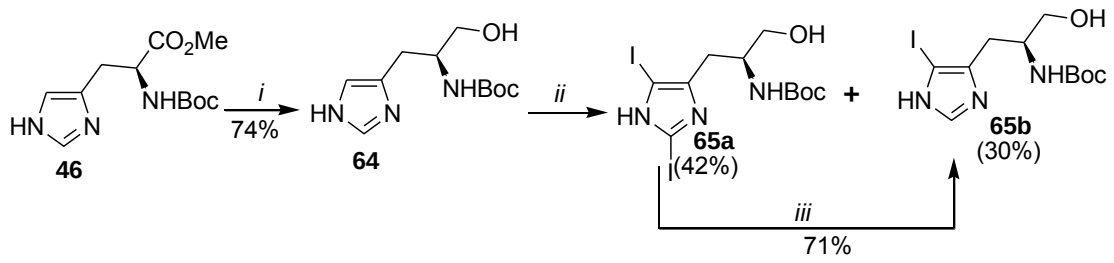

Scheme 2.12: Synthesis of 5-iodo histidinol. *Reagents and conditions:* i) $NaBH_4$, MeOH/THF, 50^{o}C, 20 min; ii) NIS, CH_3CN, N_2, dark, rt, 2 h; iii) NaH, thiophenol, isopropanol, 35^{o}C, 30 min.

Since the C-C coupling reaction utilizes strongly basic nBuLi, it was necessary to remove all acidic protons from the starting materials. The oxazolidine ring structure as a protecting group for α-amino alcohols was found ideal for this purpose (Kise *et al*, 1998). Thus, compound **65b** upon treatment with a large excess of 2,2-dimethoxypropane in dry DCM, gave a mixture of cyclic oxazolidine **67** and the alternative 7-membered ring analogue **66** in 19% and 26% yield respectively (scheme 2.13). Both cyclic products displayed diagnostic six-proton signals in their ^{1}H NMR spectra. Compound **66** displayed singlets for two methyl groups at δ 1.68 and δ 1.77 while compound **67** showed two three-proton singlets further up-field at δ 1.45 and δ 1.47. However, a significant difference, which helped with the assignment of the structures was the appearance of a signal for the α-N-H proton in the ^{1}H NMR spectrum of **66**, which was absent in the spectrum of **67**.

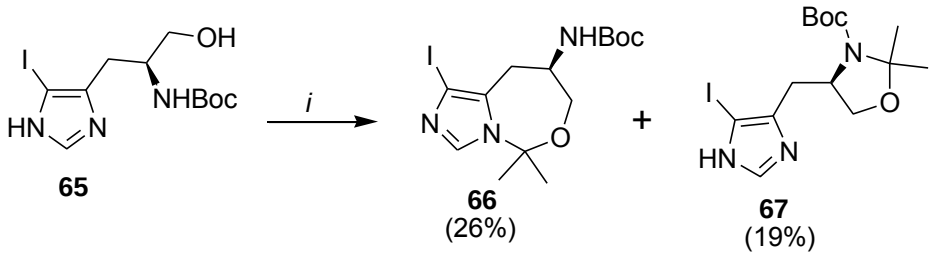

Scheme 2.13: Synthesis of oxazolidine based nucleophile: *Reagents and conditions:* i) 2,2-dimethoxypropane, DCM, TsOH (cat), reflux, 18 h.

Since compound **66** was not suitable for coupling because of the α-N-H acidic proton, attempts were made to synthesis **67** exclusively by first protecting the participating imidazole's N-1 in **65** prior to ring closure (scheme 2.14).

Thus, compound **68** (Scheme 2.14), obtained by protecting the carboxyl group of compound **44** (Vaz *et al*, 2003), was reduced with $NaBH_4$ in MeOH-THF mixture to form alcohol **69**. This was then subjected to the oxazolidine ring-forming conditions described in Scheme 2.13 but the reaction produced the mixed acetal **70** instead, without any traces of **71** even after stirring the mixture at reflux for 3 days. **70** was identified by ^{1}H NMR analysis, with the proton spectrum showing a methoxy signal at δ 3.13.

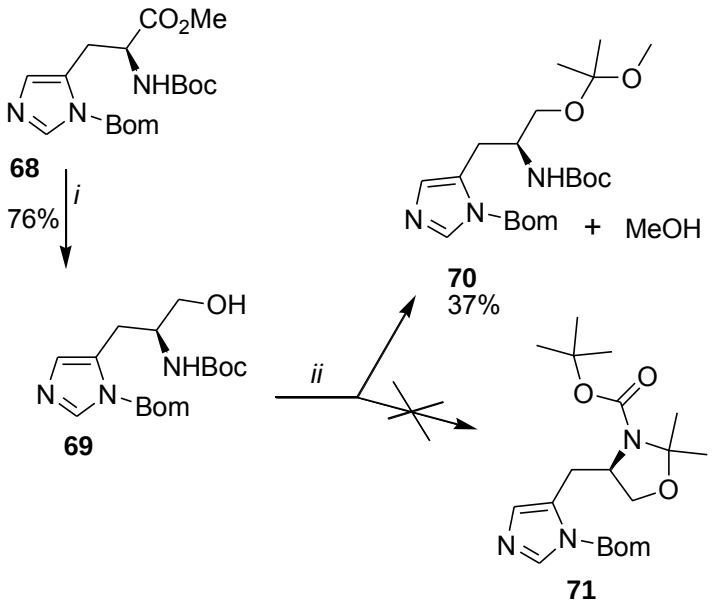

Scheme 2.14: Attempted synthesis of oxazolidine based nucleophile. *Reagents and conditions*: i) $NaBH_4$, MeOH/THF, 50°C, 20 min; ii) 2, 2-dimethoxypropane, DCM, TsOH (cat), reflux, 3 days.

2.3.4.2.2. Synthesis of oxazoline based nucleophile

Failure to synthesize the oxazolidine derivatives in reasonable amounts led to the adoption of a different approach to synthesizing suitably protected histidine derivatives for the proposed lithium-mediated coupling reaction shown in scheme 2.7. A variation on protection as a cyclic derivative was proposed, whereby the α-amino alcohols were protected by the oxazoline ring system.

Compound **72** (scheme 2.15) was proposed as suitable starting material for the synthesis of oxazoline-protected histidine derivatives **80a** and **80b** (scheme 2.17). Protected α-amino alcohol **73** was prepared in good yield by reduction of commercially available **72** with $NaBH_4$ in MeOH-THF (Kumar *et al*, 2002). The absence of the methoxy proton signal coupled with the presence of signals for the new β-protons in the ^1H NMR spectrum of **73**, clearly confirmed the formation of the amino alcohol. Treatment of **73**

with 2.1 equivalents of *para*-toluenesulfonyl chloride in dichloromethane afforded fully protected oxazoline product **75** *albeit* in poor yield (21%) together with the N-tosyl amino alcohol **74** in moderate yield (66%) after 24 hour (scheme 2.15) (Peer *et al*, 1996).

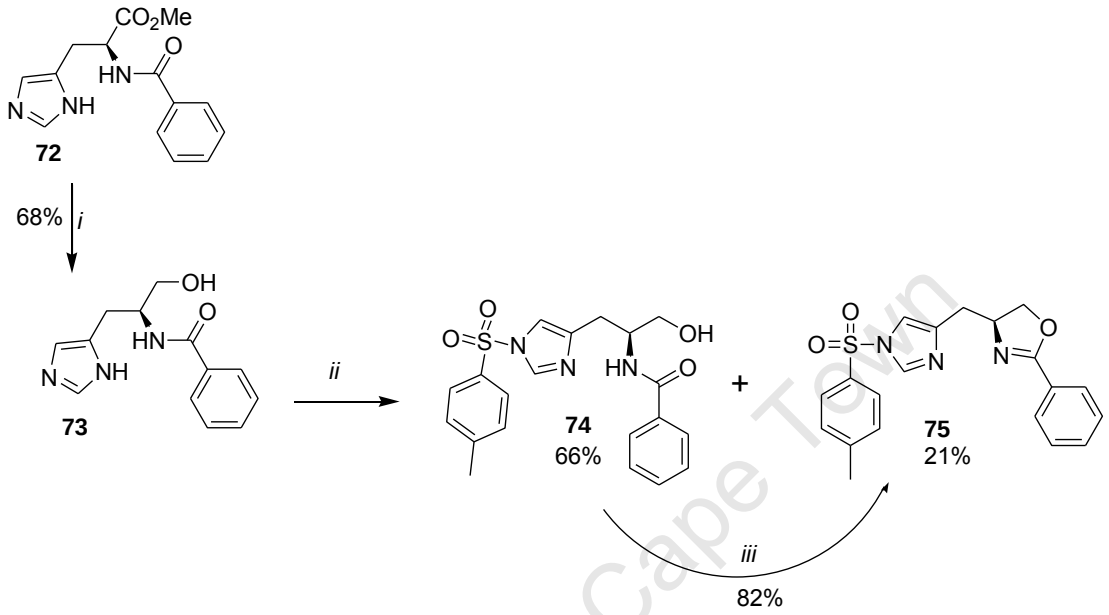

Scheme 2.15: Synthesis of oxazoline derivative of histidine: *Reagents and conditions:* i) $NaBH_4$, MeOH/THF, 50°C, 20 min; ii) and iii) TsCl, Et_3N, DCM, rt, 16 h.

Isolated and purified amino alcohol **74** was treated with another 2 equivalents of *para*-toluenesulfonyl chloride under similar conditions for a further 24 hours, giving the product **75** in excellent yield, and showing that the reaction needed a larger excess of *para*-toluenesulfonyl chloride reagent to go to completion. Attempts were made to halogenate **75** using N-iodosuccinimide to obtain either 2,5-di-iodinated derivative **77** or mono-iodinated, **78**, but without success. A previous study had found that certain protective groups prevent imidazole halogenation (Crich and Banerjee, 2006).

It therefore became apparent that the removal of the N-tosyl group from **75** may be necessary in order to achieve halogenation of imidazole ring of the oxazoline derivatives. Thus, compound **75** was reacted with caesium carbonate in a mixture of anhydrous methanol and THF at 50°C for 2 hours to give the deprotected product **76** in excellent

yield, *albeit* on a small scale (scheme 2.16) (Bajwa *et al*, 2006). However, on scaling up, small amounts of starting material remained unreacted, and it proved difficult to separate the product from the remaining starting material on a large scale. This problem could be overcome by halogenation of the crude reaction products containing **76** using electrophilic halogenating reagents (N-iodo- and N-bromo-succinimide) in acetonitrile, to afford the ring halogenated oxazoline derivatives in moderate to good yields (scheme 2.16). The attempted iodination of the crude **76** with 1.1 equivalents of N-iodosuccinimide did not go to completion, though it gave a mixture of the di-iodo derivative **77** as the major product, and the desired 5-iodo derivative **78** as the minor product (scheme 2.16) However, bromination with N-bromosuccinimide afforded the desired 5-bromo derivative **79** in good yield without noticeable amounts of the di-bromo derivative (scheme 2.16).

Identification of the halogenated compounds was accomplished mainly by analysis of the ^{1}H NMR spectra which did not show a signal at δ 6.88 corresponding to H-4 on the imidazole ring. In **78** the ^{1}H NMR spectrum showed that both imidazole protons signals had disappeared, indicating substitution of both protons by iodine.

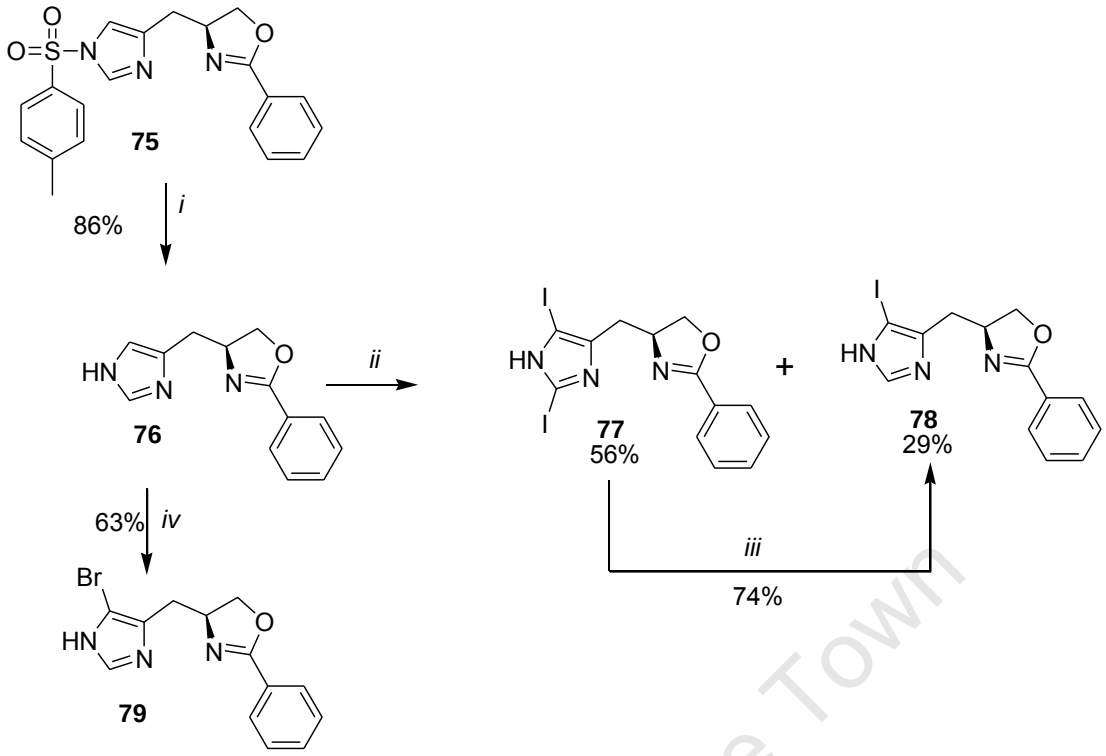

Scheme 2.16: Synthesis of 5-iodinated histidine oxazolines: *Reagents and conditions:* i) Cs_2CO_3, MeOH-THF, 50°C, 2 h; ii) NIS, CH_3CN, N_2, dark, rt, 2 h; iii) NaH, thiophenol, isopropanol, 35°C, 30 min.; iv) NBS, CH_3CN, N_2, dark, rt, 2 h.

Regio-selective deiodination of **77** with sodium thiophenolate in MeOH-THF mixture gave **78** in good yield and the product had the same analytical profile as the one obtained by direct iodination in step *ii*, also showing the H-2 signal at δ 7.64 ppm (Iddon *et al*, 1987). Synthesis of the target halogenated histidine, suitably protected for lithium mediated coupling, was concluded with N-tosyl protection of compounds **78** and **79**, using tosyl chloride in dichloromethane to give the desired **80a** and **80b** in good yields (scheme 2.17) (Peer *et al*, 1996).

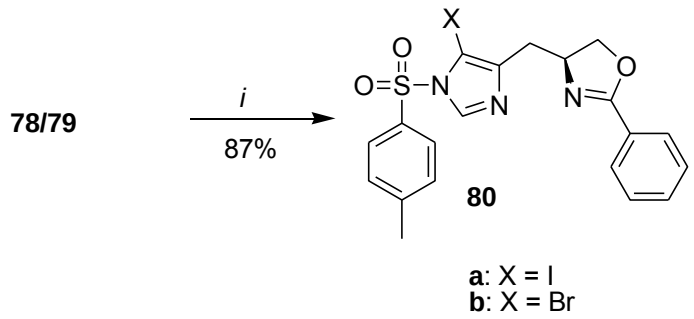

Scheme 2.17: Synthesis of protected 5-iodinated histidine oxazolines: *Reagents and conditions:* i) TsCl, Et_3N, DCM, rt, 16 h.

The ^{1}H NMR spectra of the products **80a** and **80b** displayed signals for the methyl group at δ 2.4 and for the aromatic protons, thus confirming the presence of N-tosyl group.

2.3.5. C-C coupling of oxazoline nucleophile and oxazole electrophile mediated by lithium

Having successfully synthesized the electrophile (**63**) and halogenated histidine derivatives (**80a** and **80b**), the stage was set for the lithium mediated coupling reaction. This would provide a crucial intermediate (scheme 2.7) from which the target compounds in figure 2.3 could be prepared.

Success of a lithium mediated coupling reaction relies on successful lithium-halogen exchange, and generation of a reasonably stable lithium species that can then be quenched with a suitable electrophile to generate a C-C bond (Carver *et al.*, 1997).

2.3.5.1. Quenching oxazole-lithium species with water

Many N-protecting groups are labile towards nBuLi even at low temperatures (Carver *et al.*, 1997). It was therefore necessary to obtain preliminary evidence that the lithiated

species could be formed by treatment with nBuLi, and could undergo further reaction without compromising the protecting groups.

Compound **80a** was therefore reacted with 1.1 equivalents of nBuLi in dry THF at -78^{o}C, and the presence of lithium species **81** (not isolated) investigated by quenching the reaction with water. This gave **75** in good yield (scheme 2.18), as was evident from the ^{1}H NMR spectrum which showed the presence of the imidazole's H-5 proton signal at δ 6.92. NMR also revealed that the N-tosyl group had not been removed, with a singlet at δ 2.48 for the methyl group and multiplets at δ 7.83–7.33 for the aromatic protons.

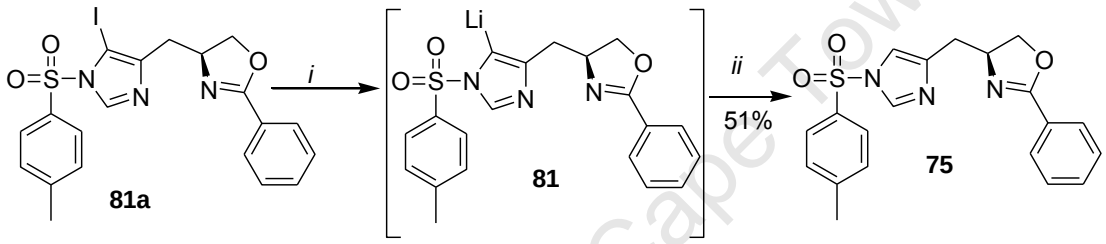

Scheme 2.18: Quenching lithium-carbon species with water: *Reagents and conditions:* i) nBuLi, THF, -78^{o}C, 10 min; ii) H_2O, rt, 1 h.

2.3.5.2. Quenching oxazole-lithium species homoserine aldehyde electrophile (63)

Results obtained in scheme 2.18, provided some confidence that lithium mediated nucleophilic C-C coupling reaction in histidine C-5 could be possible. Thus, a nucleophilic lithium species was generated by reacting protected halogenated histidine derivative **80a** with nBuLi in dry THF (scheme 2.19). Subsequent quenching of the reaction with homoserine aldehyde **63** afforded the coupled product **82**, *albeit* in poor yield, 19 % (Scheme 2.19). The identification of the product was by analysis of the ^{1}H and ^{13}C NMR spectra. The aromatic (δ 7.32-7.97) and *tert*-butyl (δ 1.41) proton signals were evident in the ^{1}H NMR spectrum, and the corresponding carbon signals were

evident in the ^{13}C NMR spectrum. The methyl protons in the tosyl group gave a singlet at δ 4.45.

While the successful formation of cross-coupled product **82** was encouraging, attempts to improve the yield of product **82** by repeating step *i* in scheme 2.19 were unsuccessful. Instead, more of dehalogenated side product **75** was obtained, which suggested that the lithiated species was forming and that aldehyde **63** contained some residual water that quenched the lithium species. This problem could not be overcome, even after prolonged drying of reactants under high vacuum. This problem was investigated by attempting to repeat the reaction using an alternative aldehyde as described below.

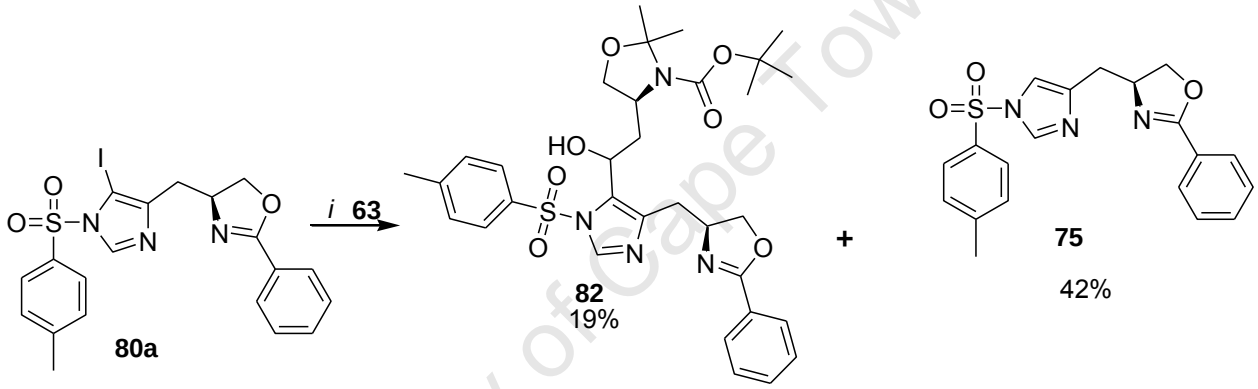

Scheme 2.19: Quenching lithium-histidine species with homoserine aldehyde electrophile: *Reagents and conditions:* i), nBuLi, THF, -78°C, 10 min.

2.3.5.3. Quenching oxazole-lithium species with dimethylformanide DMF

Lithiated species **81** (scheme 2.18) was generated from bromo-derivative **80a** and quenched immediately with DMF in an attempt to generate formyl derivative **83**. However, as before, the formation of the C–C bond was not successful (scheme 2.20), with only the debrominated product **75** being isolated, showing again the successful formation of the lithiated species but rapid quenching by protons.

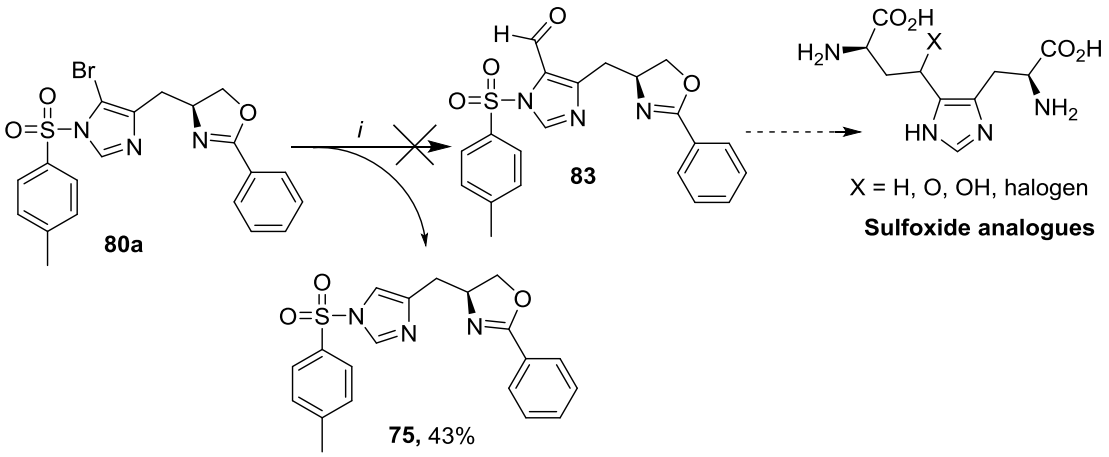

Scheme 2.20: Quenching of the histidine-lithium species with DMF: *Reagents and conditions:* i) nBuLi, DMF, THF, -78^{o}C, 10 min.

While working on protected imidazoles, Groziak and Wei (1991) noted that exchange of lithium from C-5 to C-2 took place *via* an inter-molecular process, particularly if the reaction was not quenched rapidly after addition of nBuLi (Scheme 2.21). However we did not find any evidence for C-2 formylated product after the reaction described in scheme 2.20.

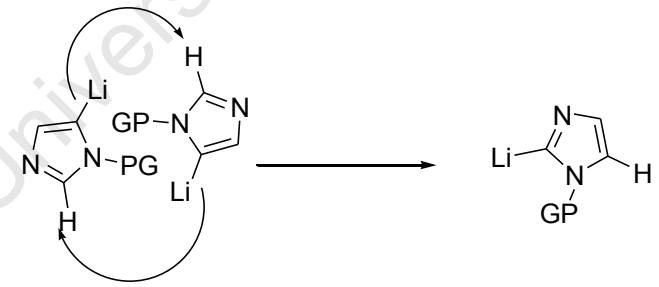

Scheme 2.21: Exchange of lithium from C-5 to C-2

Due to time constraints no further attempts were made to quench lithiated species **80** using other aldehydes. However, the initial success demonstrated in this reaction, and the evidence obtained for successful formation of the lithiated species suggest that future optimization of this method is worth pursuing, as a method for preparation of novel histidine derivatives with C-C functionalization.

CHAPTER 3:

CHARACTERIZATION AND INHIBITION OF OVOA FROM *ERWINIA TASMANIENSIS*

3.1. Introduction

3.1.1. Dioxygen activation in biological systems

OvoA and EgtB are iron-dependent sulfoxide synthases which activate molecular oxygen in order to afford oxidative sulfur transfer onto their respective substrates in ovothiol and ergothioneine biosynthesis (Seebeck, 2010 and Braunshausen and Seebeck, 2011). Ovothiol and ergothioneine are small molecule thiols believed to play a role as antioxidants in pathogenic trypanosomes and mycobacteria, respectively (Hollar *et al.,* 1988 and Melville *et al.,* 1957). Enzymes involved in dioxygen activation have been subjects of interest to scientific researchers, because they mediate biological reactions that have environmental, pharmaceutical, and medical significance (Bruijnincx *et al.,* 2008). Dioxygen activating enzymes can be classified as either heme or nonheme containing enzymes. Although reactions catalyzed by these enzymes may be similar, the enzymes differ in the way they coordinate the iron metal. Heme containing enzymes utilize a heme cofactor while nonheme enzymes make use of amino acid side chains to coordinate the iron metal. A classical example of heme containing enzymes is cytochrome P450, which mediates a variety of important biological reactions, such as conversion of polyunsaturated fatty acids into active molecules, metabolism of drug and xenobiotics etc. (Denisov *et al.,* 2005).

3.1.2. Nonheme iron enzymes

The nonheme iron enzyme superfamily itself can be divided into two groups called mononuclear and binuclear nonheme iron enzymes. Methane monooxygenase is a binuclear iron enzyme that catalyzes the very difficult reaction of oxidation of methane to

methanol (Bruijnincx *et al.,* 2008). Availability of enzyme crystal structure data in the past twenty years has allowed classification and characterization of the mononuclear nonheme iron enzymes and the way they coordinate to iron metal (Costas *et al.,* 2004). An iron-binding structural motif consisting of two histidine residues and one carboxylate of either glutamate or aspartate was identified in more than thirty of the crystal structures of mononuclear nonheme iron enzymes. The ligands were found to be facially coordinated to the iron metal and on that basis a 2-His-1-carboxylate facial triad was coined to describe the structural feature of the mononuclear iron enzyme subfamily (Bruijnincx *et al.,* 2008).

3.1.3. 2-His-1-carboxylate facial triad and mechanism of oxygen activation

In the metal resting state, the carboxylate ligand can either be monodentate (single coordination) or bidentate (double coordination) (scheme 3.1). The other two or three available binding sites are vacant or occupied by solvent, such as water molecules in biological systems. At the resting stage the metal center has very low affinity toward molecular oxygen. Binding of the substrate to the complex, sometimes by replacing a water molecule, increases dioxygen binding affinity of the complex (B). Coupling reactivity with substrate binding is believed to be a protection mechanism against self-inactivation (Bruijnincx *et al.,* 2008).

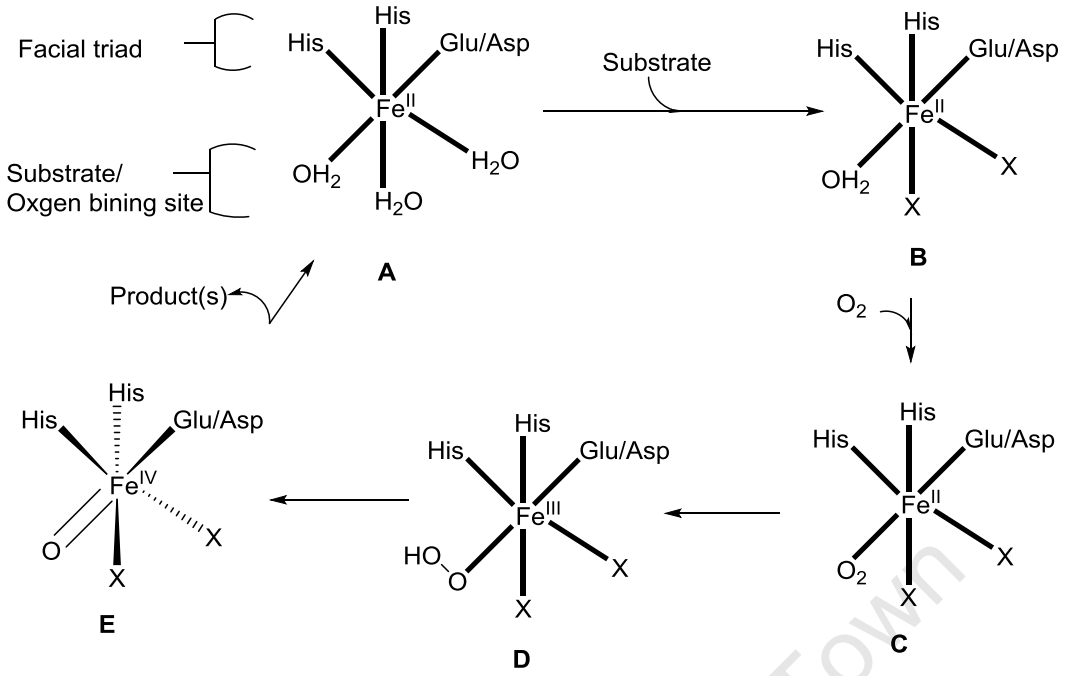

Scheme 3.1: General mechanistic pathway of 2-His-1-carboxylate iron dependent enzymes.

Binding of dioxygen to the metal center evokes formation of iron(III)-superoxide through oxidative electron transfer from the iron metal to the molecular oxygen (C → D). From this point different reactions can happen. For most characterized mechanisms of mononuclear iron enzymes, another electron transfer to the peroxide breaks the O-O bond leading to formation of water and a high-valent iron(IV)-oxo ($Fe^{IV}O$) species (E) which is believed to be the actual substrate oxidant mainly through hydrogen abstraction (Bruijnincx *et al.,* 2008). The existence of an even stronger oxidant, such as high-valent iron(V)-oxo ($Fe^{V}O$) species has also been postulated as the main oxidant (Costas *et al.,* 2004).

3.2. OvoA and EgtB as mononuclear iron enzymes

The first step in ovothiol biosynthesis involves oxidative addition of cysteine at C-5 of histidine, in a reaction that requires molecular oxygen, and is mediated by OvoA (Vogt *et al.,* 2001 and Braunshausen and Seebeck, 2011) (scheme 3.2). OvoA is a synthase enzyme whose activity was first reported by Steenkamp and colleagues (Vogt *et al.,* 2001). In their work the researchers found that the activity required molecular oxygen and addition of

iron. This was a unique enzyme-catalyzed reaction of which the only precedent had been the corresponding ergothionine biosynthetic enzyme, which was found to mediate oxidative transsulfuration at the C-2 position of hercynine using cysteine as substrate (Ishikawa *et al.,* 1974). Recently, Seebeck identified EgtB as the enzyme involved in the transsulfuration step in ergothioneine biosynthesis and found γ-glutamylcysteine as the possible natural substrate (Seebeck, 2010) for the enzyme (scheme 3.2). On the basis of the similarity of reactions of these systems, the Seebeck group later identified the synthase which mediates the transsulfuration step in ovothiol biosynthesis and named it OvoA (Braunshausen and Seebeck, 2011). *In vitro* characterization of the enzymes confirmed that both EgtB and OvoA were iron-dependent enzymes which utilize iron to activate dioxygen to afford the unique oxidative sulfur transfer. In line with the structural requirement of mononuclear iron enzymes, the group found that both OvoA and EgtB possess a conserved motif consisting of HX_3HXE, believed to be the iron binding site.

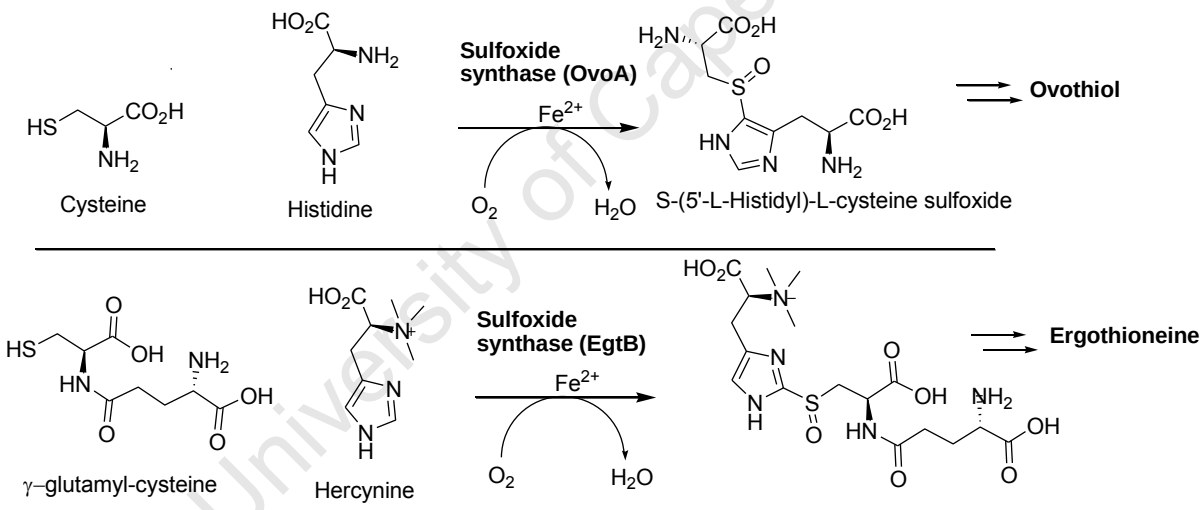

Scheme 3.2: OvoA and EgtB catalysed reactions

Gene sequence search identified homologous genes for OvoA in a number of other organisms, including bacteria. In the initial characterization of the enzyme from *Erwinia tasmaniensis* and *Trypanosoma cruzi,* which had been cloned in *E. coli,* it was found that the bacterial enzyme was more stable and active than the trypanosomal enzyme. The enzyme also displayed high selectivity towards the sulfur donor, preferring cysteine over other naturally occurring sulfur donors that were tested (Braunshausen and Seebeck, 2011). Mechanistic aspects of the OvoA and EgtB reactions still remain elusive and this

was the driving force for initiation of this study, which was oriented towards understanding the transsulfuration reaction mechanism mediated by OvoA and EgtB. A series of chemically synthesized and naturally occurring histidine analogues were thus used to characterize the OvoA reaction.

In this study we show that OvoA is activated by ascorbate and isoascorbate, and that the enzyme used a series of histidine analogues as sulfur acceptors. Kinetic characterization showed similar K_M for cysteine, histidine and histidine analogues but higher specificity for histidine. The enzyme displayed maximum activity at pH 7.5, and was limited by low substrate specificity at low pH. Enzyme inhibition was poor with many of the evaluated histidine analogues, with only 5-fluorohistidine showing about 80% inhibition. Although most amino acid metabolizing enzyms are enantioselective, OvoA was found to turnover both D- and L-histidines. However, using D-histidine as substrate, two products were obtained, one corresponding to transsulfuration at C-2 and the other corresponding to transsulfuration at C-5, suggesting that the outcome of transsulfuration was dependent on the orientation of the imidazole unit in the active site in OvoA. Lack of solvent isotope effects was observed, suggesting that the transsulfuration step does not happen via acid-base proton exchange and that iron(III)-superoxide seems to be the initial oxidant that activates sulfur to attack the histidine imidazole ring. Detailed evidence for these conclusions is presented in the following discussion.

3.2. MATERIALS AND METHODS

3.2.1. Materials

All standard reagents were purchased from Aldrich/Sigma if not otherwise stated. Histidine, 4(5)-methylimidazole and ammonium sulphate were purchase from Fluka. Cysteine, Tryptophan, Imidazole, FeSO4 and NaCl were purchased from Acros Organics. Histidinamide, 2-thiohistidine, 3-pyridyl alanine, 2-pyridyl alanine, H-(3Me)-His-OH and Histidine methyl ester were purchase from Bachem. D_2O and Ni-NTA were purchased from Roth and QIAGEN, respectively. 5-fluorohistidine and 2-fluorohistidine were a generous gift from Kenneth Kirk, National Institutes of Health, DHHS, Bethesda; 5-chlorohistidine, 5-bromohistidine and 5-iodohistidine were chemically synthesized as described here in chapter 2 and experimental section.

3.2.2. Standard OvoA assay conditions

A 250 µL reaction mixture contained 2 mM TCEP, 2 mM ascorbate, 1 µM $FeSO_4$, 20 mM NaCl, 20 mM Tris-HCl buffer, pH 8.0 at 26^{o}C. Concentration of substrate and enzyme were not always the same, and these differences were recorded on figure legends in the results section. After incubation for various times as required, reactions were stopped with addition of half a volume of 1 M phosphoric acid before analysis by HPLC. For larger scale, up to 1 mL reaction was prepared with reaction components added proportionally. Substrates and reagents were all prepared in 20 mM Tris-HCl, pH 8, except for iron-ascorbate mixture which was kept at pH of about 5.5 in 20 mM Tris-HCl buffer. Tris-HCl buffer was herein referred to as Tris buffer).

3.2.3. HPLC

All HPLC analyses were performed on Shimadzu Prominence HPLC system using Luna 5µ SCX 100A cation exchange column. The system was first equilibrated with relevant buffers before injection. A volume of 20 µL sample was injected for all qualitative analyses while up to 100 µL samples were injected for larger scale. The flow rate was maintained at 1 mL/min. The ASCII files from HPLC were analyzed on Origin Pro 8 program. For qualitative measurements, products were separated on 1 mM NaCl gradient in 20 mM phosphate buffer, pH 2 (method 1), and a gradient of 500 mM ammonium formate at pH 5.5 was used to separate products for further characterization. For identification purposes HPLC was run using ammonium formate based buffers in method 2 amd method 3. Method 2: samples were analysed with 10% gradient of 10 mM ammonium formate to 500mM while for Method 2, samples were analysed with 25% gradient of 10 mM ammonium formate to 500mM.

3.2.4. Product Identification

OvoA reaction mixtures were separated by HPLC using either HPLC method 2 or 3 (see section 3.2.3 above). Enzyme products of L-histidine, D-histidine and 2-fluorohistidine were separated using HPLC method 2 while products of histidinamide, histamine, histidine methyl ester and 4(5)-methylimidazole were separated using HPLC method 3. Products of enzyme reaction were collected from HPLC, the fractions pooled together and lyophilized. The products were re-dissolved in minimal volumes of nano pure water before being analysed by either electro-spray ionization mass spectrometry (ESI-MS), nuclear magnetic resonance (NMR), high resolution mass spectrometry (HRMS) or HPLC-Mass spectroscopy.

3.2.5. Isotope effect

Reaction mixtures, (2 x 1 mL) contained 800 µM cysteine, 800 µM histidine, 2 mM TCEP, 2 mM ascorbate, 1 µM $FeSO_4$, 20 mM NaCl and 20 mM Tris buffer. Reaction mixtures were lyophilized overnight, one was re-dissolve in 1 mL H_2O (control) and the

other in 1 mL D_2O (experimental). The samples were re-lyophilized overnight. The control sample was re-dissolved in H_2O while the experimental sample was re-dissolved in D_2O. The samples were split to make 250 µL volumes into which about 283 nM OvoA was added to start the reactions. The assays were performed in triplicates.

3.2.6. pH dependence assays

For pH dependence assays 50 mM Britton-Robinson buffer was used instead of 20 mM Tris. Assays were carried out at various pH values ranging from 5.5 to 10.0 in Britton-Robinson buffer. Substrates and reagents were prepared in 50 mM Britton-Robinson buffers at relevant pH, except for the iron-ascorbate mixture which was kept at pH of about 5.5. Britton-Robinson buffer: 50 mM H_3BO_3, 50 mM H_3PO_4, 50 mM CH_3COOH, pH adjusted with NaOH solution.

3.2.7. Inhibition

Reaction mixtures (250 µL) contained 50 µM histidine, 5 mM inhibitor, 1 mM cysteine, 2 mM TCEP, 2 mM ascorbate, 10 µM $FeSO_4$, 20 mM NaCl and 20 mM Tris-HCl, pH 7.5, 280 nM OvoA. At intervals of 1, 2, 4 and 8 minutes, 40 µL samples were quenched with 20 µL 1 M phosphoric acid solution and analyzed by HPLC method 1.

3.3. RESULTS AND DISCUSSION

3.3.1. Purification of OvoA

OvoA enzyme from *Erwinia tasmaniensis* was produced in the laboratory of Prof. Florian Seebeck using the described method (Braunshausen and Seebeck 2011). Recombinant *E. tasmaniensis* OvoA was cloned and expressed in *Escherichia coli*, BL-21 cells using IPTG induction and then purified on Ni-NTA agarose. Before use the enzyme purity was evaluated by SDS-Page with staining using Coomassie blue stain. No visible protein contaminants were observed, even in the lane where the enzyme was loaded two fold (lane A, figure 3.1). *E. tesmaniansis* OvoA is a relatively large protein, a monomer with 567 amino acids and a theoretical weight of about 85 kDa. On the basis of SDS-Page analysis, the enzyme was regarded as about 90 % homogeneous and suitable for the enzyme kinetics.

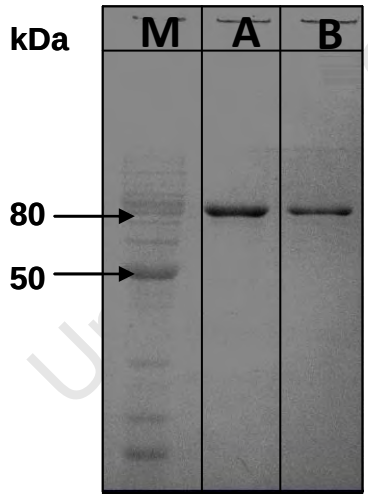

Figure 3.1: SDS-PAGE analysis of OvoA. Molecular weight marker (M), OvoA 2 x concentrated (A), OvoA 1x concentrated (B)

3.3.2. Characterization of OvoA

3.3.2.1. OvoA assay optimization

3.3.2.1.1. OvoA assay and product identification

OvoA was assayed according to the method described in the methods section with cysteine and histidine at 1000 μM concentration. HPLC analysis of the assay mixture after three hours of incubation led to identification of a new peak with a retention time of about 3.2 minutes (figure 3.2). The new product had absorption at both 220 nm and 254 nm, while the histidine substrate did not absorb at 254 nm. The product peak was well resolved from both ascorbate and histidine peaks, which eluted at 2.1 and 5.2 minutes, respectively.

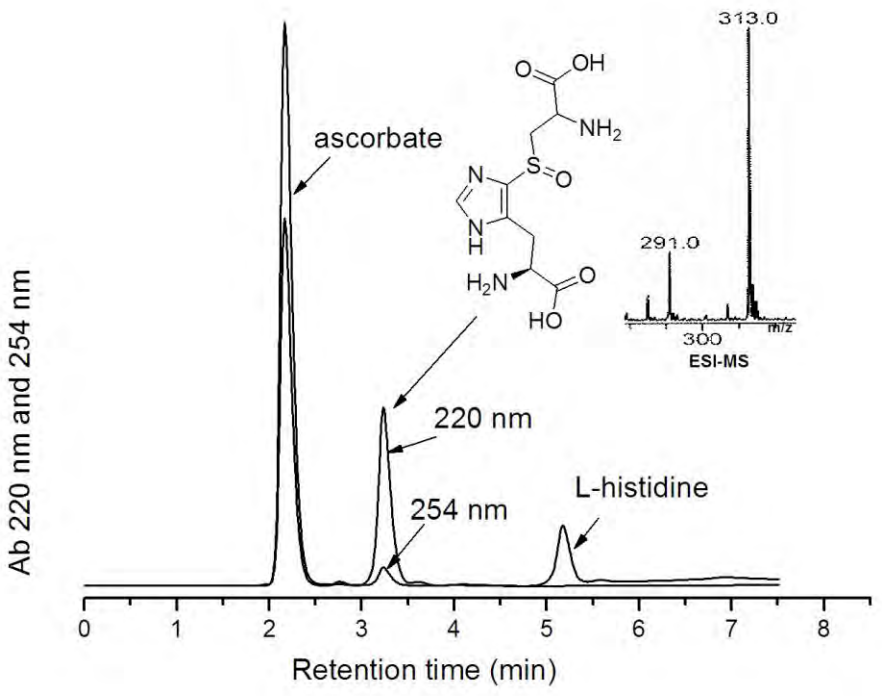

Figure 3.2: HPLC chromatogram of OvoA reaction with natural substrates. A reaction mixture containing 20 mM Tris pH 8.0, 20 mM NaCl, 2 mM TCEP, 2 mM ascorbate, 1μM $FeSO_4$, 1000 μM cysteine, 1000 μM histidine, 283 nM OvoA was incubated for three hours at 26^{o}C. About 30 μL of the reaction was quenched with addition of 15 μL before analyzed using HPLC method 1.

The product peak was collected using HPLC method 2, which utilizes ammonium formate buffer (described in section 3.2.3). After lyophilization and dissolution in nano pure water, the product was analyzed by ESI-MS, which revealed a product with m/z 291.0, corresponding to M+1 for 5-histidyl-cysteine sulfoxide. The sodium ion mass ion signal at m/z 313.0 for M+Na also provided confirmation of the identity of the product.

3.3.2.1.2. Effect of iron and ascorbate on OvoA reaction

Ascorbate is a good electron donor and is used widely in iron dependent reactions. Depending on the oxidant, ascorbate can undergo either one or two electron oxidations. One electron oxidation results in ascorbate radical while a two electron oxidation leads to the formation of a more stable form, dehydroascorbate. The ability of ascorbate to donate electrons coupled with the stability of its radical makes it a good antioxidant in biological systems. Here ascorbate was used in OvoA reaction mixture to keep iron within the enzyme in the ferrous state.

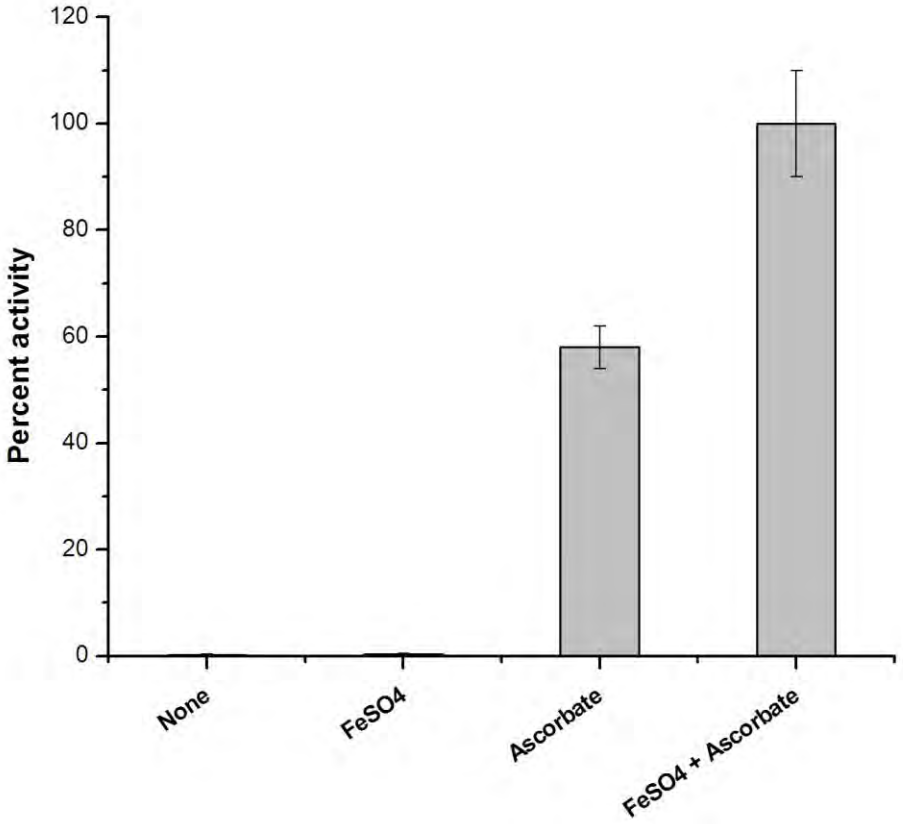

Figure 3.3: Effect of Iron and ascorbate on OvoA reaction: Reaction mixtures contained 20 mM Tris pH 8.0, 20 mM NaCl, 2 mM TCEP, 1000 μM cysteine, 1000 μM histidine, 283 nM OvoA, 1 μM $FeSO_4$ and or 2 mM ascorbate and were incubated at 26^{o}C. At intervals of 1, 2, 4 and 8 minutes, 30 μL aliquots of the reactions were quenched by addition of 15 μL 1 M phosphoric acid and analyzed using HPLC method 1.

The effect of 2 mM ascorbate on the OvoA reaction was evaluated. Our earlier study had shown that at 2 mM ascorbate, the optimal iron concentration was 1 μM (see appendix for results). Results in figure 3.3 show the importance of ascorbate as an activator of OvoA, since its omission from the reaction mixture ("None" and "$FeSO_4$") leads to very little enzyme activity even in the presence of 1 μM iron ($FeSO_4$). By adding ascorbate alone, about 60 % of the enzyme activity was restored while in the presence of 1 μM $FeSO_4$, ascorbate restored 100% OvoA activity. These results indicated that OvoA retained about 60% of its iron cofactor throughout the purification process but possibly in the wrong oxidation state, which then required ascorbate for re-activation. However it could not be ruled out that activation of OvoA by ascorbate was a result of possible direct binding to the enzyme or ascorbate being utilized by OvoA as one of its substrates. For

example ascorbate was found to bind into the active site of ACC oxidase, a nonheme iron containing enzyme that mediates the last step in biosynthesis of ethylene, a plant hormone. (Thrower et al, 2001). Since ascorbate is a chiral molecule, its binding to OvoA could be strictly stereo-selective. With this in mind OvoA was assayed with isoascorbate, the enantiomer of ascorbate to investigate if OvoA could differentiate between the isomers.

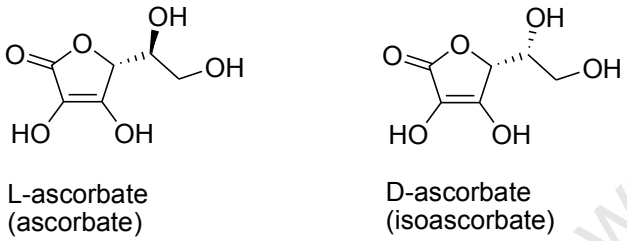

Figure 3.4: Chemical structures of ascorbate and isoascorbate

The results showed that OvoA did not differentiate between ascorbate and isoascorbate because the same reaction rates were obtained when OvoA was assayed in the presence of the two compounds (see appendix). Flashman et al. (2010), showed that isoascorbate could activate prolyl hydrolase, a nonheme iron enzyme, to the same extent as did L-ascorbate. Future work to investigate how OvoA is activated by the isomers of ascorbate could be fruitful: for example, crystallizing the enzyme in the presence of the compounds could lead to location of the binding site on the enzyme molecule.

3.3.2.2. Determination of kinetic constants of OvoA substrates

Having established assay conditions, the stage was set for determination of enzyme kinetics. The best assay conditions obtained were as follows: 20 mM Tris pH 8.0, 20 mM NaCl, 2 mM TCEP, 2 mM ascorbate and 1 μM $FeSO_4$ at 26^{o}C. The enzyme was therefore assayed by integration of product peaks, using a standard curve generated by allowing complete conversion of known concentrations of histidine substrate into 5-histidyl cysteine sulfoxide product (**3**, scheme 1.4) (see standard curve in appendix section).

Previous results of OvoA assays with numerous naturally occurring sulfur donors showed cysteine as the only sulfur donor (Braunshausen and Seebeck, 2011). Therefore in this study there was no further evaluation of other potential sulfur donors, and consequently this study was limited to a determination of the kinetic constants for cysteine as the sulphur donor. For the sulfur acceptor, the kinetics of histidine and other naturally occurring analogues were determined. Thus OvoA activity was assayed in the presence of various substrates using standard reaction conditions described earlier, and kinetic results shown in table 3.1 were determined using Michaelis-Menten graphs (Appendix). OvoA was characterized by a K_M value of 347 ± 27 μM for cysteine, a k_{cat} of 3.13 s^{-1} and k_{cat} / K_M of $9.02x10^3$ (Table 3.1). The enzyme had similar kinetic constants with L-histidine while displaying about 20 fold low specificity towards the D-histidine substrate. High K_M, 818 μM, showing suboptimal binding of D-histidine to the enzyme, was the probable reason for the low kinetics constant of 0.35 s^{-1} found.

Table 3.1: Michaelis-Menten kinetics of OvoA substrates

Substrate	V_{max} ($x10^{-9}$M/s)	OvoA ($x10^{-9}$ M)	K_{cat} (s^{-1})	K_M ($x10^{-6}$ M)	k_{cat}/K_M ($s^{-1}M^{-1}$)
Histidine	943 ± 45	289	3.26	339 ± 22	9617
Cysteine	920 ± 44	294	3.13	347 ± 27	9020
Histidinamide	156 ± 3	371	0.42	308 ± 27	1364
Histamine	99.9 ± 1.4	377	0.26	227 ± 6	1145
D-Histidine	121 ± 0.06	346	0.35	818 ± 12	427

Histidine analogues, histidinamide and histamine were turned over by OvoA with just 7 times less efficiency than L-histidine and cysteine, with specificity constants of 1364 $s^{-1}M^{-1}$ and 1145 $s^{-1}M^{-1}$, respectively. Although histidinamide and histamine also bear an imidazole ring, the kinetic constants were influenced by structural changes in the side chain, presumably the loss of the negative charge on the carboxyl group. The result with D-histidine also shows that the specificity of the enzyme is determined not only by the imidazole ring.

3.3.2.3. Effect of pH on OvoA reaction with histidine substrates

pH plays an important role in biological systems including enzyme catalyzed reactions. The ionization state of substrates and amino groups in the active site of enzymes can influence the kinetic parameters of the enzymes. Histidine and cysteine, natural substrates of OvoA, also contain ionizable side chains, the ionization of which affects their turnover. The enzyme also contains two histidine residues in the active site involved in iron metal coordination in what is referred to as a 2-His-1-carboxylate facial triad.

The effect of pH on the OvoA reaction was determined using the Britton-Robinson buffer over a pH range of 6.0 to 8.5 under the standard reaction conditions described in the methods section. Michaelis-Menten graphs were used to determine the kinetic constants. At low pH, Michaelis-Menten graphs were more linear while at high pH the graphs were more hyperbolic (figure 3.5, A). Above pH 8.5 very little activity was observed.

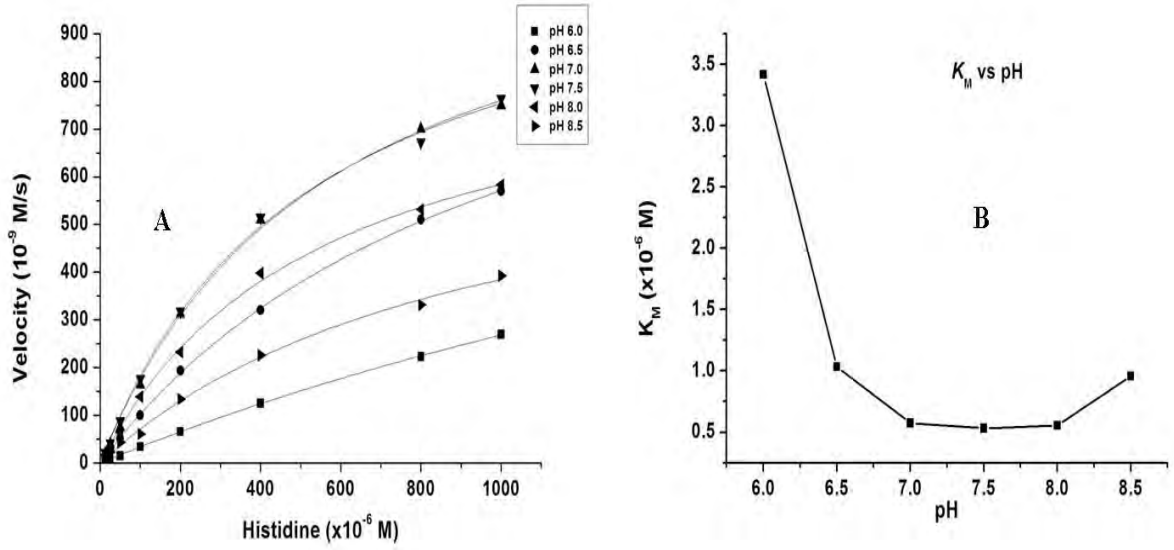

Figure 3.5: Effect of pH on histidine kinetics. 250 µL reaction mixtures at 26°C contained 800 µM cysteine, histidine (12.5 – 1000 µM), 2 mM TCEP, 2 mM ascorbate, 1 µM $FeSO_4$, 20 mM NaCl, 283 nM OvoA in 50 mM Britton-Robinson buffer at different pHs (6 – 8.5). At intervals of 1, 2, 4 and 8 minutes, 40 µL sample were quenched with 20 µL 1 M phosphoric acid solution and analyzed by HPLC using method 1. (A): Michaelis-Menten graphs and (B): K_M vs pH.

A sharp decrease in K_M from pH 6.0 to pH 6.5 as observed in figure 3.5 suggested that an ionizable group either on the substrate (possibly the histidine imidazole unit) or the enzyme significantly affected binding of substrate into the active site. Such a decrease in K_M might have also implied that the protonated histidine substrate species was not recognized as substrate by OvoA. This would follow from the fact that a reduction in pH simultaneously increased the concentration of protonated histidine species and reduced that of deprotonated species by the same amount. Investigation of the hypothesis that the observed high K_M was as a result of protonation of the histidine imidazole ring would have required utilization of histidine analogues with low imidazole p*K*a such as 2-fluorohistidine (pK_a = 1.8). However, because of limited the limited amounts of 2-fluorohistidine available, such a study could not be performed at this time.

The K_M remained unchanged between pH 7 and pH 8, implying that there was no significant acid-base ionization involving side chains in the enzyme structure or the substrates.

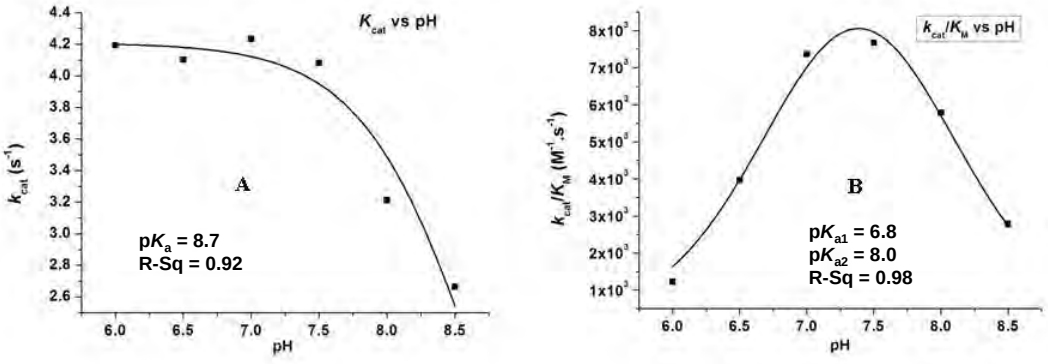

Figure 3.6: Effect of pH on histidine specificity and kinetic constant. 250 µL reaction mixtures at 26°C contained 800 µM cysteine, histidine (12.5 – 1000 µM), 2 mM TCEP, 2 mM ascorbate, 1 µM $FeSO_4$, 20 mM NaCl, 283 nM OvoA in 50 mM Britton-Robinson buffer at different pHs (6 – 8.5). At intervals of 1, 2, 4 and 8 minutes, 40 µL sample were quenched with 20 µL 1 M phosphoric acid solution and analyzed by HPLC using method 1. (A): k_{cat} vs pH, (B): k_{cat}/K_M vs pH.

The effect of pH on the specificity of OvoA towards histidine substrate was characterized by a bell a shaped curve (figure 3.6, B) with pK_as of 6.8 and 8.0 and maximum activity observed at pH 7.3 (figure 3.6). The observed pK_as indicated involvement of protonation/deprotonation of two amino acids. pK_as values of 6.8 and 8.0 corresponded to the pK_as of the histidine imidazole and cysteine sulfur, respectively, again suggesting involvement of cysteine and histidine side chains. The kinetic constant was found to be limited only at high pH with pK_a of about 8.7. At low pH the enzyme required saturating concentrations of histidine. Although the results indicated protonation/deprotonation as the probable limiting factor at high pH, binding destabilization on iron metal at high pH could not be overruled as the limiting factor.

The log k_{cat}/K_M graph assisted in the estimation of the amount of ionizable groups involved during catalysis. To the acid side from pH 7.0 to 6.0, there was a change in log k_{cat}/K_M of about 0.8 per pH unit, suggesting involvement of one ionisable group, such as the histidine imidazole. On the alkaline side, the same change of about 0.8 log k_{cat}/K_M was observed from pH 8.0 to 8.5, again implying involvement of one ionisable group, such as the cysteine side chain (figure S4, appendix).

3.3.2.4. Effect of pH on OvoA kinetics using histidinamide and histamine substrates

To investigate association of high K_M and low pH, histidinamide and histamine were used as substrate. Because of their low pKa, it was expected that at specific activity curves will shift to the left with low pK_a corresponding to the pK_a of the substrate imidazole. According to pK_a data in table 3.2, histamine and histidinamide have low pK_as.

Table 3.2: pKas of imidazole rings of histidine and some histidine analogues

	Imidazole[1]	**Histidine[1]**	**Histamine[2]**	**Histidinamide[3]**	**2-fluorohistidine[4]**
pK_a	7.0	6.2	5.0	5.3	~1

1. Giralt *et al.,* 1979, 2: Dawson *et al.,* 1959, 3: Giralt *et al.,* 1985, 4: Wimalasena *et al.,* 2007.

Thus the optimal pH for OvoA reaction with histidinamide and histamine as sulfur acceptors was determined using 1 mM concentrations for all the substrates and specific activities were obtained.

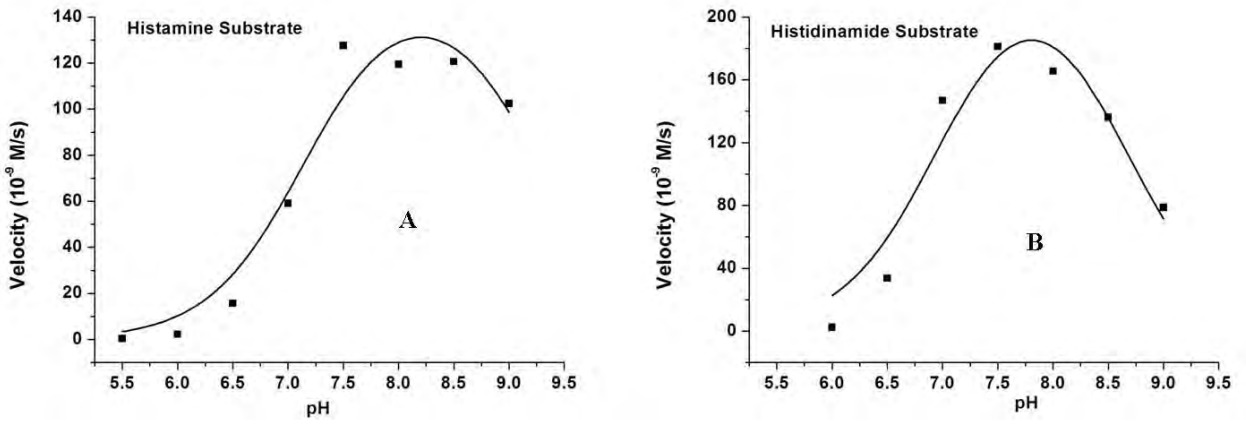

Figure 3.7: Michaelis-Menten graph of OvoA with histidinamide substrate. Reaction mixtures containing 20 mM Tris pH 8.0, 20 mM NaCl, 2 mM TCEP, 2 mM ascorbate, 1 µM $FeSO_4$, 800 µM cysteine, histamine or histidinamide (25 – 2000 µM) and 371 nM OvoA were incubated at 26°C. After intervals of 2, 4, 8 and 16 minutes, 30 µL aliquots of the reactions were quenched by addition of 15 µL 1 M phosphoric acid and analyzed for the formation of 5-histidinamidal cysteine sulfoxide using HPLC method 1. Data plotted here were averages of two determinants.

For these analogues, OvoA shows maximum activity at similar pH of 7.8 and 8.0 for histidinamide and histamine, respectively. Unexpectedly, the analogues showed higher p*K*as than those obtained with histidine (figure 3.6). This phenomenon could not be explained but may be related to the lack of a carboxylic group in these substrates. Half of maximum velocities were reached at pH 7.1 and 9.3 for histamine while for histidinamide half velocities were achieved at pH 7.0 and 8.6. These unexpected results could have been caused by the different functional groups on the amino group moieties of the substrates to that of histidine. Therefore, a more accurate comparative study would be to use histidine isosteric compounds, like 2-fluorohistidine which is characterized by a very low pK_a of around 1.0 (Wimalasena *et al.,* 2007). This was again not possible in this work, due to the limited amounts of 2-fluorohistidine available.

3.3.2.5. Solvent isotope effect of OvoA reaction

A chemical isotope effect on the OvoA catalysed reaction was not observed for the OvoA-mediated transsulfuration reaction during initial characterization of the enzyme. The histidine substrate of which C-Hs had been replaced by C-Ds was found to be used at

a similar rate to normal histidine by OvoA (Braunshausen and Seebeck, 2011). Here the solvent isotope was investigated to establish whether proton exchange was the rate limiting step in transsulfuration reaction. Two reactions were performed in duplicates, one using D_2O while the other reaction used H_2O as liquid medium. The reaction rates of 16 µM/min in D_2O and 19 µM/min in H_2O were obtained (figure 3.8). This solvent isotope effect of 1.2 is not considered significant, suggesting that hydrogen exchange was not the rate limiting step.

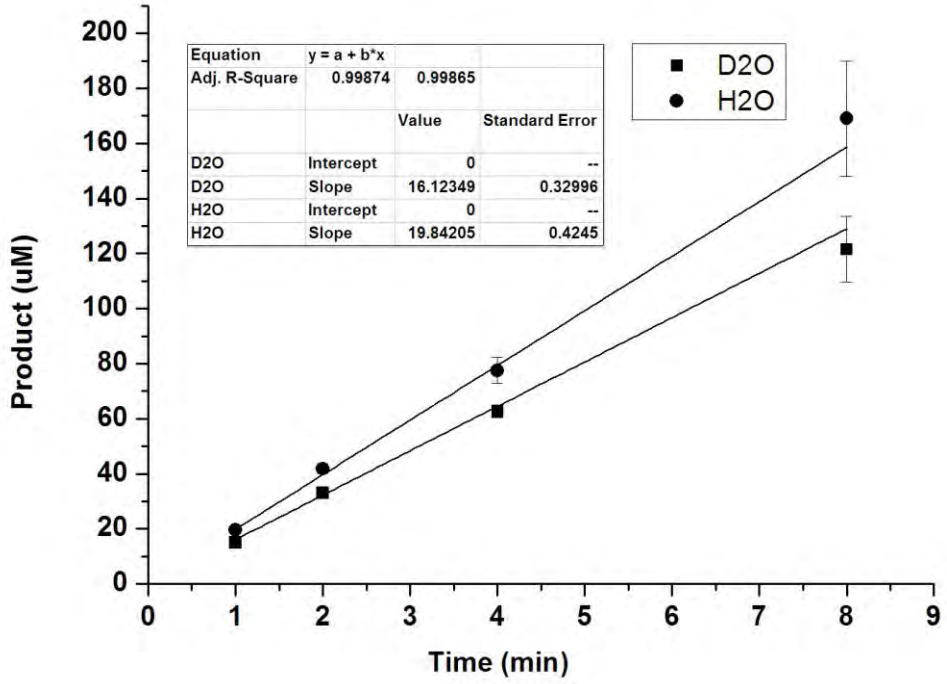

Figure 3.8: Isotope effect on OvoA reaction. Reaction mixtures (250 µL) containing 800 µM cysteine, 800 µM histidine, 2 mM TCEP, 2 mM ascorbate, 1 µM $FeSO_4$, 20 mM NaCl, 283 nM OvoA in 20 mM Tris buffer, pH 8.0 were incubated at 26°C. One reaction was performed in H_2O (control) and the other took place in D_2O (experimental), as described in materials and methods. The results were averages of three determinants.

3.3.2.6. Inhibition of OvoA by histidine and imidazole analogues

Different histidine structural analogues were then tested as potential inhibitors of OvoA. Some of the compounds were commercially sourced while others were chemically synthesized (as described in Chapter 2 and the experimental section). Some of these compounds bore modifications on the amino acid while others contained modifications on the imidazole side chain. Also included were structures lacking the amino acid moiety, and those that had imidazole replaced by pyridyl rings.

Inhibition assays were performed using standard reaction condition with 50 μM histidine at pH 7.5. Inhibitor concentration was increased 100 fold with respect to the histidine substrate.

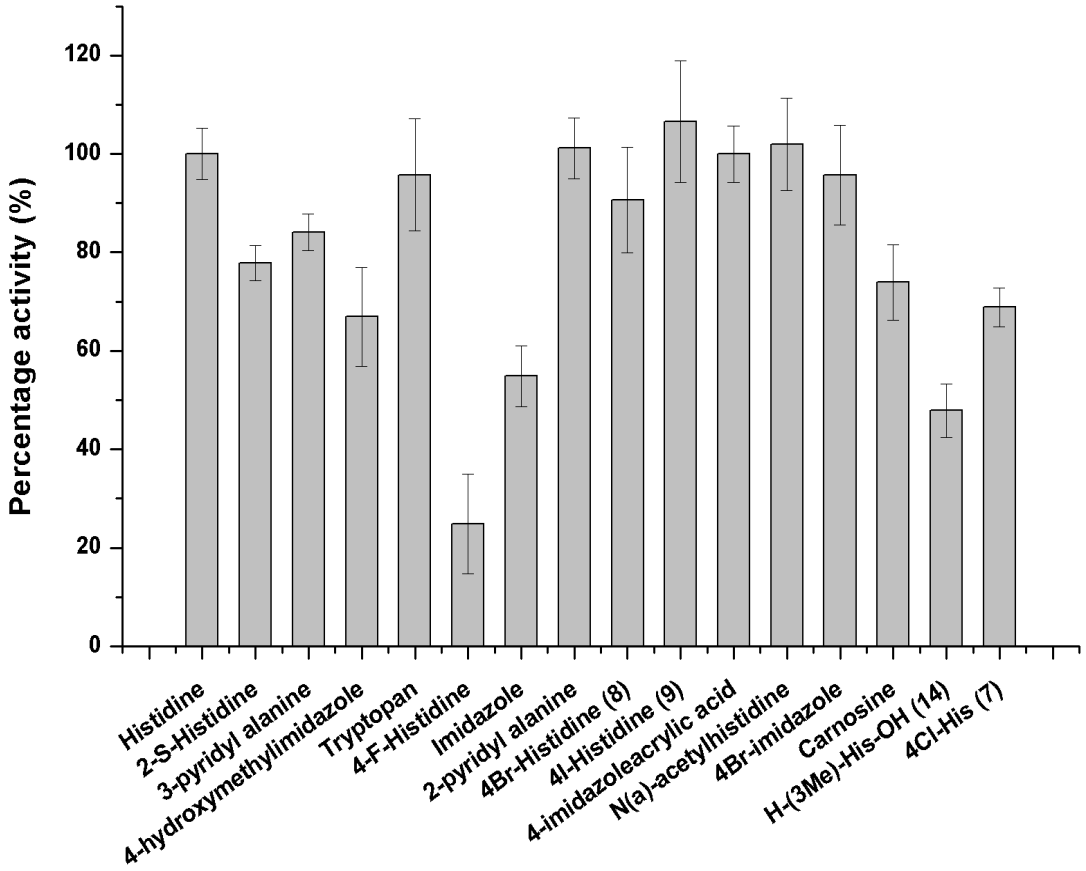

Figure 3.9: OvoA inhibition histidine structural analogues. 250 μL reaction mixtures containing 50 μM histidine, 5 mM inhibitor, 1 mM cysteine, 2 mM TCEP, 2 mM ascorbate, 10 μM $FeSO_4$, 20 mM NaCl, 20 mM Tris buffer, pH 7.5 and 280 nM OvoA were incubated at 26^{o}C. At intervals of 1, 2, 4 and 8 minutes, 40 μL sample was quenched with 20 μL 1 M phosphoric acid solution and analyzed using HPLC method 1.

Only three compounds displayed significant inhibition, *viz.* 5-fluorohistidine (80%), H-(3-Me)-his-OH (50%) and imidazole (40%). Some compounds such as carnosine, 4-chlorohistidine and hydroxymethylimidazole exhibited very mild inhibition of about 30% while most compounds did not show inhibition (figure 3.9). An important observation was the significant inhibition of the enzyme by 4-fluorohistidine. The data indicated that modification of the imidazole ring by the larger halogens iodine, bromine and chlorine abolished inhibitory effect observed with 4-fluorohistidine. These large halogens possibly contributed to very limited interaction of the imidazolyl compound with the enzyme due to steric hindrance.

Although OvoA accepted α-N-methylated histidine as substrate (figure 3.20), the enzyme did not turnover nor was inhibited by α-N-acetylhistidine. There seemed to be a slight activation of OvoA by 5-iodohistidine, though the presence of traces of histidine contaminants may have accounted for this. 2, 5-diiodohistidine was found to be unstable in the presence of TCEP, with removal of iodine seemed to be occurring (results not shown).

3.3.2.7. Evaluation of histidine analogues as OvoA substrates

Although OvoA was found to have high selectivity towards a sulfur donor, the enzyme was however found to be promiscuous when it came to sulfur acceptors. In addition to histidine, α-N-methylhistidine and α-N,N,-dimethylhistidine were also found to be OvoA substrates (Braunshausen and Seebeck, 2011). Therefore a further range of naturally occurring and chemically synthesized histidine analogues were evaluated as sulfur acceptors in OvoA reaction.

3.3.2.7.1. D-histidine

D- and L-histidines are enantiomers. Evaluation of D-histidine as an OvoA substrate was crucial as it would provide valuable information about the orientation of the amino acid in the active site. Analysis of the OvoA reaction mixture on HPLC showed a new peak

with retention time similar to that obtained with L-histidine. The new product had the HPLC characteristics of sulfoxide as it displayed absorption at both 220 nm and 254 nm wavelengths (figure 3.10).

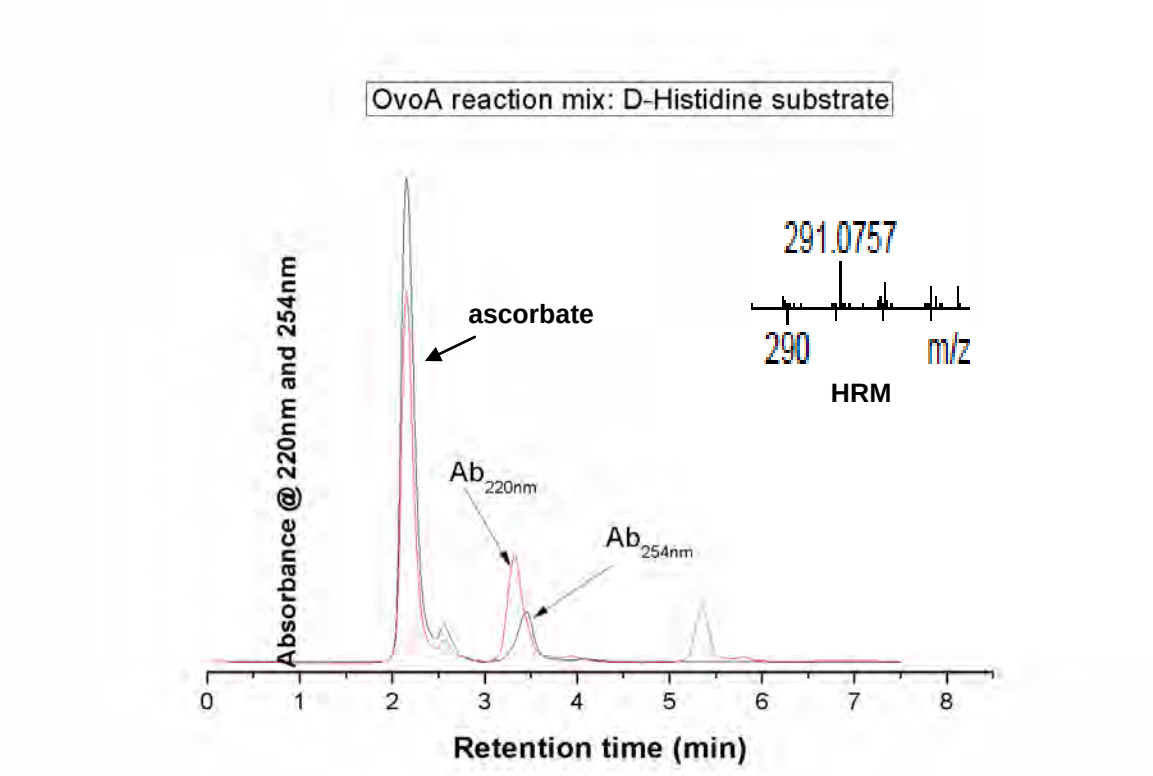

Figure 3.10: HPLC chromatogram of OvoA reaction with D-histidine substrates. A reaction mixture containined 20 mM Tris pH 8.0, 20 mM NaCl, 2 mM TCEP, 2 mM ascorbate, 1 µM FeSO4, 1000 µM cysteine, 1000 µM D-histidine and 283 nM OvoA. After overnight reaction (about 16 hours) 40 µL reaction mixture was quenched with 20 µL 1 M phosphoric acid solution and analyzed using HPLC method 1. Insert shows mass of new product as determined by ESI-MS.

Analysis of the new peak by high resolution mass spectroscopy after separation using HPLC method 2 produced a component with mass 291.0757 which corresponded with M+H of the D-histidine-5-sulfoxide (figure 3.10). On closer inspection it was noted that the product peak of D-histidine had a stronger absorption at 254 nm than that of L-histidine in figure 3.2. Further analysis of the product using NMR revealed that it was a mixture of 37% 2-histidyl cysteine sulfoxide and 63 % 5-histidyl cysteine sulfoxide (figure 3.11).

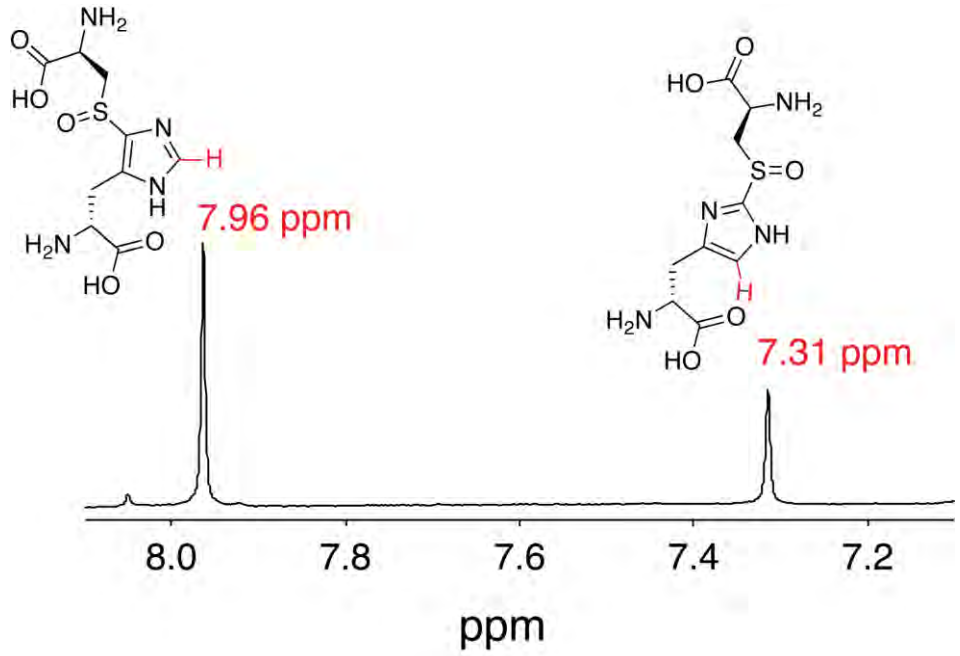

Figure 3.11: NMR of OvoA reaction product with D-histidine.

Therefore, the high absorbance at 254 nm was associated with sulfoxidation at the C-2 position, and this was used as another distinguishing feature of the position of transsulfuration when other histidine analogues were tested. More work comparing D- and L-histidine reactions was carried out and the results are discussed in a separate section (section 3.3.2.7.10).

3.3.2.7.2. 2-fluorohistidine

Substitution of a hydrogen by a fluorine on a carbon atom of an organic molecules leads to changes in electronic properties. Due to its high electronegativity, fluorine withdraws bonding electrons from carbon making it electron deficient. The presence of fluorine in 2-fluorohistidine reduces the pK_a of the imidazole from about 6.2 to around 1.0 (Wimalasena *et al.,* 2007) making the nitrogen less reactive than in normal histidine. Evaluation of 2-fluorohistidine as an OvoA substrate would therefore provide some insights on the interaction of the histidine imidazole with the iron metal cofactor of OvoA. Using HPLC method 4, analysis of the OvoA reaction mixture with 2-

flourohistidine as sulfur acceptor produced a new peak with a retention time of 4.8 minutes. Using the same method, analysis of the OvoA reaction mixture containing both 2-fluorohistidine and histidine in the same reaction mixture as sulfur acceptors lead to appearance of two well separated product peaks, a peak for 2-flourohistidyl cysteine sulfoxide at 4.8 minutes and one for 5-histidyl cysteine sulfoxide at 7.2 minutes (figure 3.12).

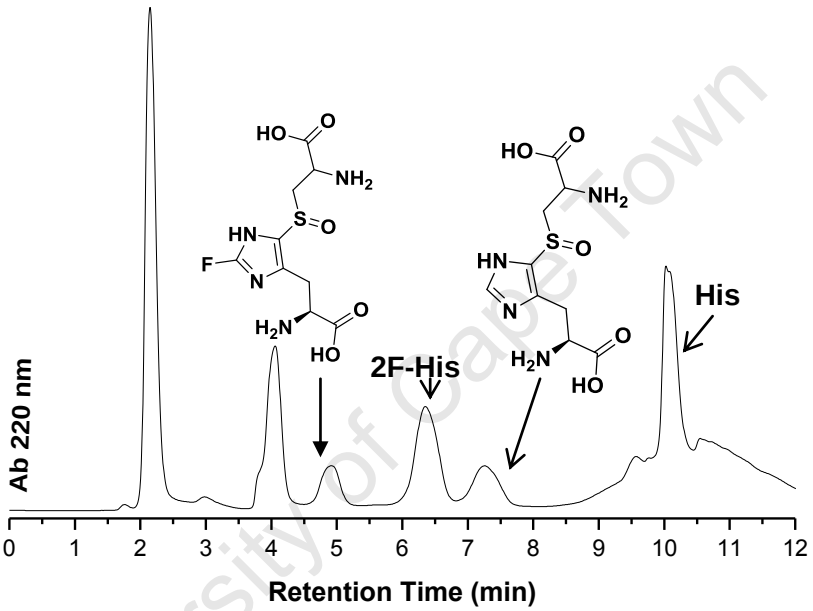

Figure 3.12: HPLC profile of OvoA reaction with 2-fluorohistidine and histidine. Reaction mixture (250 µL) contained 20 mM Tris buffer, pH 8.0, 1000 µM cysteine, 1000 µM histidine, 1000 µM 2-fluorohistidine, 2 mM TCEP, 2 mM ascorbate, 1 µM $FeSO_4$, 20 mM NaCl and 283 nM OvoA. After 16 minutes 40 µL sample was quenched with 20 µL 1 M phosphoric acid solution and analyzed using HPLC method 1.

After separation using HPLC method 2, a compound with mass 309.1 m/z was detected by ESI-MS, corresponding to M+H for 2-fluorohistidyl cysteine sulfoxide. Also found were signals at 331.1 and 353.0 indicating the presence of M+Na and M+2Na, respectively (figure 3.13).

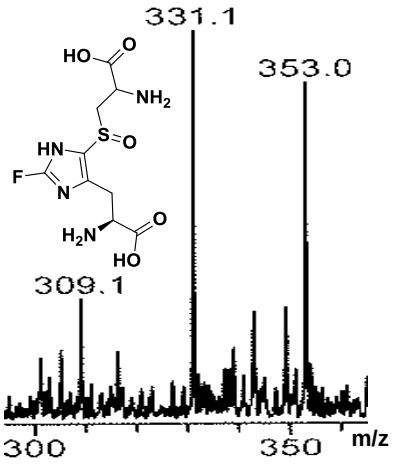

Figure 3.13: ESI spectrum of 2-fluorohistidyl cysteine sulfoxide.

The substrate specificity of OvoA toward 2-fluorohistidine was compared to that of the histidine substrate. As seen in figure 3.14, the enzyme turned over 2-fluorohistidine at a similar rate to histidine, with rates of 10.2 μM/min and 9.5 μM/min observed, respectively. However, due to lack of sufficient quantities of 2-fluorohistidine, no kinetic constants were determined.

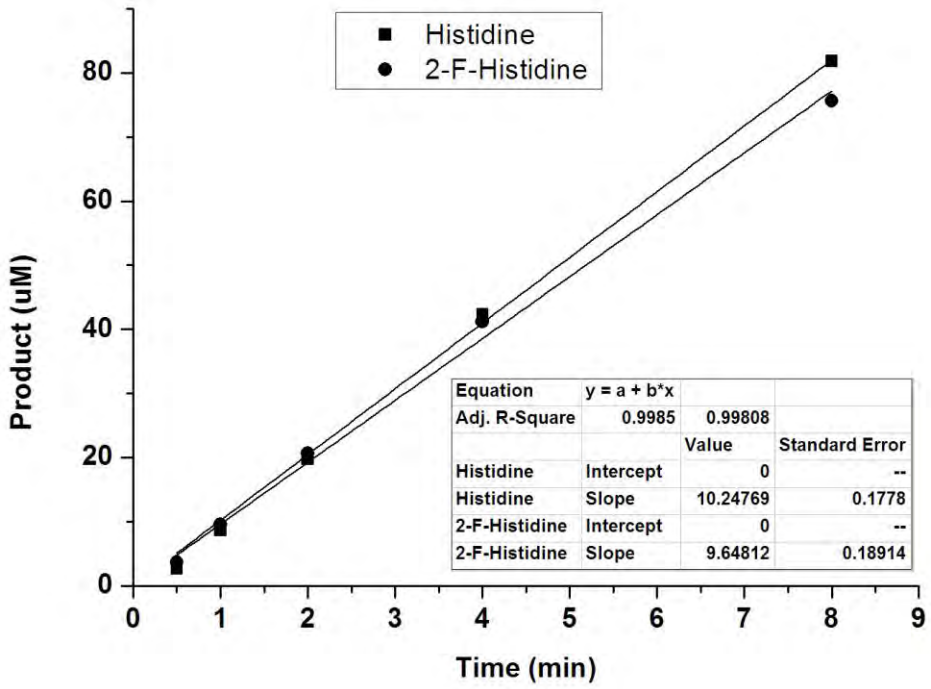

Figure 3.14: OvoA reaction; comparison of L-histidine and 2-Fluoro-L-histidine. 250 µL reaction mixtures incubated at 26°C, contained 20 mM Tris buffer, pH 8.0, 1000 µM cysteine, 1000 µM L-histidine or 2-fluoro-L-histidine, 2 mM TCEP, 2 mM ascorbate, 1 µM $FeSO_4$, 20 mM NaCl and 283 nM OvoA. At points 1, 2, 4 and 8 minutes, 40 µL sample was quenched with 20 µL 1 M phosphoric acid solution and analyzed using HPLC method 4.

3.3.2.7.3. Histidinamide

Histidinamide is a histidine analogue with a primary amide group replacing the carboxyl group. Such a modification increases the overall charge and decreases the pK_a (table 3.2) of the molecule. Evaluation of histidinamide as sulfur acceptor in the OvoA reaction was envisaged to provide more insights into the interaction of amino acids in the enzyme active site with the amino acid moiety of sulfur acceptors.

A new peak with retention time of 4.5 minutes was detected when a standard reaction mixture containing histidinamide as sulfur acceptor was analysed on HPLC (figure 3.15).

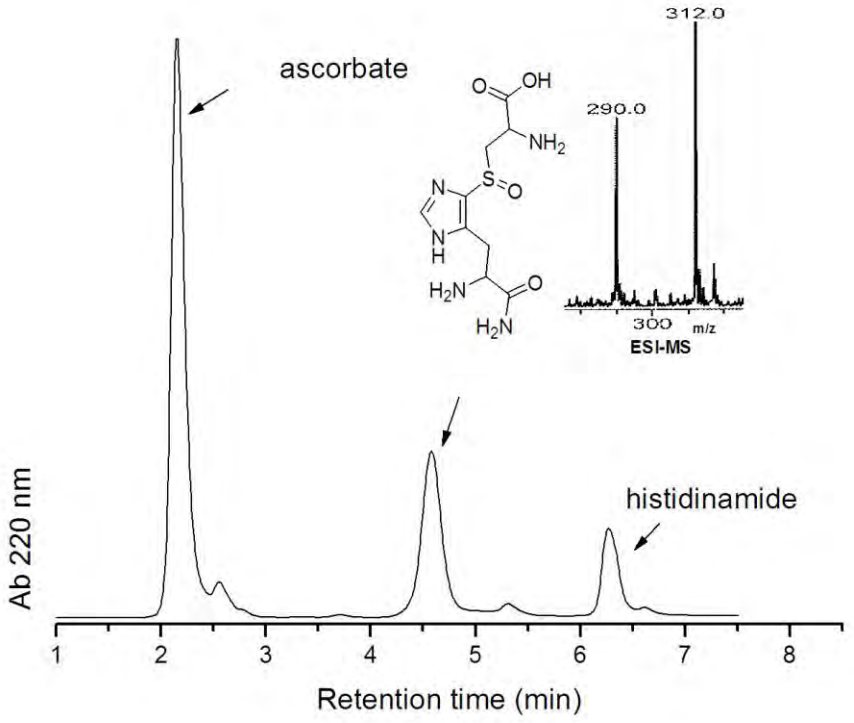

Figure 3.15: HPLC profile of OvoA reaction with histidinamide substrate. A 250 µL reaction mixture containing 20 mM Tris buffer, pH 8.0, 1000 µM cysteine, 1000 µM L-histidinamide, 2 mM TCEP, 2 mM ascorbate, 1 µM $FeSO_4$, 20 mM NaCl and 283 nM OvoA was incubated at 26^{o}C. After three hours, a 40 µL sample was quenched with 20 µL 1 M phosphoric acid solution and analyzed using HPLC method 1.

Analysis of the product by ESI-MS after separation using HPLC method 3, led to detection of a component with m/z 290.0, which corresponded with M+H for 5-histidinamidal cysteine sulfoxide. The M+Na signal was also detected at 312.0 m/z, (figure3.15).

3.3.2.7.4. Histamine

Evaluation of histamine as a sulfur acceptor in the OvoA reaction was predicted to provide information concerning the requirement and significance of the histidine carboxyl group for catalysis. The HPLC profile of three-hour OvoA reaction mixture using histamine as the substrate, showed a new peak eluting at about 5.3 minutes (figure 3.16). The peak was well resolved from the histamine starting material which eluted at about 6.7 minutes. The new peak and that of histamine appear relatively late compared to histidine and 5-histidyl cysteine sulfoxide, perhaps because of increased positive charge on histamine.

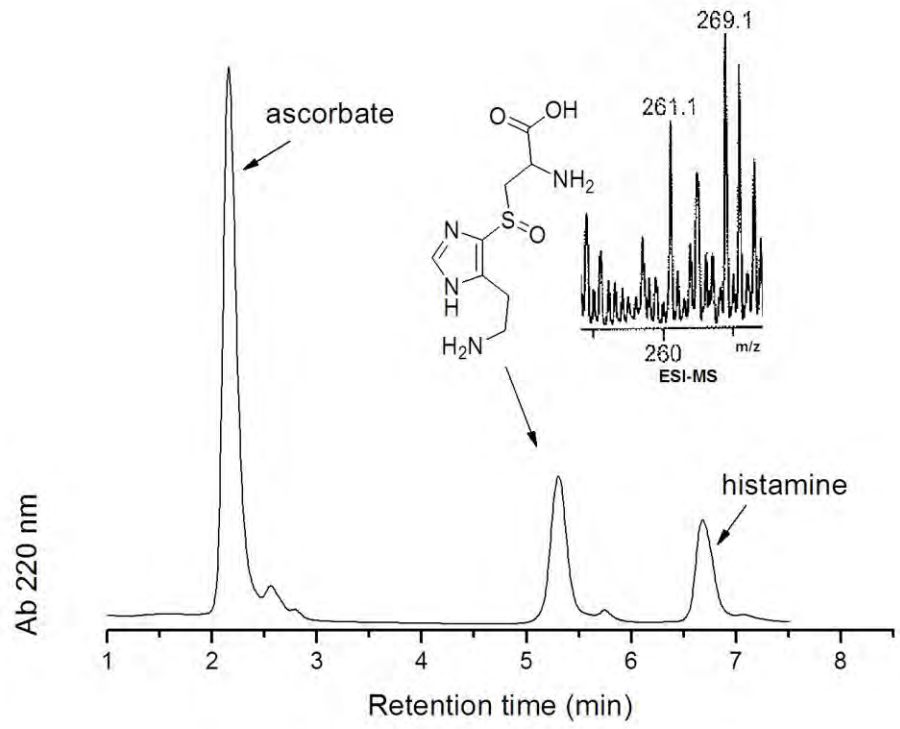

Figure 3.16: HPLC profile of OvoA reaction with histamine substrate. A 250 µL reaction mixture at 26°C contained 1000 µM cysteine, 1000 µM histamine, 2 mM TCEP, 2 mM ascorbate, 1 µM $FeSO_4$, 20 mM NaCl, 283 nM OvoA and 20 mM Tris buffer, pH. After three hours, a 40 µL sample was quenched with 20 µL 1 M phosphoric acid solution and analyzed using HPLC method 1.

The new product was isolated using HPLC method 3 and analysed by ESI-MS. The observed ion at m/z 269.1 corresponded with M+Na+H for 5-histamine cysteine sulfoxide.

3.3.2.7.5. Histidine methyl ester (HOMe)

The importance of the substrate amino acid group in the OvoA reaction was further investigated by evaluation of histidine methyl ester (His-Ome). This was envisaged to provide further insights on the effect of less reactive hydrophobic methyl ester on substrate OvoA reaction. Analysis of the OvoA reaction mixture with histidine methyl ester using HPLC method 1 revealed the presence of two new peaks. The first peak eluted at 3.5 minutes while the second one eluted at 5.5 minutes (figure 3.17). The peak at 3.5 minutes was later found to be due to 5-histidyl cysteine sulfoxide that could have resulted from histidine contamination, although HPLC analysis of the His-Ome alone did not show histidine contamination (data not shown). This suggests that histidine may have been produced enzymatically *in situ* from histidine methyl ester.

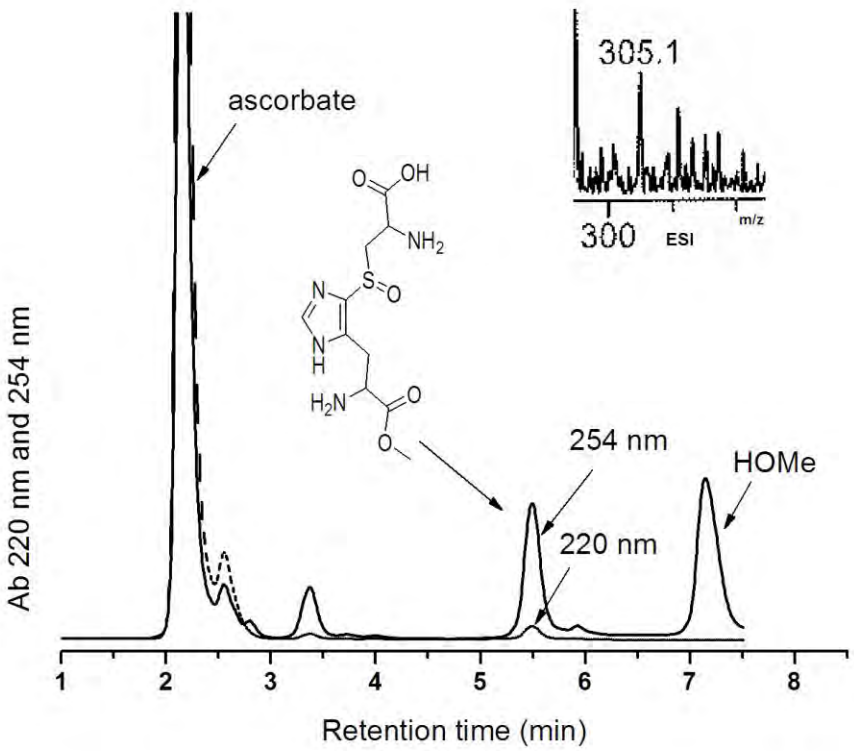

Figure 3.17: OvoA reaction with L-histidine methyl ester substrate. A 250 µL reaction mixture contained 1000 µM cysteine, 1000 µM L-histidine methyl ester, 2 mM TCEP, 2 mM ascorbate, 1 µM $FeSO_4$, 20 mM NaCl and 283 nM OvoA wt, 20 mM Tris buffer. After three hours, a 40 µL sample was quenched with 20 µL 1 M phosphoric acid solution and analyzed using method 1. Dashed line: Ab 220 nm and solid line: Ab 254 nm.

Analysis of the peak eluting at 5.4 minutes by ESI-MS revealed an ion at m/z 305 corresponding to HOMe cysteine sulfoxide (figure 3.17). However, because of an apparent competing reaction with the histidine contaminant noted above, no kinetic constants were determined for HOMe substrate. Further studies using more stable histidine esters such as ethyl ester could be fruitful.

3.3.2.7.6. 4(5)-Methylimidazole

Evaluation of 4(5)-methylimidazole as sulfur acceptor in OvoA reaction was imperative as it would provide crucial information about requirement with regard to the imidazole amino groups in histidine for catalysis. HPLC analysis of the OvoA reaction using HPLC method 1 showed two new very small peaks at 4.0 minutes and 6.0 minutes (figure 3.18). The reaction mixture was analysed using HPLC method 3 which contained ammonium formate buffer, allowing for easy removal by lyophilization. However, using this method the two peaks could not be separated and were therefore collected and analyzed together. After repeated lyopholization, the residue was analysed by HPLC-mass spectroscopy and an ion at m/z 218.1 was detected, which corresponded to M+H for methylimidazole cysteine sulfoxide.

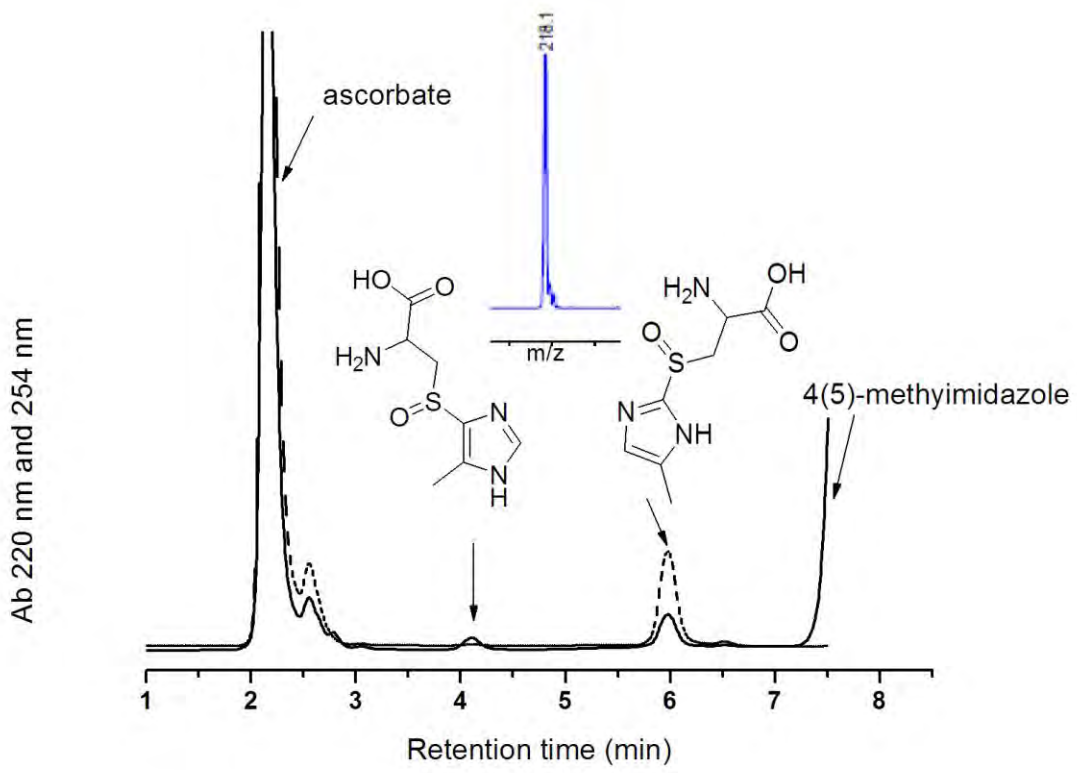

Figure 3.18: OvoA reaction with 4(5)-methylimidazole. A 250 µL reaction mixture contained 1000 µM cysteine,1000 µM 4(5)-methylimidazole, 2 mM TCEP, 2 mM ascorbate, 1 µM $FeSO_4$, 20 mM NaCl, 283 nM OvoA in 20 mM Tris buffer, pH. After three hours, a 40 µL sample was quenched with 20 µL 1 M phosphoric acid solution and analyzed by HPLC method 1. Solid: Ab 220 nm dashed line: Ab 254 nm and. The HPLC

program ended before the substrate peak had fully eluted, however no peaks were observed after the 4(5)-methylimidazole peak when the program was extended by 3 more minutes (data not shown).

The two peaks were identified as 4(5)-methylimidazole products having the sulfoxide moiety at different positions on the imidazole ring, one with a C-2 sulfoxide (rt: 4.1 min and the other having the sulfoxide at the C-5 position on imidazole. This conclusion was based on the previous observation (figure 3.10) that sulfoxidation at C-2 produced a product that absorbs more strongly at 254 nm than the product with the C-5 sulfoxide. As seen in figure 3.18, the enzyme turned over 4(5)-methylimidazole to make more of C-2 sulfoxide intermediate (dashed line, figure 3.18) than the C-5 sulfoxide intermediate (solid line, figure 3.18).

3.3.2.7.7. α-N-methyl histidines

From the previous observations in this study, it became apparent that the amino group of histidine was not required for OvoA catalytic transsulfuration and formation of sulfoxide. Ovothiol A, B and C are mercaptohistidine derivatives differing only in the extent of methylation at the α-amino group. Ovothiol A lacks methylation while ovothiol B and ovothiol C contain one and two methyl groups, respectively. It is not clear whether methylation at the amino acid happens before or after the transsulfuration step. Therefore evaluation of α-amino methylated histidine derivatives as sulfur acceptors in the OvoA reaction would provide significant insights. When the reaction mixture from the OvoA reaction using α-N-methyl histidine as sulfur acceptor substrate was analysed using HPLC method 1, two new peaks were detected (figure 3.19).

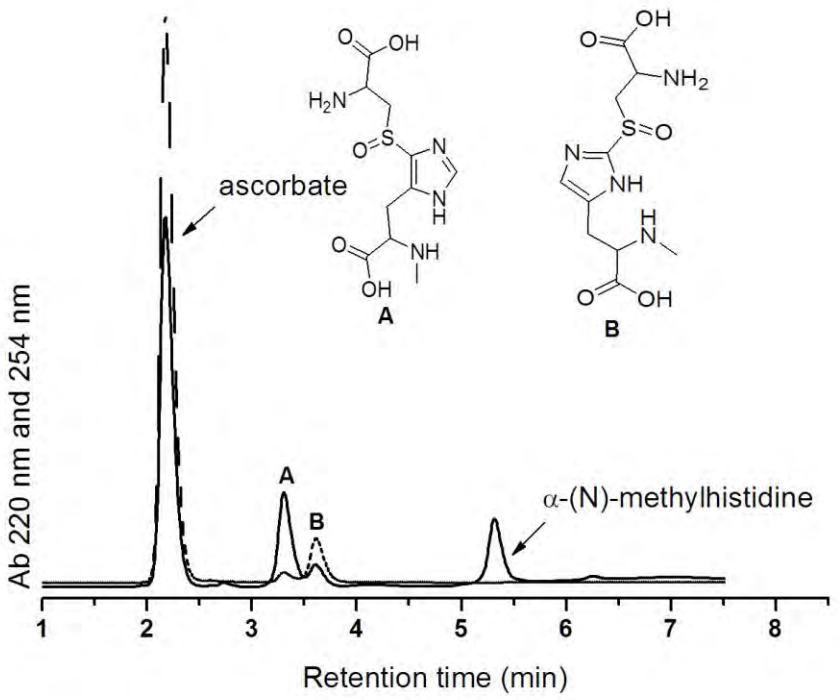

Figure 3.19: OvoA reaction with α-N-methylhistidine. A 250 µL reaction mixture at 26°C contained 1000 µM cysteine,1000 µM α-N-methylhistidine, 2 mM TCEP, 2 mM ascorbate, 1 µM FeSO4, 20 mM NaCl, 283 nM OvoA and 20 mM Tris buffer, pH 8.0. After overnight, a 40 µL sample was quenched with 20 µL 1 M phosphoric acid solution and analyzed by HPLC method 1. Solid line: Ab 220 nm, dashed line: Ab 254 nm.

Again, as shown in figures 3.10 and 3.18, difference in absorption characteristics at 254 nm was used to identify the two products, with the C-2 sulfoxide eluting at 3.3 minutes followed by the C-5 intermediate at 3.6 minutes (figure 3. 19). The results also confirmed earlier observations made by Braunshausen and Seebeck, 2011 that OvoA utilizes α-N-methylhistidine as an alternative substrate.

3.3.2.7.8. α-N,N-dimethylhistidine

Analysis of the OvoA reaction mixture using α-N,N-dimethylhistidine as sulfur acceptor produced two new peaks with retention times of 4.0 minutes (B) and 4.6 minutes (A) (figure 3.20). On the basis of their absorption at 254 nm, the products were identified as before as the C-2 intermediate (A) and C-5 intermediate (B).

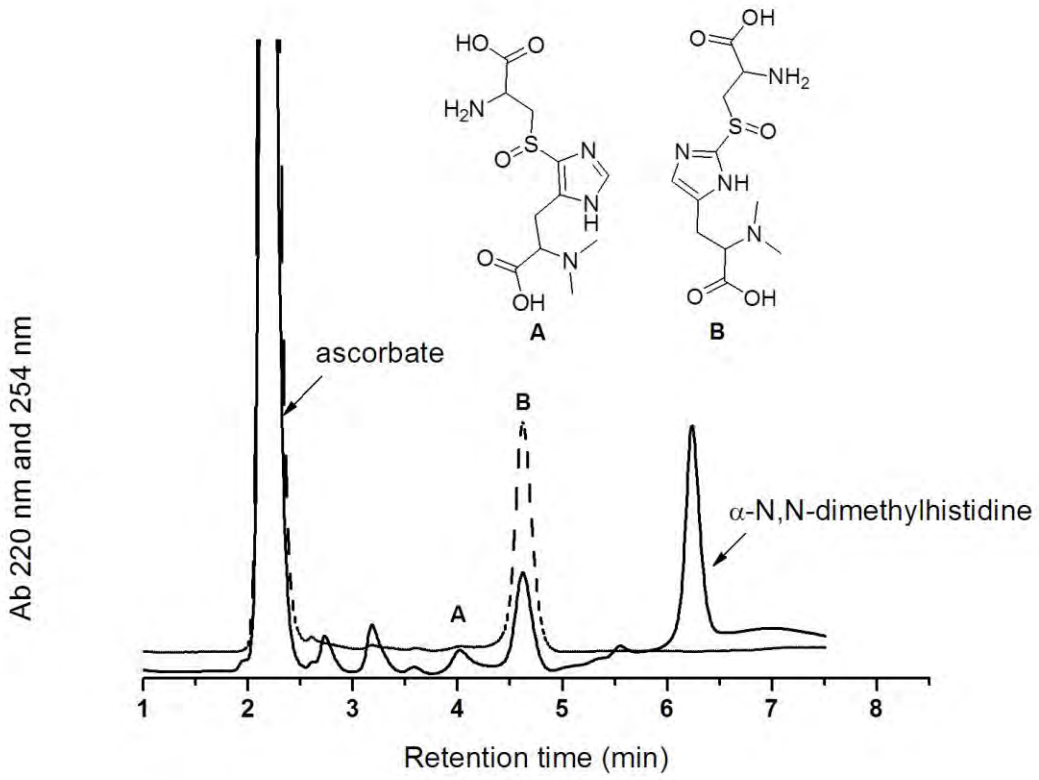

Figure 3.20: OvoA reaction with α-N,N-dimethylhistidine. A 250 µL reaction mixture at 26°C contained 1000 µM cysteine, 1000 µM α-N,N-dimtheylhistidine, 2 mM TCEP, 2 mM ascorbate, 1 µM $FeSO_4$, 20 mM NaCl, 283 nM OvoA and 20 mM Tris buffer, pH 8.0. After overnight, a 40 µL sample was quenched with 20 µL 1 M phosphoric acid solution and analyzed using HPLC method 1. Solid line: Ab 220 nm and dashed line: Ab 254 nm.

A further observation was that the C-5 sulfoxide intermediates eluted earlier than the C-2 intermediate for all products formed with histidine analogues used in this study. The utilization of α-N,N-dimethylhistidine by OvoA was first reported by Braunshausen and Seebeck, 2011, and was confirmed in the current study. This will be important because it will mean that the two enzymes mediating the last two steps in ovothiol biosynthesis also utilize α-amino methylated intermediates as substrates. Attempts were made to use a chemically- synthesized histidine betaine as sulfur acceptor without success. The reason for this failure was not apparent but poor substrate stability and high affinity of the substrate for the column were suggested as probable reasons. Continuation of this work in future will be very important in the light of possibility the OvoA could synthesis

intermediates of the ergothioneine biosynthetic pathway, a system found in different organisms.

3.3.2.7.9. Evaluation of other histidine analogues as OvoA substrates

In the quest for further potential cysteine sulfur acceptors in the OvoA reaction, more histidine analogues were evaluated (figure 3.21). Pyridylalanines in group B in figure were selected to test if OvoA could transfer sulfur onto other aromatic rings other than imidazole. Successful sulfuration of 4(5)-methylimidazole observed here, led to evaluation of other imidazole derivative in group A. Group C contained histidine analogues bearing modifications at α-amino and imidazole ring. However, none of the compounds in figure were found to be OvoA substrates as determined by HPLC analysis of their respective reaction mixtures (data not shown).

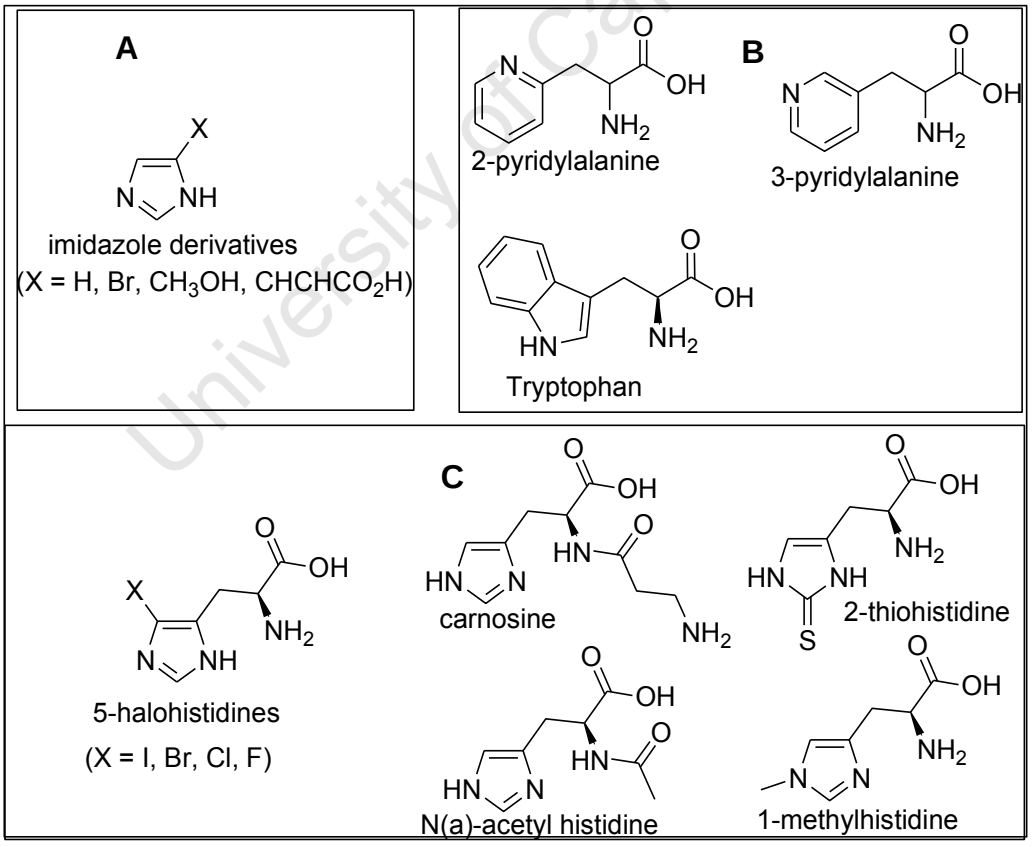

Figure 3.21: OvoA substrate specificity: A list of compounds tested as cysteine sulfur acceptors in OvoA reaction. Standard reaction mixtures contained 1 mM compound, 283 nM OvoA and 1 mM cysteine.

3.3.2.7.10. OvoA and OvoB reactions: conversion of 5-histidyl cysteine sulfoxides into 5-thiohistidines

In ovothiol biosynthesis, OvoA mediates the transsulfuration step to form 5-histidyl cysteine sulfoxide from histidine and cysteine substrates. The lysis step mediated by OvoB involves formation of 5-mercapto-histidine from the 5-histidyl cysteine sulfoxide substrate (Braunshausen and Seebeck, 2011). Reactions of OvoA and OvoB using L-histidine and D-histidine were monitored by HPLC. In the first reaction (L-His OvoA), OvoA was incubated with L-histidine until most substrate was converted to 5-histidyl cysteine sulfoxide, thereby providing substrate for the second reaction mediated by OvoB (L-His OvoB). Using HPLC method 1, the OvoA product 5-L-histidyl cysteine sulfoxide eluted at about 3.3 minutes (figure 3.22), while the OvoB product (L-His OvoB) eluted later at about 3.5 minutes. It was clear that after 10 minutes of incubation all 5-histidyl cysteine sulfoxide was consumed.

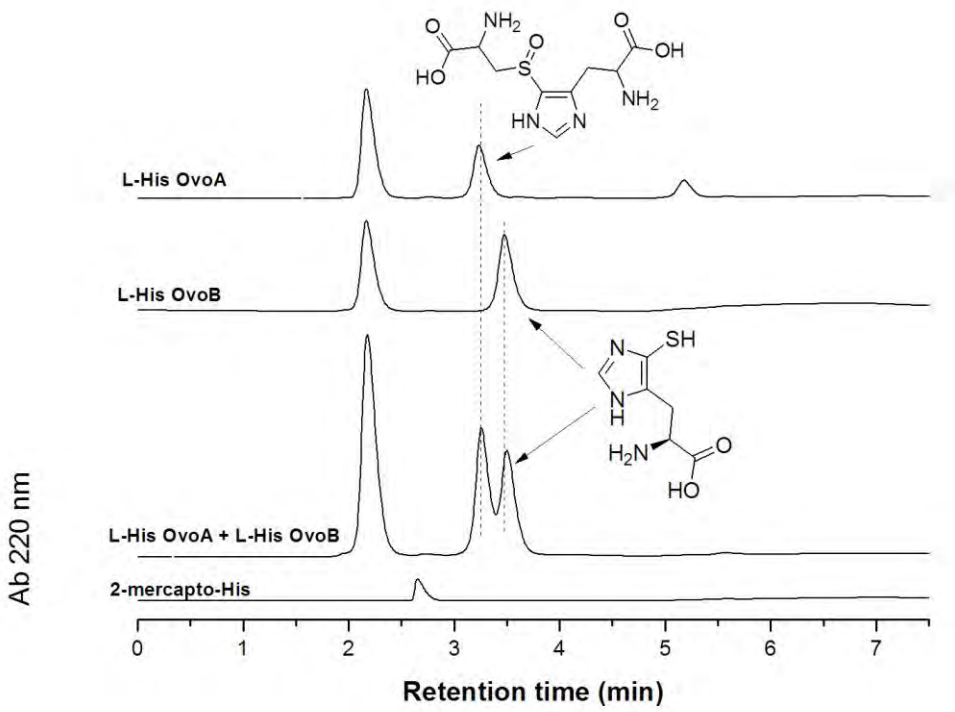

Figure 3.22: OvoA and OvoB reactions with L-Histidine: A 1 mL µL reaction mixture contained 1.2 mM cysteine, 1 mM L-histidine, 2 mM TCEP, 2 mM ascorbate, 1 µM $FeSO_4$, 20 mM NaCl and 680 nM OvoA in Tris buffer pH 8, was incubated at 26°C overnight. The reaction was split into 2 x 500 µL. OvoB was added into one sample while the other served as a control without OvoB. Reactions were incubated at 26°C for 10 min,

before 40 µL of the reactions were quenched with 20 µL 1 M phosphoric acid and analyzed using HPLC method 1.

In the next experiment, separate reaction mixtures of OvoA and OvoB which had been stopped by acid (L-His OvoA + L-His OvoB) were combined prior to injection on HPLC. The HPLC chromatogram showed two distinct overlapping peaks (L-His OvoA + L-His OvoB, figure 3.22). None of the OvoA and OvoB produced a peak that corresponded to the one produced by 2-mercapto-histidine (2-mercapto-His). This confirmed that no transsulfuration happened at C-2 when L-histidine was used as substrate. When similar experiments were performed using D-histidine as substrate, different results were obtained. The OvoA reaction mixture with D-histidine (D-His OvoA, figure 3.23) produced one broad peak eluting at about 3.3 minutes, the same elution time as the product obtained when L-histidine was used as substrate (L-His OvoA, figure 3.22). However, when OvoB was added into the OvoA reaction mixture, two distinct peaks were observed, one at 2.6 minutes and the other one at 3.5 minutes (figure 3.23).

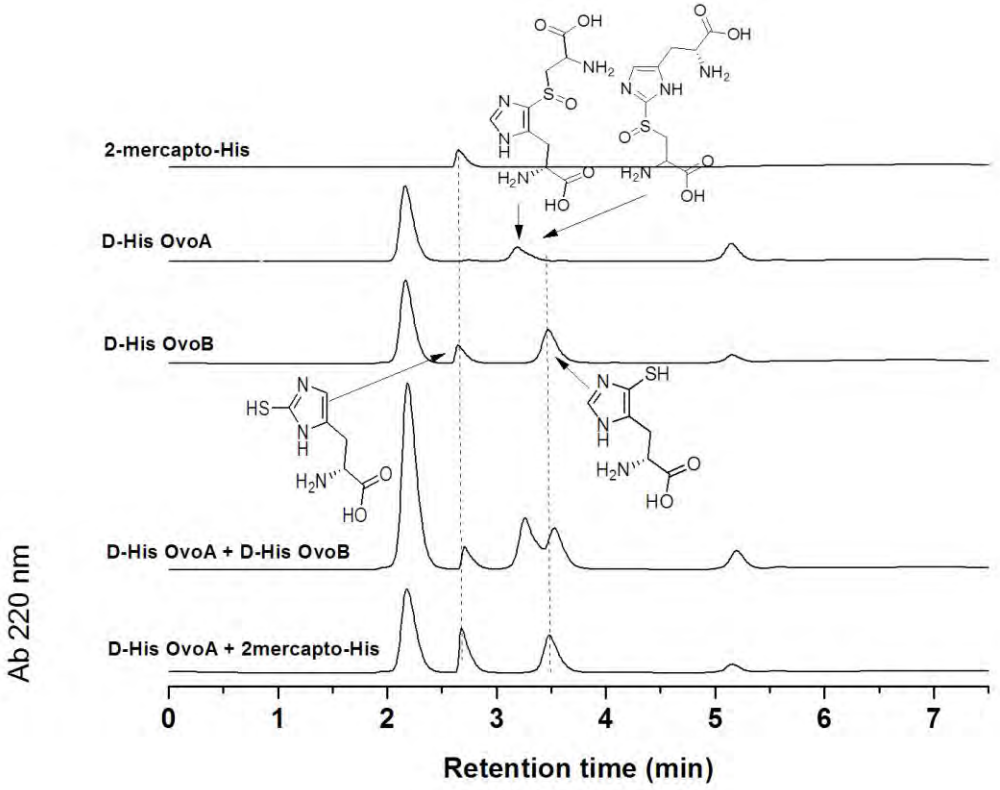

Figure 3.23: OvoA and OvoB reactions with D-Histidine: A 1 mL reaction mixture contained 1 mM cysteine, 1 mM D-histidine, 2 mM TCEP, 2 mM ascorbate, 1 µM $FeSO_4$, 20 mM NaCl and 680 nM OvoA in Tris-HCl pH 8, was incubated at 26°C overnight. The reaction was split into 2 x 500 µL. OvoB was added into one sample while the other served as a control without OvoB. Reactions were incubated at 26°C for 10 min.

The first peak at 2.6 minutes had the same retention time as 2-mercaptohistidine (2-mercapto-His) while the second peak eluted at the same time as the product produced in the reaction of OvoB with L-histidine intermediate (L-His OvoB, figure 3.22). Two distinct products were therefore produced when D-histidine was used as OvoA substrate. However, the chemical structures of the two products were so similar that they could not be separated by HPLC under conditions used here, hence the broad peak observed for the (D-His OvoA) experiment. Based on HPLC analysis, it was confirmed that OvoA mediated transsulfuration at both C-2 and C-5 of D-histidine but only at C-5 of L-histidine. Also important was the observation that OvoB was able to turn over both the C-2 and C-5 sulfoxide intermediates into their respective mercaptohistidine products. Another significant observation was the potent smell emerging from OvoB reaction mixtures, suggesting formation of thiols from 5-histidyl cysteine sulfoxide precursors.

CHAPTER 4:

EFFECT OF HALOGENATED HISTIDINES ON ERGOTHIONEINE BIOSYNTHESIS IN *MYCOBACTERIUM SMEGMATIS*

4.1 INTRODUCTION

Ergothioneine is a trimethylbetaine of 2-thio-L-histidine that was first isolated in 1909 by Tanret from ergot fungus*, Claviceps purpurea* (Tanret, 1909). Ergothioneine was found to be produced by non-yeast fungus and various Actinobacteria (Melville et al., 1956, Melville *et al*., 1957). It is widely present in vertebrates and plants where is taken up from nutrients. Ergothioneine has been found to accumulate in specific human cells and tissues such as liver, erythrocytes, lens and cornea of eyes, seminal fluid and kidney (Cheah and Halliwell, 2012). Accumulation of ergothioneine in these human cells and tissues is associated with expression of *SLC22A4* gene, which encodes a transport protein (OCTN1). This organic cation transporter has been found to be specific for ergothioneine transport across cellular membrane. At physiological conditions, ergothioneine exists as a thione form as opposed to thiol form. It has high thiol-redox potential of – 0.06 V in contrast to – 2 and – 32 V of other naturally occurring thiols and unlike glutathione, ergothioneine does not readily undergo autoxidation which can generate free radicals (Cheah and Halliwell, 2012). Physiological roles of ergothioneine are still a subject of speculations. Various functions have been attributed to ergothioneine including metal chelation, regulation of gene expression, immune regulator and antioxidant. *In vitro*, ergothioneine has been found to be a powerful scavenger of hydroxyl radicals, hypochlorous acid and peroxynitrite (Van Lear *et al*, 2013 and Cheah and Halliwell, 2012).

Genes involved in biosynthesis of ergothioneine were recently identified in *Mycobacterium smegmatis* (Seebeck *et al*, 2010). The ergothioneine biosynthesis begins with formation of histidine betaine (**84**), transulfuration at C-2 of histidine betaine using γ-glutamylcysteine as sulfur donor to form product **85**, hydrolysis of the glutamate and finally lysis of pyruvate to form ergothioneine, **87** (scheme 4.1). The key reactions were

found to be the formation of histidine betaine and transsulfuration steps (Seebeck *et al*, 2010. The transsulfuration step in ergothioneine biosynthesis is similar to that found in ovothiol biosynthesis and such a rare chemical reaction has not been found in any other biological systems. Therefore understanding the mechanism of transsulfuration step in ergothioneine might provide insights on the same reaction in ovothiol and vice versa.

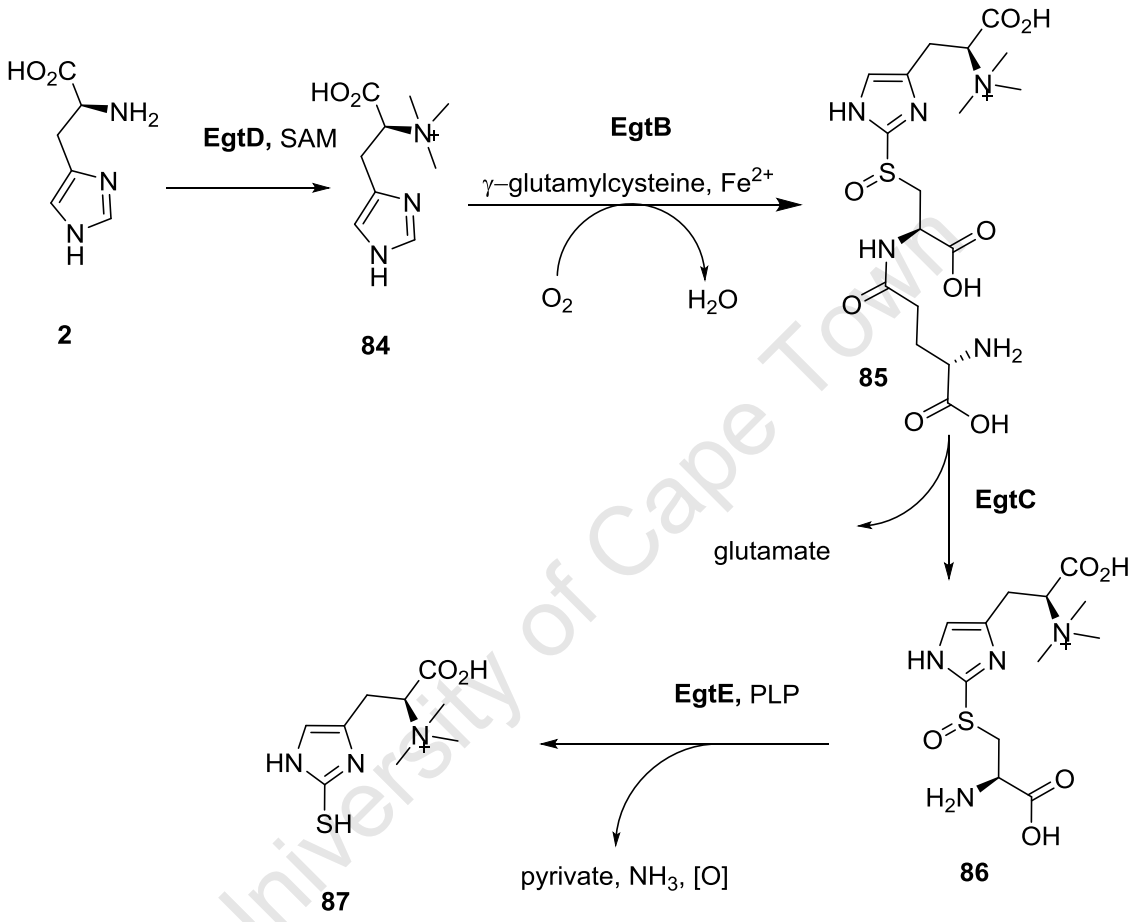

Scheme 4.1: Biosynthesis of ergothioneine (adapted form Seebeck *et al*, 2010)

On the basis of structural similarities with the betaine, halogenated histidines in figure 4.1 were envisaged as potential inhibitors of EgtB, the enzyme mediating the transsulfuration step. Fluorinated histidines were of particular interest because although the fluorine atom has almost a similar size as hydrogen, it confers different electronic properties to the molecule. The presence of fluorine at C-2 and C-5 of the imidazole ring of histidine might also shed light on the electron transfer mechanism involved in the transsulfuration reaction in ergothioneine biosynthesis as this still remains a mystery. Synthesis of these

compounds was described in other chapter 2 here, except for 2- and 5-fluorohistidine which were a gift from Prof. Kenneth Kirk.

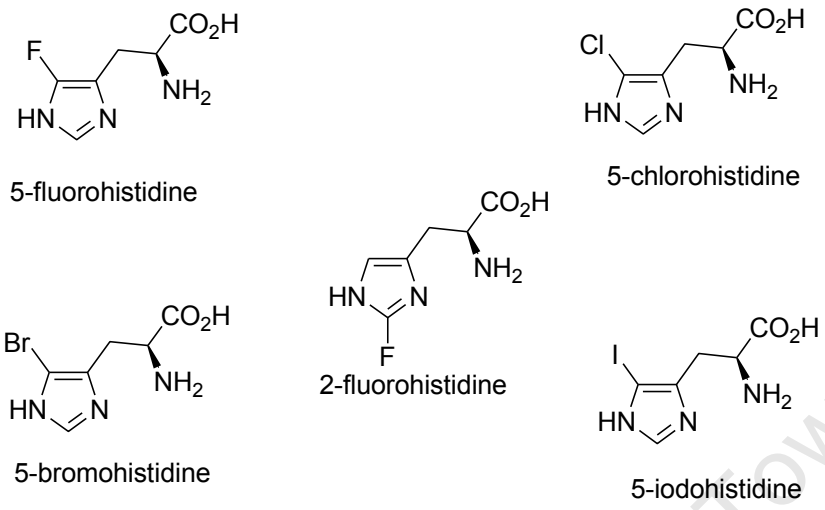

Figure 4.1: Chemical structures of halogenated histidines used in the study of ergothioneine biosynthesis

4.2. MATERIALS AND METHODS

4.2.1. Materials

All standard reagents were purchased from Aldrich/Sigma if not otherwise stated. Bacto Middlebrook was purchased from Dicfo. Perchloric acid and luna 5µ C-18 HPLC column were purchased from BDH and Phenomenex, respectively.

4.2.2. Effect of halogenated histidines on the growth of M. smegmatis

M. smegmatis cells, harvested at the late log phase, were diluted to OD of 0.1 in Bacto Middlebrook 7H9 medium pH 7.8, containing 0.05% Tween 80 and 5% glycerol as the only carbon source. The cells (20 mL) were transferred into 10 x 50 mL sterilized Erlenmeyer flasks. A 250 µL aliquot of 5-chloro, 5-bromo, 5-fluoro- and 5-Iodo-histidine solutions, which had been prepared in water, was added into the flask to achieve 250 µM final concentrations. The cultures were shaken in an incubator at 200 rpm at 37^{o}C until they reached stationary phase. The cells were harvested by centrifugation. For 2-fluorohistidine, 500 nM concentration was used as it had earlier been found that the compound was very toxic towards *M. smegmatis* cells (see section 4.2.3 and figure 4.2).

4.2.3. The growth of *M. smegmatis* in varying concentrations of 2-fluorohistidine

The *M. smegmatis* cells harvested at late log phase were diluted into the Middlebrook medium as in section 2.1 above. The cultures were grown to early exponential phase and 10 mL quantities of the cells were then transferred into 25 mL conical flasks. 2-fluoro-histidine was then added from stock solution of 20 mM in water to obtain final concentrations of 25, 50, 200 and 500 nM. Cultures lacking 2-fluorohistidine were used as controls. The flasks were incubated, with shaking at 200 rpm at 37^{o}C. The OD_{600} of the cultures were recorded at 3, 6, 9 and 12 hour.

4.2.4. Evaluation of the effect of halohistidines on ergothioneine biosynthesis in M. smegmatis and derivatization of thiols.

4.2.4.1. Treatment of *M. smegmatis* culture with halohistidine

The cells were treated and cultured as described in section 2.2. The cells, 1 mL, were harvested when they reached the early stationary phase at OD_{600} of 9.6. The harvested pellets were suspended in a 200 µL extraction buffer [acetonitrile: 0.75M perchloric acid, (2 : 1)]. The mixtures were vortexed for 3 x 20 seconds. The denatured proteins and other cellular debris were removed by centrifugation at 13200 rpm for 5 minutes at room temperature. The supernatants were transferred into new Eppendorf tubes and then centrifuged for a further 5 minutes at 13200 rpm. The supernatants (about 157 µL) were neutralized by adding13 µL of a 2 M K_2CO_3 solution. The mixtures were centrifuged to remove potassium perchlorate.

4.2.4.2. BAN derivatization of thiols

A 20 µL of 50 mM Li_2CO_3 (pH 9.0) buffer was added to 170 µL of the neutralized mixtures, followed by 10 µL of 10 mM 2-bromo-2'-acetonapthone (BAN) in acetonitrile. The reaction mixtures were allowed to react for 2 hrs at room temperature in the dark. A 100 µL quantity of the reaction mixture was diluted two-fold by addition of 100 µL 0.1% trifluoroacetic acid to lower the acetonitrile concentration to about 15% prior to analysis on HPLC.

4.2.4.3. HPLC analysis of derivatized thiols

The BAN derivatized thiols were analysed by HPLC on a Luna 5µ phenyl-hexyl column (250 x 4.60 mm) that had been equilibrated with a mixture of 95% solution A (0.1% TFA) and 5% solution B (100% acetonitrile) at a flow rate of 0.8 ml/min. The column was eluted as detailed in Table 1 below.

Table 4.1: Analysis of BAN derivatized thiols

Time (min)	0	5	10	40	45	50	55
Solution A	95%	80%	70%	20%	10%	10%	95%
Solution B	5%	20%	30%	80%	90%	90%	5%

The column effluent was monitored by measuring absorbance at 248 nm and the fractions corresponding to derivatized thiols were collected for analysis by mass spectroscopy.

4.3. RESULTS AND DISCUSSION

4.3.1. Effect of halohistidines on the growth of *M. smegmatis*

Halogenated histidine analogues have been shown to inhibit microbial growth (Howard *et al*., 1986). It was therefore crucial to look at the growth profile of *M. smegmatis* in increasing concentrations of these compounds before the study on ergothioneine biosynthesis could start. A concentration of 250 µM was found to be the most tolerable one for all the compounds except for 2-fluorohistidine. Even at 250 µM 2-fluorohistidine was found to be toxic to the cells (see figure 4.2).

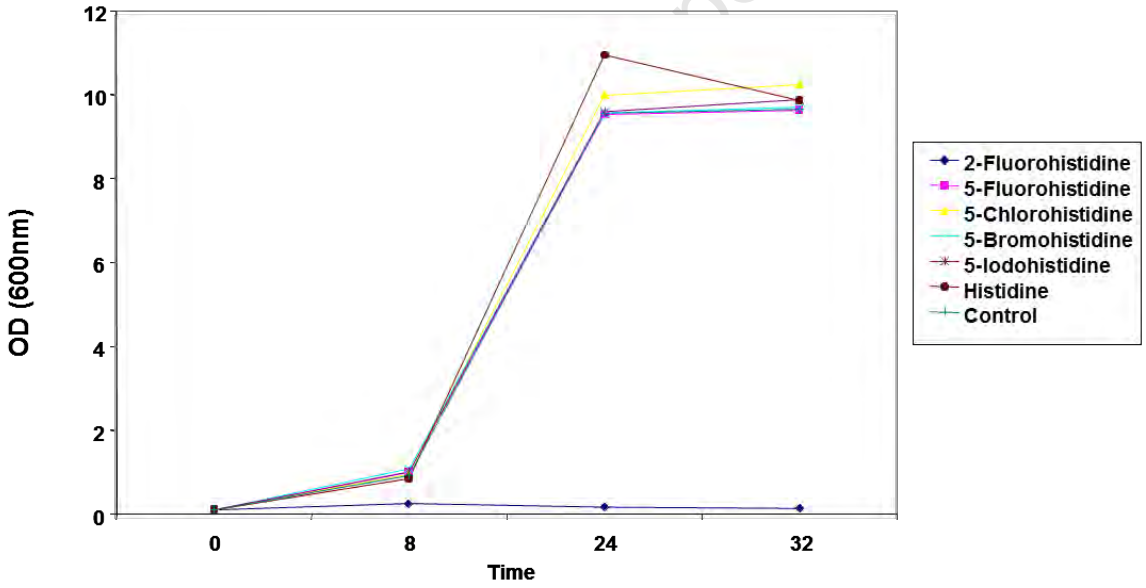

Figure 4.2: Effect of halogenated histidines (250 µM) on growth of *M smegmatis* cells.

Growth inhibition by 2-fluorohistidine was previously observed in malaria parasites (PANTON *et al*., 1988 and Howard *et al*., 1986). The growth inhibitory effect of 2-fluorohistidine could be attributed to the fact that they can be incorporated into proteins (Torrence *et al*., 1979 and Eichler *et al*., 2005). The presence of fluorine on the imidazole

ring of histidine reduces the imidazole pKa from 6.8 to ~ 1.0 (Yeh *et al*. 1975 and Wimalasena *et al.,* 2007). The reduced pKa may negatively impact on the function of the histidine imidazole side chain found in the active site of many enzymes. Although it is not clear how it inhibited growth of *M. smegmatis*, 2-fluorohistidine was found to inhibit histidine uptake in malaria parasites (Panton *et al*., 1988), and in other studies was found to be more readily incorporated into proteins than 4-fluorohistidine (Eichler *et al*., 2005).

4.3.2. Growth of *M. smegmatis* culture in varying concentrations of 2-fluorohistidine

Due to high levels of toxicity displayed by 2-fluorohistidine to *M. smegmatis* cells (figure 4.2), it was necessary to establish the sub-lethal concentrations of the compound prior to investigating its effect on ergothioneine biosynthesis. *M. smegmatis* cultures were subjected to varying concentrations of 2-fluorohistidine. At 500 nM concentrations of 2-fluorohistidine, the culture grew to just over halve the cell density of the control culture after 12 hours (figure 4.3). The subsequent studies to evaluate the effect of 2-fluorohistidine on ergothioneine biosynthesis were therefore carried out using 500 nM 2-fluorohistidine.

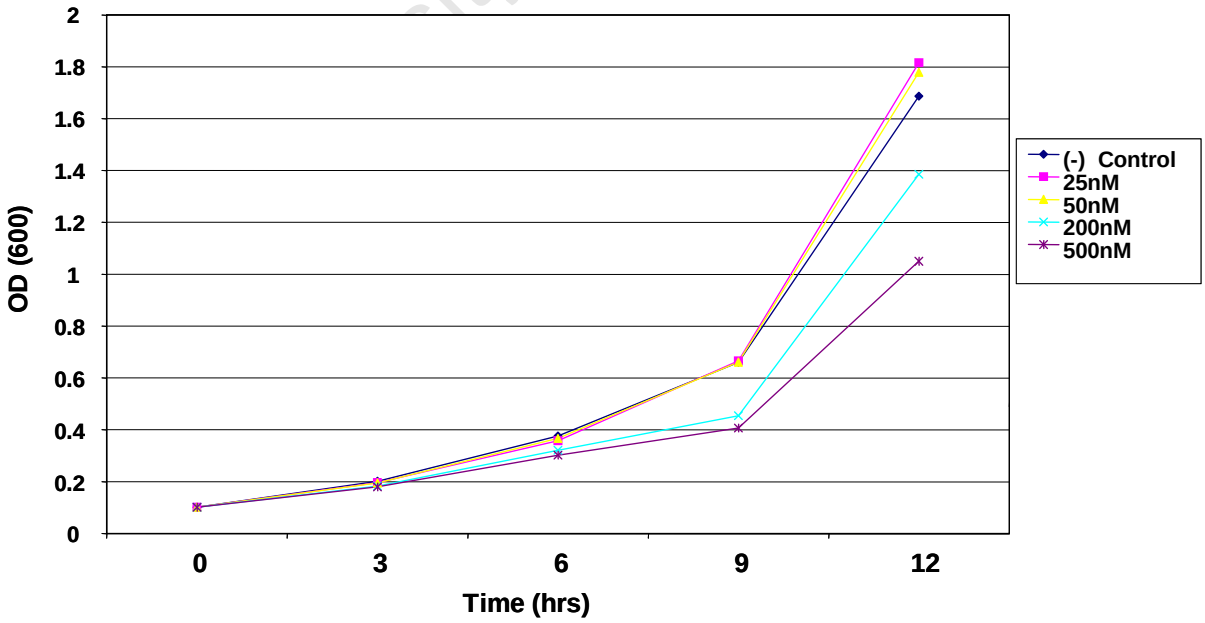

Figure 4.3: Effect of 2-fluorohistidine on growth of *M. smegmatis* cells.

4.3.3. Identification of M. smegmatis thiols by HPLC

The amounts of ergothioneine from cultures treated with halogenated histidines were compared to that of untreated cultures. *M. smegmatis* cultures were exposed to halogenated histidines at early exponential phase, and then harvested once they had reached the stationary phase. Cell-free extracts were prepared and thiols derivatized by incubation with BAN as outlined in the methods section. After 2 hours of derivatization the mixtures were analysed by HPLC at 248 nm. The mixture of BAN derivatized thiol produced well resolved peaks on HPLC, with significant components eluting at 3.84, 22.26, 23.45, 35.64 and 36.80 min (figure 4.4). The BAN reagent itself eluted at 36.80. Peaks at 3.84 22.26 and 35.64 were collected and analysed by mass spectroscopy for identification.

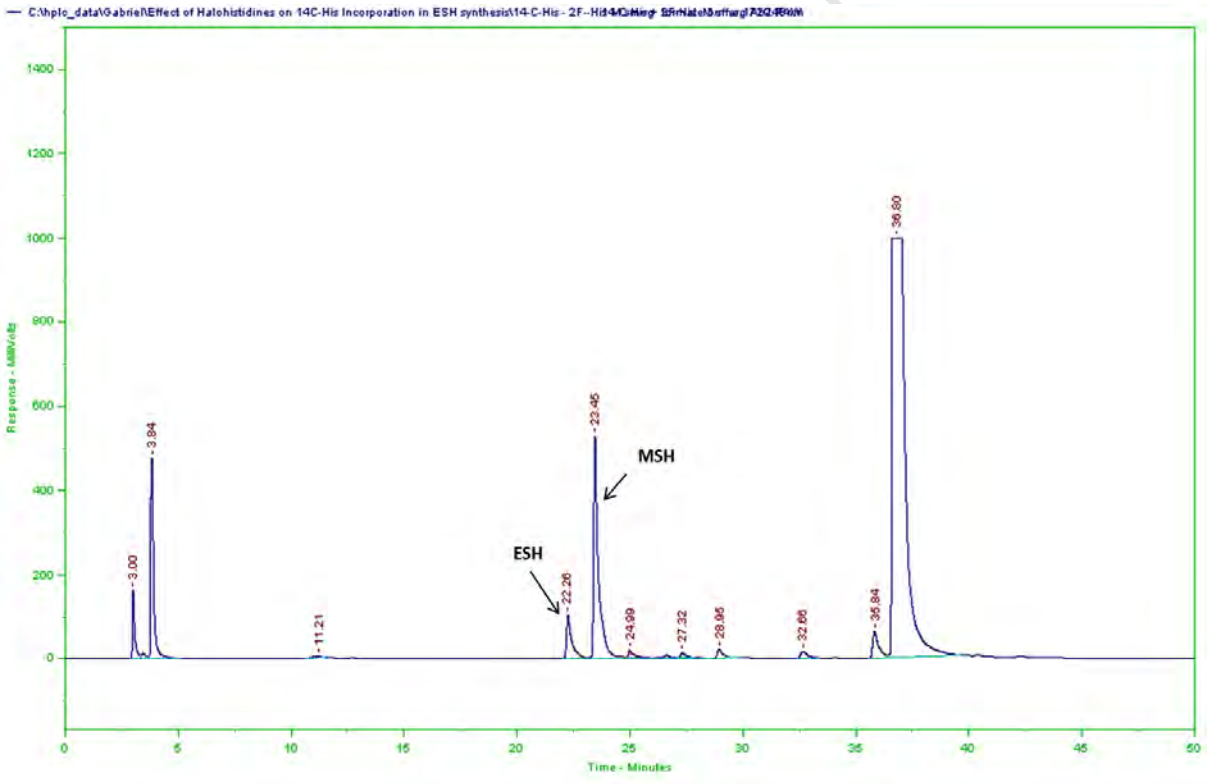

Figure 4.4: A typical HPLC elution profile of BAN derivatized thiols from *M. smegmatis* cells. Peaks at 22.26 and 23.45 minutes were later identified by mass spectrometry as BAN derivatized ergothioneine (ESH) and mycothiol (MSH) respectively.

The mass of the product eluting at 22.64 minutes was 398.4, corresponding to the mass of BAN derivatized ergothioneine (figure 4.5). The 23 minute peak gave a mass of 656 which corresponded to the BAN derivatized mycothiol (figure 4.6). The 3.84 minutes peak was found to have a mass of 481 and could not be identified.

The same HPLC profiles were observed for *M. smegmatis* cells treated with halogenated histidines and cells not treated with halogenated histidines, indicating that the halogenated histidines were either not substrates or their respective thiols could not be derivatized with BAN.

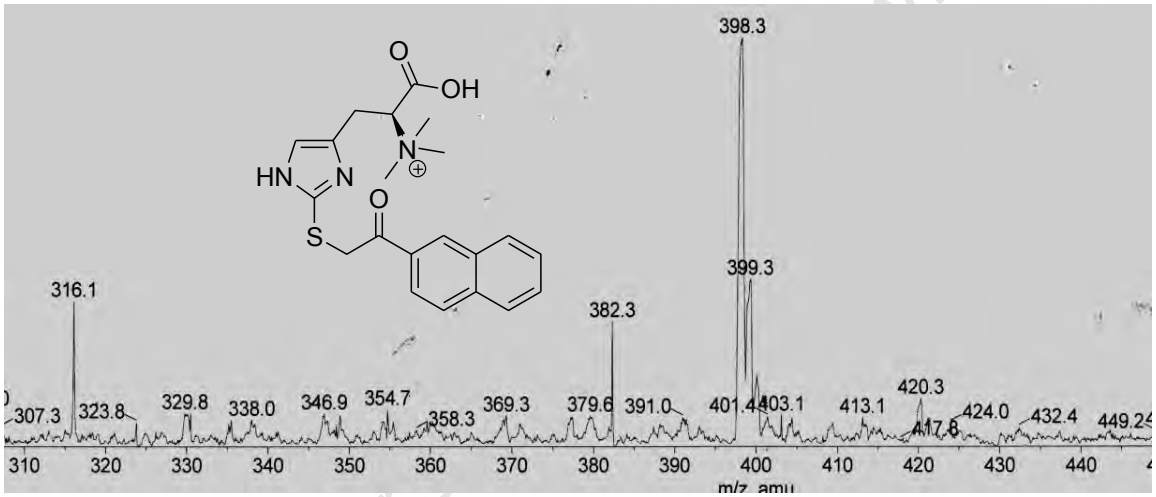

Figure 4.5: Mass spectrum of BAN derivatized ergothioneine from *M. smegmatis*. Mass spectrum of a compound that eluted at 22 minutes from in the HPLC run shown in Fig 4.4 of BAN derivatized M. smegmatis cell fraction. The major peak at 398.3 corresponds to the BAN derivatized ergothioneine.

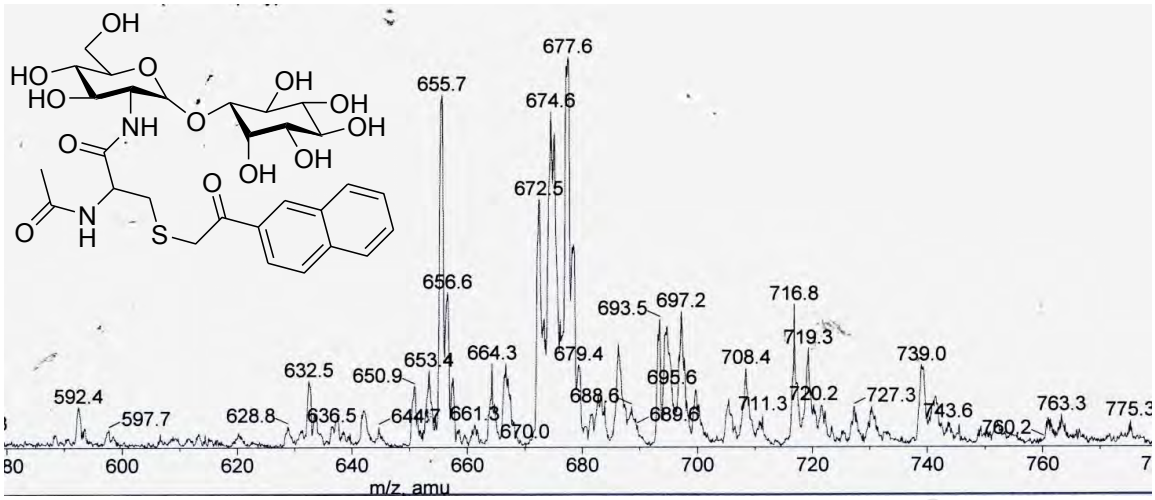

Figure 4.6: Mass spectrum of BAN derivatized mycothiol from *M. smegmatis*. Mass spectrum of a compound eluted at 23.45 minutes in the HPLC run of Fig 4.4. The major peak at 655.7 corresponds to the BAN derivatized mycothiol. These results were of the M. smegmatis culture not treated with any halogenated histidines. The peak at 677.6 is probably a sodiated species, but the ones at 674.6 and 672.5 are difficult to assign.

4.3.4. Effect of halohistidines on ergothioneine biosynthesis

Having successfully separated the ergothioneine derivative from the mycothiol derivative the effect of halohistidines on the biosynthesis of ergothioneine in *M smegmatis* could then be investigated. The peak area of mycothiol peak at 23.45 min was used to correct any variation on ergothioneine, the assumption being that mycothiol production would not be affected by halogenated histidines.

The cells were first grown to the early stationary phase before they were treated with halogenated histidines (OD_{600} of 9.6). Due to its toxicity cells were only then treated with 500 nM 2-fluorohistidine, while for the other compounds concentrations of 250 μM were used. The cells were harvested, thiols derivatized by BAN and the mixtures analysed by HPLC. The effect of halogenated histidines on ergothioneine biosynthesis was monitored by changes in ergothioneine peak area relative to a control which contained histidine. Ergothioneine produced in control sample was regarded as 100%.

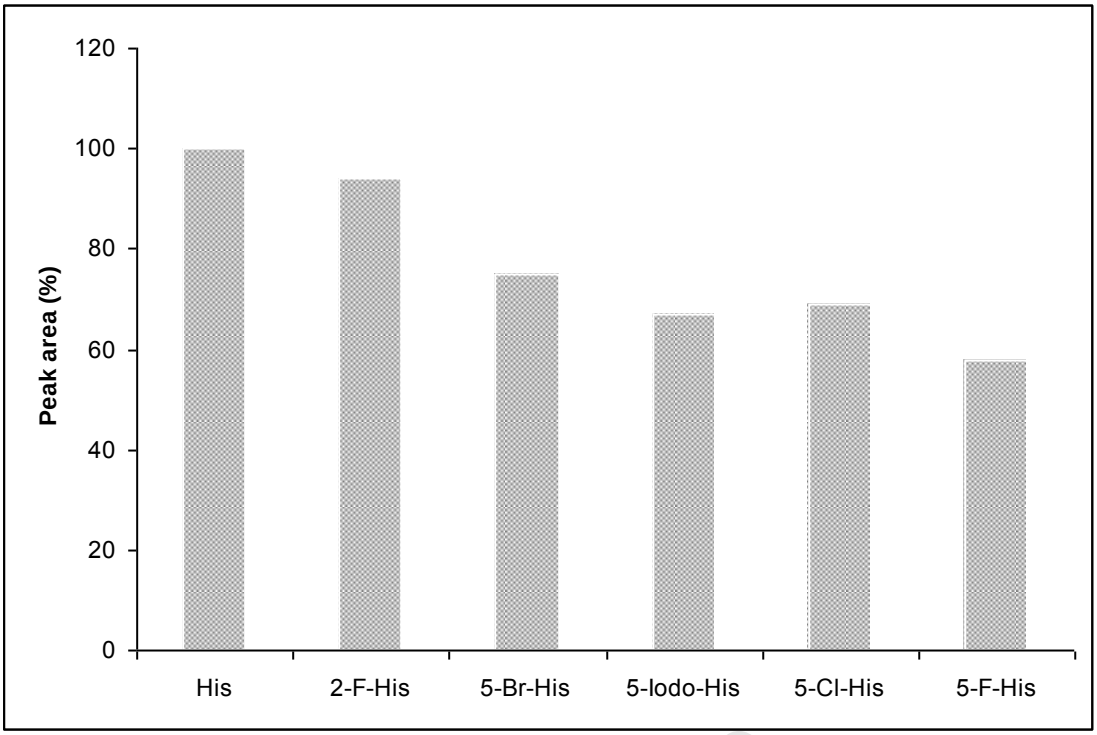

Figure 4.7: Inhibition of ergothioneine biosynthesis by 5-halogenated histidines. Ratios (ergothioneine/mycothiol) of BAN derivatized ergothioneine to BAN derivatized mycothiol showing the effect of halogenated histidines on ergothioneine biosynthesis in *M. smegmatis*. The cultures were treated with 250 μM halogenated histidines except for 2-fluorohistidine, in which case the concentration was 500nM. The ratios indicated are averages of two determinations.

The 5-halohistidines showed significant inhibition of ergothioneine formation, with 5-fluorohistidine showing most inhibition at over 40% (table 4.2). In contrast 2-fluorohistidine did not show any significant reduction in ergothioneine amounts, perhaps due to the low concentration used for the compound. Use of higher concentrations than 250 μM would have provided crucial information about the effect of 5-halogenated histidine on ergothioneine biosynthesis, but toxicity observed at concentration above 250 μM prevented such a study.

Table 4.2: Inhibition of ergothioneine biosynthesis by 5-halogenated histidines

Compound	**2-F-His**	**5-F-His**	**5-Cl-His**	**5-Br-His**	**5-Iodo-His**
ESH inhibition (%)	**5**	**42**	**31**	**25**	**33**

The validity of a study of the effect of compounds on a biosynthetic pathway using whole cells would be limited by the possibility that the substrate may be channelled into other pathways. For example, the toxicity of 2-fluorohistidine suggests that the compound may have been used up in a manner other than in the ergothioneine biosynthetic pathway since the compound's toxicity did not correlate with ergothioneine reduction. Furthermore it should be pointed out that when this work was conducted, no enzymes of ergothioneine and ovothiol biosynthetic pathway were available. With all enzymes in both pathways now identified, it will be crucial to re-investigate the effect of halogenated histidines on ergothioneine biosynthesis.

CHAPTER 5: GENERAL DISCUSSION

Ovothiol is a 3-methyl-5-mercaptohistidine which was discovered in sea urchin eggs and later isolated from other organisms including pathogenic trypanosomes. The ovothiol biosynthetic pathway was first elucidated using a cell extract of *Crithidia fasciculata* (Vogt *et al.,* 2001). Following elucidation of the corresponding genomes the sulfoxide synthase activity was purified from homologous genes in *E. tasmaniensis* and *Trypanosoma cruzi* and was named OvoA (Braunshausen and Seebeck, 2011). OvoA was confirmed as an iron dependent enzyme that activates molecular oxygen to convert histidine and cysteine into 5-histidyl cysteine sulfoxide.

Here recombinant OvoA was purified from *E. coli* B21 cells using Ni-NTA agarose as described before (Braunshausen and Seebeck, 2011) and SDS-Page analysis showed that the enzyme was more than 90% homogenous (figure 3.1). Components of the OvoA reaction mixture were separated on HPLC using ion exchange column and the reaction products were monitored by absorption at 220 nm and 254 nm wavelengths while the histidine substrate had absorption only at 220 nm. HPLC was able to detect as little as 30 ng of the sulfoxide product from the OvoA reaction mixture (calibration curve, appendix). The isolated sulfoxide products were identified by mass and strong absorbance at 254 nm.

Assay optimization showed that addition of 2 mM ascorbate activated OvoA activity over 100 fold (figure 3.3). A similar phenomenon has been reported in another nonheme iron-dependent enzyme, where the ascorbate binding site was also found located in the enzyme pocket (Thrower et al, 2001). OvoA was also found to be activated to the same level by isoascorbate (D-ascorbate), the enantiomer of ascorbate (L-ascorbate). Isoascorbate activation of iron depend enzymes was also reported on prolyl hydrolase (Flashman *et al.,* 2010). Nonheme iron enzyme are characterized by poor retention of the iron metal, but here OvoA was found to have retained about two thirds of the iron metal because addition of $FeSO_4$ into the reaction mixture increased OvoA activity by about 40% (figure 3.3). The optimal OvoA assay mixture was found to contain 20 mM NaCl, 20 mM Tris-HCl, pH 8.0, 2 mM TCEP and 1 μM $FeSO_4$ at 26^{o}C.

OvoA was characterized by histidine and cysteine K_M of 339 and 347 μM, respectively. The enzyme was found to be most active at pH 7.5 flanked by acid and alkaline pK_as of 6.8 and 8.0 respectively (table 3.1), which indicated the presence of ionizable groups that affected the reaction. The ionizable group with pK_a of 6.8 was believed to be the imidazole of the histidine substrate. At high pH the enzyme was thought to be limited by ionization of the cysteine side chain, or perhaps by a loss of iron metal above pH 9. The histidine K_M was found to be low and constant between a pH of 6.0 and 8 (figure 3.5, **B**), indicating no effect of ionizable group on the enzyme reaction. Here, the effect of imidazole ionization on the enzyme reaction could not be confirmed by the use of histidinamide and histamine, histidine analogues which have low imidazole pK_a, because the specific activity graphs produced with these analogues showed a shift towards the alkaline instead of expected acidic side for substrate with lower pK_a. The difference in amino acid group of these substrates compared to histidine introduced another variable which perhaps made these substrates not suitable candidates to study the effect of ionization group on OvoA reaction. A 2-fluorohistidine which has a very low pK_a of about 1.0 (Wimalasena *et al.,* 2007) would be a suitable substrate, but the compound was not available in sufficient amounts to perform the study.

Table 5.1: Michaelis-Menten kinetics of OvoA substrates

Substrate	V_{max} (x10^{-9}M/s)	OvoA (x10^{-9} M)	K_{cat} (s^{-1})	K_M (x10^{-6} M)	k_{cat}/K_M ($s^{-1}M^{-1}$)
Histidine	943 ± 45	289	3.26	339 ± 22	9617
Cysteine	920 ± 44	294	3.13	347 ± 27	9020
Histidinamide	156 ± 3	371	0.42	308 ± 27	1364
Histamine	99.9 ± 1.4	377	0.26	227 ± 6	1145
D-Histidine	121 ± 0.06	346	0.35	818 ± 12	427

Initial characterization of OvoA revealed the enzyme promiscuity towards sulfur acceptors while showing high specificity towards the sulfur donor. Histamine and histidinamide were turned over at about 5 times less efficiency than histidine, which is believed to be the enzyme's natural substrate (table 3.1). The use of 4(5)-methylimidazole as OvoA substrate and other histidine analogues bearing various

modifications at the amino acid part, indicated that the enzyme does not require the amino acid moiety for catalysis. However, the results provided some important information about the role played by the amino acid part in this reaction. When D-histidine was used as substrate, the enzyme lost its selectivity towards C-5 as transsulfuration target location, because 2-D-histidyl cysteine sulfoxide was also identified as one of the reaction products (figure 3.11). It appears therefore that by changing the orientation of the amino acid functional group the specificity of the reaction is significantly affected.

Histidine analogues that have modifications at the α-amino group were all sulfurated at the C-2 position of the imidazole ring, including 4(5)-methylimidazole, which does not have an amino acid group (figure 3.18). A further observation was that an increased degree of methylation on the histidine α-amino group resulted in increased formation of the C-2 sulfoxide product while reducing the amount of C-5 sulfoxide product (figure 3.19 and figure 3.20). These results place interaction of α-amino group at the center of transsulfuration location in the enzyme. Perhaps the same interaction is the one separating ovothiol from ergothioneine biosynthetic systems, because the main difference between these two systems seems to be the position of transsulfuration (figure 3.2).

Initial characterization of OvoA did not find a substrate kinetic isotope effect, suggesting that hydrogen abstraction was not a rate limiting step for the transsulfuration step (Braunshausen and Seebeck, 2011). The results reported here also did not find a solvent isotope effect because reaction in water was found to be only 1.2 times faster than in deuterium oxide under similar conditions (figure 3.8). Lack of solvent isotope effect perhaps means that proton exchange is not a rate limiting step for the OvoA mediated transsulfuration step either. Another important finding of this study was the fact that OvoA used 2-fluorohistidine as substrate, converting it into 2-fluorohistidyl cysteine sulfoxide at nearly the same rate as histidine (figure 3.14). The presence of fluorine at histidine C-2 was found to reduce the pK_a of histidine imidazole group almost seven times, which makes the 2-fluorohistidine imidazole much more electron deficient (Wimalasena *et al.,* 2007 and Yen *et al.,* 1975).

The lack of a substrate kinetic isotope effect previously found by Braunshausen and Seebeck in 2011, lack of solvent isotope effect, and efficient turnover of electron deficient 2-fluorohistidine substrate found here led to a proposal about mechanistic aspects of the transsulfuration step catalyzed by OvoA. In some nonheme iron-dependent enzymes, the iron-metal complex generates high valent iron(IV)-oxo species which is believed to be the main initiator of substrate oxidation by abstracting a hydrogen atom from the substrates. However, such a route would be unlikely for electron poor substrates such as 2-fluorohistidine (pK_a of about 1). Observed efficient turnover of 2-fluorohistide to the respective sulfoxide prompted a suggestion of a different mechanism from the one followed by many characterized nonheme iron-dependent enzymes scheme 3.1 (Bruijnincx *et al.,* 2008). The mechanism proposed here suggested that the cysteine thiyl radical, generated by enzyme iron(III)-superoxide, is the initiator of the transsulfuration reaction by attacking the histidine double bond, leading to homolytic cleavage of the C-H bond through hydrogen transfer to the iron(II)-superoxide to form iron-hydroperoxide. Through electron rearrangement, oxygen is then transferred to the sulfur and the iron returns to its ground state.

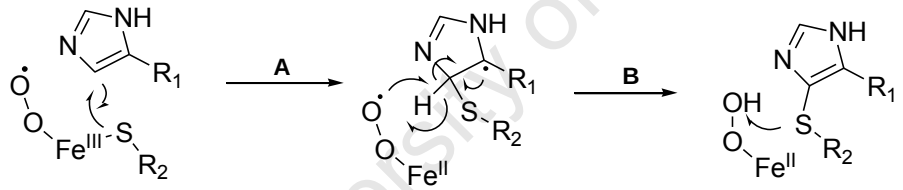

Scheme 5.1: Proposed catalytic mechanism of OvoA

Inhibition of the OvoA reaction by histidine analogues revealed 5-fluorohistidine as a superior inhibitor resulting in 80% OvoA inhibition at inhibitor concentration 100 times more than the histidine substrate. Also, OvoA did not turn over 5-fluorohistidine into the respective 5-fluorohistidyl cysteine sulfoxide. Determination of inhibition constants of 5-fluorohistidine would have provided crucial insights on inhibitor-enzyme interaction. However insufficient amounts of 5-fluorohistidine prevented such a study at this time. Other 5-halogenated histidines showed poorer inhibition of the enzyme from undetectable levels (5-iodohistidine) to 20% (4-chlorohistidine) (figure 3.9). It is speculated that this may be due to steric hindrance caused by the bulkier halogens.

Although OvoA turned over 4(5)-methylimidazole into the respective sulfoxide the enzyme did not use similar compounds, 4(5)-bromoimidazole and 4(5)-hydroxymethylimidazole as substrates, and was not significantly inhibited by these compounds. The enzyme was moderately inhibited by imidazole, which showed almost 50% inhibition. Because no measurable turnover was observed with imidazole substrate, the inhibition was not linked to two substrates competing for the enzyme activity. Imidazole and imidazole containing compounds are known metal chelators, so it could not be out ruled that imidazole inhibition of OvoA was through coordination to the enzyme metal center.

OvoA promiscuity towards sulfur donors was however not extended to other aromatic compounds, as substitution of imidazole by pyridine and indole rings did not result in any measurable turnover of 2- and 3-pyridylalanine, and tryptophan, and none of the compounds exhibit significant inhibition of OvoA. Perhaps these results pointed to the small and restrictive catalytic pocket to which only imidazole can bind on OvoA. On the amino acid side, the enzyme did not turnover histidine analogues bearing α-N-amidation, and none of these compounds inhibited the enzyme, as seen with α-acetylhistidine and carnosine (figure 3.9 and figure 3.21). Perhaps, oxygen of the amide group dislocates the imidazole ring by interacting with other distant side chains of the enzyme or perhaps the active side consists of hydrophobic side chains which push oxygen containing compound away or again pointing to small and restrictive catalytic pocket of the enzyme.

Sulfurization of 3-methylhistidine would suggest a possibility of another route to ovothiol biosynthesis, one which begins with methylation of the histidine imidazole prior to the sulfoxidation and lysis steps. However no measurable turnover by OvoA was observed with 3-methylhistidine substrate. Interestingly 3-methylhistidine inhibited up to 50% OvoA activity, perhaps suggesting a strong affinity to the enzyme (figure 3.9). This was an interesting result because ovothiol also contains a methyl group at a similar position. Although without sufficient data support it, such a modification may allow ovothiol to bind an allosteric site on the enzyme to regulate ovothiol biosynthesis in a feed-back inhibition mode.

When evaluated as potential inhibitors of ergothioneine biosynthesis in mycobacteria, halogenated histidine showed moderate to poor inhibition, ranging from 5 to 40% when used at 250 μM, with 5-fluorohistidine being the superior one (table 4.1). Because of observed high toxicity towards *M. smegmatis*, the concentration of 2-fluorohistidine was 400 times less than others tested. It is possible that a 500 nm concentration was too low to evaluate 2-fluorohistidine as an inhibitor of ergothioneine biosynthesis. High toxicity of 2-fluorohistidine was also observed in malaria (PANTON *et al*., 1988). The compound was also found to be incorporated into proteins (Eichler *et al*., 2005). With all the enzymes involved in ergothioneine now readily available (Seebeck, 2010), a new study of halogenated histidine on ergothioneine is possible.

Availability of sulfoxide synthases (Seebeck, 2010 and Braunshausen and Seebeck, 2011) coupled with easier methods to synthesis halogenated histidine, (excluding fluorinated histidines) and other histidine analogues described here, provide opportunity to study the physiological roles played by such important biological metabolites as ovothiol and ergothioneine, and ultimately development of new site-targeted drugs against bacterial and trypanosomal diseases.

CONCLUSION:

During the course of this work, halogenated histidine derivatives were chemically synthesized and evaluated as potential inhibitors or alternative substrates of OvoA. Recombinant *E. tasmaniensis* OvoA was expressed and purified from *E. coli* cells and then characterized. OvoA retained more than 60% of its iron and its activity increased over 100 fold with addition of 2 mM ascorbate and isoascorbate. OvoA was characterized by L-histidine an L-cysteine K_M of 339 ± 22 and 347 ± 27, respectively. Specificity constants towards it natural substrates was found to be 9.6 x10^3 $s^{-1}M^{-1}$ and 9.0 x 10^3 $s^{-1}M^{-1}$ for L-histidine and L-cysteine, respectively. The enzyme was found to be most active at pH 7.5, achieving catalytic constant of up to 3.2 s^{-1}.

Sulfur acceptor specificity study revealed that amino acid moiety of histidine is only required for transsulfuration location targeting but not for catalysis as 4(5)-methylimidazole was turned over into the respective sulfoxide product. OvoA was found to turnover histidine, histamine and L-histidine into their respective sulfoxide products just about seven times less efficient than D-histidine. Interestingly 2-fluorohistidine was turned over at the same rate as L-histidine despite its imidazole ring being almost seven fold less electron deficient than that of L-histidine. There was no observed solvent isotope effect on OvoA reaction and 80% of the enzyme activity was inhibited by 5-fluorohistidine. Modification of L-histidine at α-amino group resulted in increased transsulfuration at C-2 position of sulfur acceptor.

EXPERIMENTAL

General Procedures

Preparative: All solvents were freshly distilled. Benzene and toluene were distilled over sodium wire under nitrogen. Diethyl ether and tetrahydrofuran were distilled under nitrogen and dried over sodium wire with benzophenone. Dichloromethane was distilled over phosphorus pentoxide. Other solvents were purified according to standard procedures (Perrin and Armarego, 1988). The water used in the experimental work was distilled and deionized.

Reactions were monitored by thin layer chromatography (tlc) using aluminium-backed precoated Merck silica gel 60 F254 plates and were visualized by dipping in 2% ninhydrin in methanol followed by heating at 150^{o}C. Column chromatography was performed using Merck silica gel 60 (70-230 mesh) or Dowex 50 WX 2-200, H^{+} form. Typical work-up involved threefold extraction with organic solvents. All reagents were purchased from Aldrich, Merck or Bachem.

Analytical: Melting points were determined using a Riechert-Jung Thermovar hot plate microscope and were uncorrected. Nuclear Magnetic Rosonance spectra were recorded on a Varian Unity 400 (100 MHz for ^{13}C, 376.3 MHz for ^{19}F) or Varian Mercury 300 MHz (75 MHz for ^{13}C) and carried out in d-chloroform unless otherwise stated. Chemical shifts (δ) were recorded using residual chloroform (δ 7.24 in ^{1}H NMR and δ 77.00 in ^{13}C NMR) or tetramethylsilane (δ 0.00) as an internal standard. For D_2O, dioxane (δ 3.75 in ^{1}H NMR and δ 67.19 in^{13}C NMR) was used as an internal standard. For CD_3OD, the residual methanol peak (δ 3.31 in ^{1}H NMR and δ 49.00 in ^{13}C NMR) was used as an internal standard. All chemical shifts were reported in ppm.

tert-Butyl 1-(methoxycarbonyl)-2-(5-chloro-1H-imidazol-4-yl)ethylcarbamate (47a)

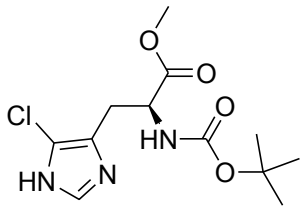

To a stirring solution of *tert*-butyl 1-(methoxycarbonyl)-2-(1H-imidazol-4-yl)ethylcarbamate, **46**, (0.2 g, 0.74 mmol) in acetonitrile (5 ml), N-Chlorosuccinimide (0.1 g, 0.75 mmol) in acetonitrile (2ml) was slowly added. The reaction mixture was stirred for two hours in the dark (flask covered with aluminium foil) under nitrogen. The reaction was stopped by removing the solvent in vacuo. The crude product was dissolved in small amount of dichloromethane and quickly transferred to a 50 ml column packed with 20 g of silica gel in petroleum ether. The column was eluted with ethyl acetate: petroleum ether (7:3) solution and the evaporation of the solvent afforded the product in as colourless oil (142 mg, 63%). δ H (300 MHz, $CDCl_3$) 7.48 (1 H, s, H-2), 5.43 (1 H, s, N-H) 4.48 (1 H, s, α-CH), 3.75 (3 H, s, OCH_3), 3.09 (2 H, ddd, J 6.3, 15.3, 22.3, β-CH_2), 1.41 (9 H, s, 3(CH_3)). δ C (75 MHz, $CDCl_3$) 171.91, 133.36, 120.64, 52.81, 29.58, 28.21, 27.94, 27.59.

2-Amino-3-(4-chloro-1H-imidazol-5-yl)propanoic acid (5-chlorohistidine) (7)

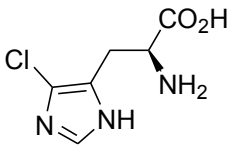

To a solution of *tert*-butyl 1-(methoxycarbonyl)-2-(5-chloro-1H-imidazol-4-yl)ethylcarbamate, **47a**, (0.1 g, 0.33 mmol) in methanol (5 ml) was added LiOH (0.024 g, 0.99 mmol) and the mixture was stirred for 3 hours at room temperature. Water (30 ml) was added and the aqueous mixture was extraction with ethyl acetate (2 x 50 ml). The organic phase was washed with saturated NaCl solution (50 ml) and dried over $MgSO_4$.

Evaporation of the solvent afforded an oily residue which was dissolved in 20% TFA in DCM (5 ml) and stirred for 2 h. The solvent was evaporated and the resulting oily residue was dissolved in 1mM HCl (3 ml) and transferred onto an ion exchange column (Dowex 50 WX 2-200, H^+ form). The column was washed with water until the eluent pH was neutral before the product was eluted with 10% NH_4OH solution. Evaporation of the solvent afforded the product as brown solid (40.7 mg, 65%). M + H: 190.0 (exp), 190.1 (obt).δ H (300 MHz, D_2O) 7.52 (1 H, s, H-2), 3.84 (1 H, t, J 6.0, α-CH), 3.11 (2 H, qd, J 6.4, 15.6, β-CH_2).

tert-Butyl 1-(methoxycarbonyl)-2-(5-bromo-1H-imidazol-4-yl)ethylcarbamate (47b)

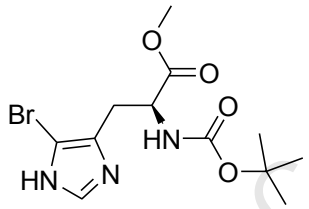

To a stirring solution of *tert*-butyl 1-(methoxycarbonyl)-2-(1H-imidazol-4-yl)ethylcarbamate, **46**, (0.2 g, 0.74 mmol) in acetonitrile (5 ml) in a 25 ml two necked round bottomed flask covered with an aluminium foil, under nitrogen atmosphere, N-bromosuccinimide (0.13 g, 0.75 mmol) in acetonitrile (2 ml) was slowly added. After stirring for two hours the reaction was stopped by removing the solvent *in vacuo*. The crude product was dissolved in small amount of dichloromethane and quickly transferred on a 50ml column packed with 20 g of silica gel in petroleum ether. The column was eluted with ethyl acetate: petroleum ether (7:3) solution. Evaporation of the solvent gave the product as colourless oil (172 mg, 67%). δ H (400 MHz, $CDCl_3$) 7.56 (1 H, s, H-2), 5.47 (1 H, s, N-H), 4.48 (1 H, s, α-CH), 3.62 (3 H, s, OCH_3), 3.08 (1 H, dd, J 5.7, 15.2, β-CH), 3.02 – 2.89 (1 H, m, β-CH), 1.38 (9 H, s, 3(CH_3)).

2-amino-3-(4-bromo-1H-imidazol-5-yl)propanoic acid (5-bromohistidine) (8)

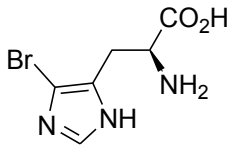

To a solution of (*tert*-butyl 1-(methoxycarbonyl)-2-(5-bromo-1H-imidazol-4-yl)ethylcarbamate, **47b**, (0.1 g, 0.29 mmol) in methanol (5 ml) was added LiOH (0.021 g, 0.87 mmol) and the mixture was stirred for 3 hours at room temperature. Water (30 ml) was added and the aqueous mixture was extraction with ethyl acetate (2 x 50 ml). The organic phase was washed with saturated NaCl solution (50 ml) and dried over $MgSO_4$. Evaporation of the solvent afforded an oily residue which was dissolved in 20% TFA in DCM (5 ml) and stirred for 2 h. The solvent was evaporated and the resulting oily residue was dissolved in 1 mM HCl (3 ml) and transferred onto ion exchange column (Dowex 50 WX 2-200, H^+ form). The column was washed with water until the eluent pH was neutral before the product was eluted with 10% NH_4OH solution. Evaporation of the solvent afforded the product as brown solid (42 mg, 62%). M + H: 233.98 (exp), 234.0 (obt). δ H (400 MHz, CD_3OD) 8.99 (1 H, s, H-2), 4.39 (1 H, dt, J 7.3, 30.5, α-CH), 3.39 (2 H, qd, J 7.6, 15.6, β-CH_2).

tert-Butyl 1-(methoxycarbonyl)-2-(5-iodo-1H-imidazol-4-yl)ethylcarbamate (47c) and _tert_-butyl 1-(methoxycarbonyl)-2-(2,5-diiodo-1H-imidazol-4-yl)ethylcarbamate (56)

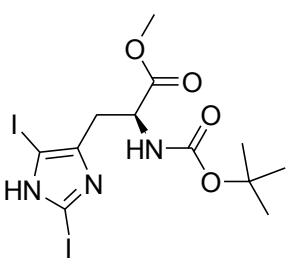

56

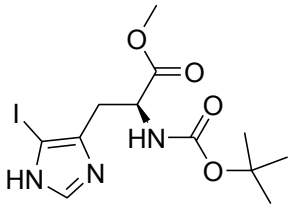

47c

To a stirring solution of *tert*-butyl 1-(methoxycarbonyl)-2-(1H-imidazol-4-yl)ethylcarbamate, **46**, (0.2 g, 0.74 mmol) in acetonitrile (5 ml) in a 25ml two necked

round bottomed flask covered with an aluminium foil, under nitrogen atmosphere, N-iodosuccinimide (0.20, 0.9 mmol) in acetonitrile (2 ml) was slowly added. After stirring for two hours the reaction was stopped by removing the solvent *in vacuo*. The crude product was dissolved in small amount of dichloromethane and quickly transferred on a 50ml column packed with 20 g of silica gel in petroleum ether. The column was eluted with ethyl acetate: petroleum ether (7:3) solution. The products were obtained as colourless oil, **47c** (170 mg, 58%) and **56** (116 mg, 30%).

47c: δ H (300 MHz, $CDCl_3$) 7.59 (1 H, s, H-4), 5.41 (1 H, s, N-H), 4.52 (1 H, d, J 7.3, α-H), 3.15 (1 H, dd, J 5.3, 15.4, β-H), 3.01 (1 H, dd, J 6.4, 15.4, β-H), 1.47 – 1.38 (9 H, m, 3(CH_3)).

56: δ H (300 MHz, $CDCl_3$) 5.41 (1H, s, N-H), 4.56 (1H, m, α-CH), 3.79(3H, s, OCH_3), 3.42 – 2.94 (2H, m, β-CH_2), 1.45 (9H, s, 3(CH_3))

2-amino-3-(4-iodo-1H-imidazol-5-yl)propanoic acid (5-iodohistidine) (9)

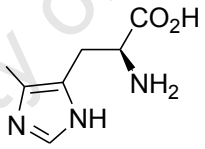

To a solution of (*tert*-butyl 1-(methoxycarbonyl)-2-(5-iodo-1H-imidazol-4-yl)ethylcarbamate, **47c**, (0.08 g, 0.2 mmol) in 5 ml methanol was added LiOH (0.014 g, 0.6 mmol) and the mixture was stirred for 3 hours at room temperature. Water (30 ml) was added and the aqueous mixture was extraction with ethyl acetate (2 x 50 ml). The organic phase was washed with saturated NaCl solution (50 ml) and dried over $MgSO_4$. Evaporation of the solvent afforded an oily residue which was dissolved in 20% TFA in DCM (5 ml) and stirred for 2 h. The solvent was evaporated and the resulting oily residue was dissolved in 1 mM HCl (3 ml) and transferred onto ion exchange column (Dowex 50 WX 2-200, H^+ form). The column was washed with water until the eluent pH was neutral before the product was eluted with 10% NH_4OH solution. Evaporation of the solvent afforded the product as brown solid (36.5 mg, 65%). M + H: 281.97 (exp), 282.0 (obt). δ

H (400 MHz, D2O) 7.69 (1 H, s, H-2), 3.96 – 3.83 (1 H, m, α-CH), 3.11 (2 H, ddd, J 6.5, 15.5, 23.1, β-CH_2).

N-(1-hydroxy-3-(1H-imidazol-4-yl)propan-2-yl)benzamide (73)

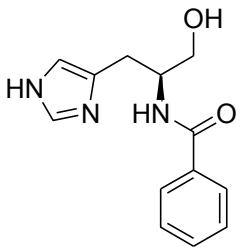

Into a stirring solution of methyl 2-(benzamido)-3-(1H-imidazol-4-yl)propanoate, **72**, (5 g, 18.3 mmol) in anhydrous methanol (50 ml) at 50°C, $NaBH_4$ (2.8 g, 74.0 mmol) was added in portions, every portion added after the effervescence had stopped. The reaction was allowed to stir at the same temperature for 2 hours. The solvent was removed in vacuo to afford crude product as a white solid. The crude product was treated with water (200 ml) and then neutralized with 2 M HCl solution. The product was extracted with hot ethyl acetate (4 x 200 ml). The ethyl acetate was removed *in vacuo* to give the product a white product (3.1 g, 68%). δ H (300 MHz, CD_3OD) 7.84 – 7.73 (2 H, m, phenyl), 7.57 (1 H, s, 2-H), 7.54 – 7.37 (3 H, m, phenyl), 6.88 (1 H, s , 4-H), 4.36 (1 H, dq, J 5.6, 8.0, α-H), 3.65 (2 H, t, J 5.7, CH_2), 2.94 (2 H, qd, J 7.0, 14.9, β-H_2).

N-(1-hydroxy-3-(1-tosyl-1H-imidazol-4-yl)propan-2-yl)benzamide (74)

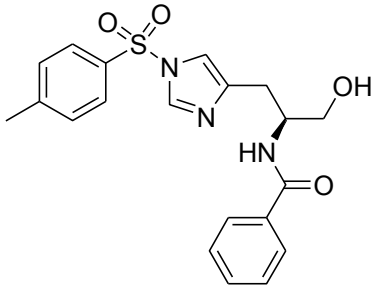

A stirring suspension of N-(1-hydroxy-3-(1H-imidazol-4-yl)propan-2-yl)benzamide, **73**, (2.5 g, 6.26 mmol) and triethylamine (5.45 ml, 37.56 mmol) in dichloromethane (40 ml)

was cooled to 0°C on ice bath before a solution of para-toluenesulfonyl chloride (2.5 g, 13.11 mmol) was slowly added. The ice bath was removed and the mixture was allowed to react at room temperature for 24 hours, at which point tlc (ethyl acetate and petroleum ether (9:1) as eluent) showed complete consumption of the starting material. The reaction was quenched with saturated NH_4Cl solution (100 ml) and extracted with dichloromethane (3 x 100 ml). The organic layer was washed with saturated $NaHCO_3$ solution (100 ml), once with distilled water (500 ml) and then saturated NaCl solution (300 ml). The organic phase was dried over $MgSO_4$. The solvent was removed by evaporation to afford a crude product which was purified by silica column using a mixture of ethyl acetate and petroleum ether (9:1) to give the product as colourless oil (1.65 g, 66%). δ H (300 MHz, $CDCl_3$) 7.96 (1 H, d, J 1.3, 4-H (imida)), 7.75 (4 H, ddt, J 1.8, 6.9, 9.7, phenyl and tosyl), 7.52 – 7.44 (1 H, m, phenyl), 7.43 – 7.33 (3 H, m, phenyl and N-H), 7.30 (2 H, d, J 8.0, tosyl), 7.13 (1 H, d, J 1.2, 2-H (imida)), 4.32 (1 H, dd, J 4.5, 11.9, α-H), 3.74 (1 H, dd, J 4.5, 11.4, β-Ha), 3.62 (1 H, dd, J 4.5, 11.4, β-Hb), 2.94 (2 H, dd, J 5.5, 6.9, CH_2), 2.41 (3 H, s, CH_3, tosyl). δ C (75 MHz, $CDCl_3$) 167.62, 146.37, 140.91, 136.33, 134.69, 134.16, 131.47, 130.43, 128.46, 127.30, 126.98, 115.04, 64.56, 51.33, 29.13, 21.67.

4-((4,5-dihydro-2-phenyloxazol-4-yl)methyl)-1-tosyl-1H-imidazole (75)

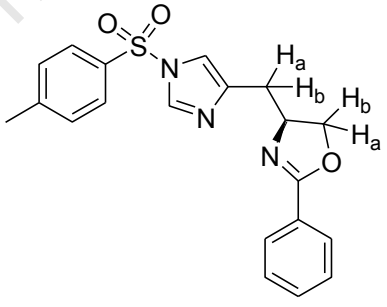

Method A: To a stirring solution of para-toluene sulfonyl chloride (5.85 g, 30.68 mmol) in dry dichloromethane (40 ml) on ice, triethylamine (15 ml, 107.6 mmol) was slowly added. The resulting mixture was stirred for 20 minutes until brown colour developed before N-(1-hydroxy-3-(1-tosyl-1H-imidazol-4-yl)propan-2-yl)benzamide, **73**, (5.85 g,

14.64 mmol) in DCM (12 ml) was slowly added. The mixture was stirred for 20 minutes before the ice bath was removed. The stirring continued overnight before the reaction was stopped with saturated $NaHCO_3$ solution (100 ml) and extracted three times with DCM (200 ml). The organic phase was washed with water (400 ml) and saturated NaCl solution (200 ml) before dried over $MgSO_4$. Upon removal of the solvent by evaporation the crude sample was loaded on silica gel and eluted with ethyl acetate-petroleum ether (7:3) mixture. The product was obtained as white crystals after the solvent was removed (4.58 g, 82%). mp 133^{o}C. M + H: 382.1 (exp), 382.1 (obt). δ H (400 MHz, $CDCl_3$) 7.96 – 7.86 (3 H, m, phenyl and 2-H (imida)), 7.80 – 7.70 (2 H, m, tosyl), 7.55 – 7.44 (1 H, m, phenyl), 7.44 – 7.37 (2 H, m, phenyl), 7.29 (2 H, dd, J 0.5, 8.5, tosyl), 7.13 (1 H, d, J 1.3, 4-H (imida)), 4.60 (1 H, dtd, J 5.3, 7.5, 12.8, α-H), 4.44 (1 H, dd, J 8.5, 9.4, CHa), 4.20 (1 H, dd, J 7.5, 8.5, CHb), 3.04 (1 H, dd, J 4.6, 14.8, βHa), 2.76 (1 H, dd, J 7.6, 15.0, β-Hb), 2.43 (3 H, s, CH_3, tosyl). δ C (101 MHz, CDCl3) 164.19, 146.07, 141.53, 136.27, 136.16, 135.08, 131.41, 130.40, 130.28, 128.32, 128.23, 127.72, 127.31, 127.20, 114.59, 114.48, 72.05, 65.90, 65.78, 34.06, 21.69.

Method B: Into a stirring solution of 5-iodo-4-((4,5-dihydro-2-phenyloxazol-4-yl)methyl)-1-tosyl-1H-imidazole, **80a**, (0.17 g, 0.33 mmol) in THF (2 ml) in an acetone-liquid nitrogen bath under nitrogen, n-butyllithium (300 µl, 0.48mmol, 1.6 M in hexane) was added drop-wise over 3 minutes. After 3 minutes a sample (about 50 µl) was quenched with water and analysed by tlc using ethyl acetate-petroleum ether (2:3) as the mobile phase. TLC showed a complete metal and halogen exchange after 3 minutes. Water (2 ml) was added into the reaction mixture and the reaction mixture was allowed to warm. While at room temperature, saturated NH_4Cl (50 ml) solution was added followed by extraction with DCM (2 x 50 ml). The organic phase was washed with 50 ml distilled water (50 ml) and then saturated NaCl solution (50 ml) solution before dried over $MgSO_4$ salt. Removal of the solvent by evaporation afforded a brown residue which was purified by chromatography using ethyl acetate-petroleum ether (2:3) as the mobile phase to give the product as a white solid (63 mg, 50%). δ H (400 MHz, $CDCl_3$) 8.14 (1 H, d, J 1.0), 7.98 – 7.87 (2 H, m), 7.83 – 7.72 (2 H, m), 7.53 – 7.45 (1 H, m), 7.45 – 7.38 (2 H, m), 7.33 (2 H, ddd, J 0.6, 8.6, 27.5), 6.92 (1 H, q, J 1.0), 4.65 – 4.52 (1 H, m), 4.45 (1 H, dt, J 8.2, 9.4), 4.03 (1 H, dt, J 7.2, 14.3), 3.18 – 2.69 (2 H, m), 2.48 – 2.38 (3 H, m).

4-((4,5-dihydro-2-phenyloxazol-4-yl)methyl)-1H-imidazole (76)

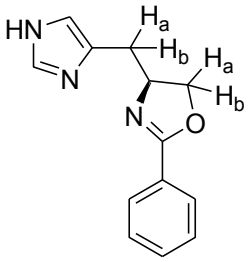

A solution of 4-((4,5-dihydro-2-phenyloxazol-4-yl)methyl)-1-tosyl-1H-imidazole, **75**, (6.5 g, 17.06 mmol) in mixture of anhydrous methanol (30 ml) and THF (2:1) was transferred in a flask containing Cs_2CO_3 (6.11 g, 18.8 mmol). The mixture was stirred at 50^{o}C for two hours, at which point a tlc showed total consumption of the starting material. The product was purified by flash chromatography using ethyl acetate and methanol (8:2) and the evaporation of the solvent afforded the product as a colourless wax (3.33 g, 86%). δ H (400 MHz, CD_3OD) 7.95 – 7.84 (2 H, m, phenyl), 7.60 (1 H, s, 4-H (imida)), 7.52 (1 H, t, J 7.4, phenyl), 7.43 (2 H, dd, J 6.9, 8.2, phenyl), 6.88 (1 H, s, 4-H (imida)), 4.59 (1 H, dd, J 7.4, 14.6, α-H), 4.48 (1 H, t, J 9.0, CHa), 4.31 – 4.19 (1 H, m, CHb), 3.06 (1 H, dd, J 5.2, 14.7, β-Ha), 2.81 (1 H, dd, J 7.8, 14.6, β-Hb). δ C (101 MHz, CD_3OD) 135.05, 131.75, 128.62, 128.37, 128.13, 127.35, 125.79, 117.37, 72.11, 65.92, 48.45, 48.03, 47.81, 47.39, 32.49.

4-((4,5-dihydro-2-phenyloxazol-4-yl)methyl)-5-iodo-1H-imidazole (78)

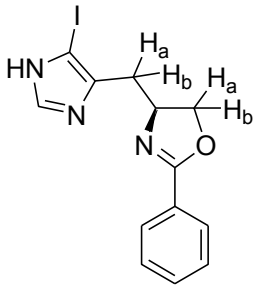

Method A: Into a stirring solution of 4-((4,5-dihydro-2-phenyloxazol-4-yl)methyl)-1H-imidazole, **76**, (3.8 g, 13.71 mmol) in anhydrous DMF (15 ml) in the dark (flask covered by aluminium foil) under nitrogen atmosphere, 1.5g N-iodosuccinimide (1.5 g,) in acetonitrile (15 ml) was added. After 2 hour of stirring at room temperature, tlc indicated

a complete conversion of the starting material. The solvent was removed *in vacou* and the crude product was purified by silica gel chromatography eluted with a mixture of ethyl acetate and petroleum ether (9:1) to give the product as a yellow solid (1.4 g, 29%). M + H: 353.0 (exp), 354.0 (obt). δ H (400 MHz, CD_3OD) 7.93 (2 H, dt, J 1.7, 8.5, phenyl), 7.64 (1 H, s, 2-H (imida)), 7.57 – 7.48 (1 H, m, phenyl), 7.48 – 7.38 (2 H, m, phenyl), 4.58 (1 H, ddd, J 6.8, 9.4, 13.2, α-H), 4.52 – 4.42 (1 H, m, CHa), 4.27 (1 H, dd, J 6.8, 8.6, CHb), 2.96 (1 H, dd, J 6.2, 14.7, β-Ha), 2.84 (1 H, dd, J 7.0, 14.7, β-Hb).

Method B: Sodium methoxide (0.374 g, 6.92 mmol) was reacted with thiophenol (0.71 ml, 6.92 mmol) in isopropanol (10 ml). When all the bubbling had stopped, 4-((4,5-dihydro-2-phenyloxazol-4-yl)methyl)-2,5-diiodo-1H-imidazole, **77**, (1.5g, 3.13 mmol) was added and the reaction mixture was allowed to continue stirring overnight at room temperature. The reaction was stopped with addition of saturated $NaHCO_3$ solution (100 ml) and extracted with ethyl acetate (3 x 50 ml). The organic phase was washed with water (200 ml) and then saturated NaCl solution (100 ml) before dried over $MgSO_4$. The solvent was evaporated and the residue was purified by chromatography using ethyl acetate-petroleum ether (9:1) to give a yellow solid (0.82 g, 74%).

4-((4,5-dihydro-2-phenyloxazol-4-yl)methyl)-2,5-diiodo-1H-imidazole (77)

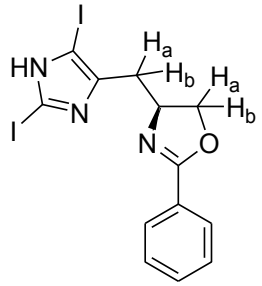

Synthetic procedure is the same as Method A for **78** above (3.7 g, 56%). M + H: 479.9 (exp), 479.9 (obt). δH (400 MHz, CD_3OD) 7.90 (2 H, dt, J 1.6, 8.5, phenyl), 7.56 – 7.48 (1 H, m, phenyl), 7.42 (2 H, tt, J 1.1, 8.3, phenyl), 4.55 (1 H, dt, J 6.6, 13.6, α-H), 4.49 – 4.41 (1 H, m, CHa), 4.26 (1 H, dd, J 6.7, 8.6, CHb), 2.96 (1 H, dd, J 6.0, 14.6, β-Ha), 2.78 (1 H, dd, J 7.6, 14.5, β-Ha).

4-((4,5-dihydro-2-phenyloxazol-4-yl)methyl)-5-iodo-1-tosyl-1H-imidazole (80a)

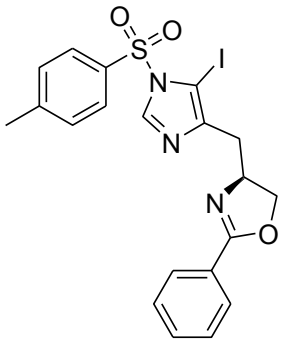

Into a cold (ice bath) mixture of 4-((4,5-dihydro-2-phenyloxazol-4-yl)methyl)-5-iodo-1H-imidazole, **78**, (1.045 g, 2.96 mmol) and (triethylamine 1.8 ml, 40 mmol) in THF (10 ml), para-toluenesulfonyl chloride (0.85 g, 4.44 mmol) in DCM (10 ml) was added. The ice bath was removed and the mixture was stirred overnight. Saturated $NaHCO_3$ solution (100 ml) was added into the mixture and the extraction was done three times with DCM (200 ml). The DCM layer portion was washed with water (200 ml), saturated NaCl solution (200 ml) and dried over $MgSO_4$. The evaporation of the solvent afforded an oily residue which was purified by chromatography to give the product as a white solid (1.3 g, 86%). M + H: 508.0 (exp), 508.0 (obt). δ H (400 MHz, $CDCl_3$) 8.38 (1 H, s, 2-H (imida)), 7.91 (4 H, ddt, J 1.7, 4.0, 8.7, phenyl and tosyl), 7.52 – 7.43 (1 H, m, phenyl), 7.44 – 7.32 (4 H, m, phenyl and tosyl), 4.64 (1 H, tdd, J 5.0, 7.2, 9.1, α-H), 4.48 – 4.38 (1 H, m, CHa), 4.27 (1 H, dd, J 7.3, 8.6, CHb), 3.06 (1 H, dd, J 5.0, 14.5, β-Ha), 2.68 (1 H, dd, J 9.0, 14.6, β-Hb), 2.46 (3 H, s, CH_3, tosyl). δ C (101 MHz, $CDCl_3$) 164.22, 147.65, 146.50, 140.95, 134.03, 131.31, 130.16, 128.60, 128.35, 128.26, 127, 65.95, 65.51, 34.58, 21.79,

***tert*-Butyl 2-((benzyloxy)carbonyl)-1-(methoxycarbonyl)ethylcarbamate (59)**

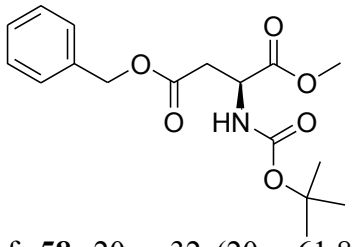

To a stirring solution of, **58**, 20 g 32 (20g, 61.85 mmol) in DMF (100 ml) at room temperature under an atmospheric air, K_2CO_3 (9 g, 65.12 mmol) was added. The

suspension was stirred for further 15 minutes before a cold (4^{o}C) aliquot of methyl iodide (12 ml, 192.67 mmol) was slowly added. The reaction mixture was stirred for two hours when a tlc with ethyl acetate: petroleum ether, 7: 3 as mobile phase showed the complete consumption of the starting material. At this point water (400 ml) was added and the product was extracted three times with a total of diethyl ether (40 ml). The combined ether fractions were washed twice with water (500 ml) before dried over Mg_2SO_4. The diethyl ether was removed *in vacou* to afford 20.3 g the product as a white solid in (20.3 g, 98%), which did not require any further purification. δ H (400 MHz, $CDCl_3$) 7.41 – 7.28 (5 H, m, aromatic), 5.11 (2 H, dd, J 4.8, 10.1, CH_2), 5.52 (1 H, s, N-H), 4.59 (1 H, s, α-H), 3.69 (4 H, d, J 5.3, OCH_3), 2.95 (1 H, d, J 0.4, β-H), 2.87 (1 H, t, J 2.0, β-H), 1.44 (10 H, s, $C(CH_3)_3$).

tert-Butyl 1,4-dihydroxybutan-2-ylcarbamate (60)

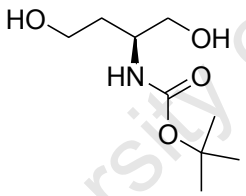

Into a *tert*-butyl 2-((benzyloxy)carbonyl)-1-(methoxycarbonyl)ethylcarbamate, **59**, (20.3 g, 60.17 mmol) in a 500 ml round bottom flask fitted with a condenser, methanol (100 ml) was added followed by THF (25 ml). The reaction mixture was stirred to afford a complete dissolution before $NaBH_4$ (12 g, 317.21 mmol) was added in portions. Caution: care should be taken when adding $NaBH_4$ to avoid losing material through effervescence as the reaction mixture gets hot and bubbles. After all the $NaBH_4$ was added the reaction was incubated for further 20 minutes and a tlc with ethyl acetate: petroleum ether (7:3) as mobile phase showed a complete consumption of the starting material. Ethyl acetate (100 ml) was added and the reaction mixture was stirred for one hour before all the solvent

was removed *in vacuo*. DCM (400 ml) was added in the mixture to form suspension which was filtered over celite and the celite was washed with DCM (50 ml). The solvent was reduced by evaporation before silica (100 g) was added. The solvent was removed and the dry silica was transferred on to a column pre-packed with a 130 g of silica. The column was first washed with ethyl acetate-petroleum ether (3:2). The product was eluted with H_2O-MeOH-EtoAc (1:2:17). The eluent was dried over $MgSO_4$ before the solvent was removed *in vacou* to give the product as an of oil (12 g, 74%). δ H (400 MHz, $CDCl_3$) 5.02 (1 H, s, N-H), 3.82 (1 H, s, α-H), 3.64 (4 H, ddd, J 5.8, 11.1, 15.6, 2(CH_2)), 3.36 – 3.04 (1 H, m, O-H), 2.81 – 2.52 (1 H, m, O-H), 1.78 (2 H, ddd, J 4.8, 9.3, 18.7, β-H_2), 1.42 (9 H, s, 3(CH_3)). δ C (101 MHz, $CDCl_3$) 157.02, 79.96, 65.38, 58.81, 49.47, 34.84, 28.34.

tert-Butyl 4-(2-hydroxyethyl)-2,2-dimethyloxazolidine-3-carboxylate (61)

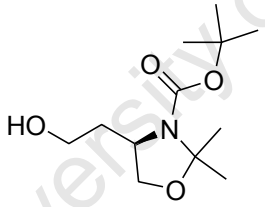

Into a stirring solution of *tert*-butyl 1,4-dihydroxybutan-2-ylcarbamate, **60**, (11.95 g, 58.22 mmol) in DCM (30 ml) under nitrogen, 2,2-dimethoxypropane (60 ml, 502.42 mmol) was added followed by p-toluenesulfonic acid (1 g, 5.82 mmol). The reaction mixture was left stirring overnight at room temperature. The solvent was removed by evaporation to afford a yellow solid which was purified by a silica column to obtain the product in yield as a white solid (6 g, 42%). δ H (300 MHz, $CDCl_3$) 4.19 (1 H, s, α-H), 3.99 (2 H, dd, J 5.5, 8.6, CH_2), 3.68 (2 H, d, J 8.6, CH_2), 1.91 – 1.64 (2 H, m, β-H2), 1.53 (3 H, s, CH_3, oxa), 1.48 (12 H, d, J 2.6, 3(CH_3) and CH3, oxa). δ C (75 MHz, $CDCl_3$) 93.62, 80.89, 68.22, 58.68, 54.00, 37.74, 28.32, 27.72, 24.35.

***tert*-Butyl 2,2-dimethyl-1,3-dioxepan-5-ylcarbamate (62)**

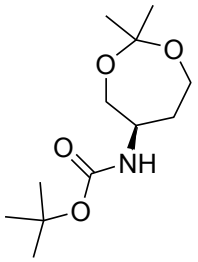

Similar reaction conditions to those described for the synthesis of **61** above were used here, (2.7 g 19%). δ H (300 MHz, $CDCl_3$) 5.14 (1 H, s, H-H), 3.73 (3 H, ddd, J 7.0, 12.4, 13.4, α-H and CH_2), 3.63 – 3.44 (2 H, m, CH2), 1.84 – 1.60 (2 H, m, β-H2), 1.45 (9 H, d, J 7.7, 3(CH_3)), 1.31 (6 H, d, J 4.8, 2(CH_3)). δ C (75 MHz, $CDCl_3$) 155.13, 101.37, 79.25, 77.41, 64.00, 57.98, 48.61, 35.83, 28.39, 24.87, 24.70.

***tert*-Butyl 4-(formylmethyl)-2,2-dimethyloxazolidine-3-carboxylate (63)**

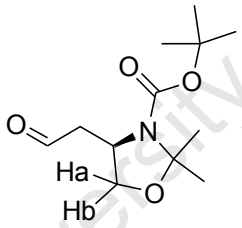

Oxalyl chloride (0.74 ml, 8.5 mmol) was added to DCM (18 ml) and the solution cooled to -78^{o}C in an acetone-liquid nitrogen cold bath. To the solution, DMSO (1.14 ml, 16 mmol) in DCM (5 ml) was slowly added and the reaction was stirred for 30 minutes. A portion of *tert*-butyl 4-(2-hydroxyethyl)-2,2-dimethyloxazolidine-3-carboxylate, **61**, (1.3 g, 5.3 mmol) dissolved in DCM (10ml) was added drop wise. After stirring the reaction for another 30 minutes triethylamine (4.3 ml, 31 mmol) was added. The reaction mixture was allowed to stir for 30 minutes at the same temperature before allowing it to warm up. Water was added and the mixture was extracted three times with DCM (200 ml). The organic layer was collected and dried over $MgSO_4$ before removed by evaporation. Material was loaded on a silica column and eluted with ethyl acetate-petroleum ether

(1:9) mixture. The product was obtained as a white crystal (1.1 g, 84%); δ H (400 MHz, $CDCl_3$) 9.79 (1 H, s, COH), 4.36 (1 H, s, α-H), 4.18 – 4.01 (1 H, m, CHa), 3.73 (1 H, dd, J 1.5, 9.3, CHb), 2.85 (2 H, d, J 124.3, β-H2), 1.58 (3 H, d, J 17.8), 1.48 (12 H, s). δ C (101 MHz, $CDCl_3$) 200.34, 67.90, 67.54, 52.68, 48.36, 47.46, 28.41, 27.51, 24.48.

***tert*-Butyl 4-(2-(4-((4,5-dihydro-2-phenyloxazol-4-yl)methyl)-1-tosyl-1H-imidazol-5-yl)-2-hydroxyethyl)-2,2-dimethyloxazolidine-3-carboxylate (82)**

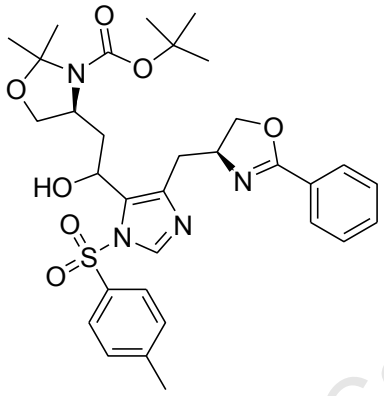

A **80a** (1.01 g, 2.0 mmol) was added in a dry round bottomed flask (flamed dried under nitrogen)). THF (20 ml) was then added and the solution was stirred vigorously. The flask was cooled over acetone-liquid nitrogen bath and left for about 20 minutes. An n-butyllithium (2 ml, 3.2 mmol, 1.6 M in hexane) was added drop-wise over 10 minutes. The reaction was monitored by tlc every 20 minutes by sampling 50 µl from the reaction mixture, quenched with water (500 µl) and extracted with DCM (200 µl). When all the starting material was completely converted, *tert*-butyl 4-(formylmethyl)-2,2-dimethyloxazolidine-3-carboxylate, **63**, (0.73 g, 3mmol) in THF (5 ml) was slowly added. The reaction mixture was left stirring for 1 hour at -78^{o}C before allowed to warm to room temperature. The reaction was stopped with saturated NH_4Cl (50 ml) solution and extracted with DCM (3 x 100 ml). The organic phase was washed with water (100 ml) and saturated NaCl solution (100 ml) before dried over $MgSO_4$. After the solvent was reduced to minimal level, the residue was transferred onto silica gel column and eluted with ethyl acetate-petroleum ether (2:3). The product was obtained as yellow oil (237 mg, 19%). δ H (400 MHz, $CDCl_3$) 8.12 – 7.96 (2-H (imida)), 7.97 – 7.71 (4 H, m, phenyl and tosyl), 7.32 (5 H, t, J 26.0, phenyl and tosyl), 5.36 – 5.20 (1 H, m, CH), 4.14 (8 H, s,),

2.45 (3 H, s, CH_3 tosyl), 2.38 – 2.08 (2 H, m, β-H2), 1.76 – 1.34 (15 H, m, 2(CH_3) and 3(CH_3)). δ C (75 MHz, $CDCl_3$) 137.05, 131.95, 130.50, 128.52, 128.45, 128.36, 127.23, 127.13, 72.28, 68.22, 66.00, 65.75, 54.91, 29.64, 28.39, 24.39, 21.67, 14.15.

2,5-dibromo-4-((4,5-dihydro-2-phenyloxazol-4-yl)methyl)-1H-imidazole (79)

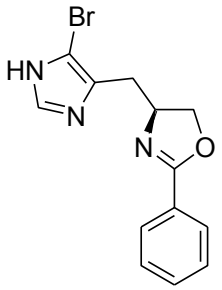

Into a stirring solution of 4-((4,5-dihydro-2-phenyloxazol-4-yl)methyl)-1H-imidazole, **76**, (1.1 g, 4.84 mmol) in acetonitrile-DMF (1:1) (10 ml) mixture in the dark (aluminium foil) under nitrogen, N-bromosuccinimide (0.8 g, 4.84 mmol) in acetonitrile (2 ml) was slowly added. After two hours of stirring, tlc showed complete conversion of the starting material. The solvent was reduced by evaporation before 10 g of silica was added. The solvent was removed in vacuo over silica and the dry silica was transferred onto a packed column and eluted with ethyl acetate-petroleum ether (2:3) to afford the product as a yellow solid (933 mg, 63%); δ H (400 MHz, $CDCl_3$) 7.95 (2 H, d, J 8.2, phenyl), 7.62 – 7.38 (4 H, m, phenyl and 2-H), 4.69 – 4.49 (2 H, m, α-H and CHa), 4.23 – 4.11 (1 H, m, CHb), 3.07 (1 H, dd, J 3.9, 15.0, β-Ha), 2.77 (1 H, dd, J 8.4, 15.0, β-Hb).

5-bromo-4-((4,5-dihydro-2-phenyloxazol-4-yl)methyl)-1-tosyl-1H-imidazole (80b)

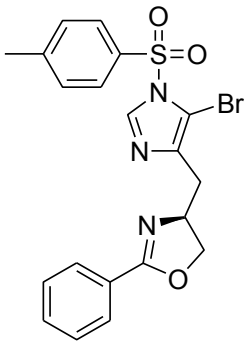

A mixture of 2,5-dibromo-4-((4,5-dihydro-2-phenyloxazol-4-yl)methyl)-1H-imidazole, **79**, (0.64 g, 2.08 mmol) and triethylamine (2.24 ml, 16 mmol) in DCM (10 ml) was cooled to 0^{o}C on ice bath before a solution of para-toluenesulfonyl chloride (0.61 g, 3.2 mmol) in DMC (5 ml) was added. The reaction mixture was stirred overnight at room temperature before stopped with saturated $NaHCO_3$ solution (50 ml). The mixture was extracted with DCM (2 x 50 ml), and the combined organic layers were washed with water (100 ml) and saturated NaCl solution (100 ml) before dried over $MgSO_4$ salt. Evaporation of the organic solvent afforded a crude solid which was purified by chromatography using ethyl acetate-petroleum ether (1:4) as the mobile phase. The product was obtained as a yellow solid (843 mg, 88%). M + H: 460.0 (exp), 460.0 (obt). δ H (400 MHz, Pyridine) 8.13 (1 H, d, J 0.9, 2-H), 8.08 – 7.98 (2 H, m, phenyl), 7.86 (2 H, d, J 8.4, tosyl), 7.55 (1 H, dd, J 4.0, 10.7, phenyl), 7.51 – 7.39 (4 H, m, phenyl and tosyl), 4.83 – 4.70 (1 H, m, α-H), 4.39 (1 H, t, J 9.0, CHa), 4.33 – 4.24 (1 H, m, CHb), 3.17 (1 H, dd, J 6.2, 14.8, β-Ha), 2.92 (1 H, dd, J 8.6, 14.8, β-Hb), 2.50 (3 H, s, CH_3, tosyl). δ C (101 MHz, $CDCl_3$) 164.42, 146.85, 137.50, 134.46, 131.49, 130.68, 128.46, 128.32, 127.56, 125.91, 120.36, 71.64, 66.02, 60.37, 30.37, 21.76.

***tert*-Butyl 1-hydroxy-3-(1H-imidazol-4-yl)propan-2-ylcarbamate (64)**

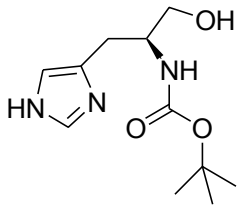

Into a stirring suspension of $LiAH_4$ (0.423 g, 11.14 mmol) in THF (18 ml) at -10^{o}C, *tert*-butyl 1-(methoxycarbonyl)-2-(1H-imidazol-4-yl)ethylcarbamate, **46**, (2 g, 7.43 mmol) in THF (5 ml) was added drop-wise over 15 minutes. The reaction was complete after 20 minutes (showed by tlc). A mixture of water-THF (1:1) (5 ml) was slowly added into the reaction mixture to stop the reaction. The mixture was quickly neutralized with 2 M NH_4Cl solutions and extraction was done with DCM (3 x 300 ml). The organic phase was washed with water (100 ml), saturated NaCl solution (100 ml) before dried over Na_2SO_4 salt. The solvent was removed to give an oily residue which was purified by chromatography using methanol-ethyl acetate (1:4) to give colourless oil (1.33 g, 74%); δ H (400 MHz, $CDCl_3$) 7.53 (1 H, s, 2-H), 6.79 (1 H, s, 4-H), 5.18 (1 H, s, N-H), 3.82 (1 H, s, α-H), 3.71 – 3.66 (1 H, m, C-H), 3.63 – 3.51 (1 H, m, CH), 2.88 (2 H, qd, J 5.8, 14.7, β-H2), 1.41 (9 H, d, J 8.1, 3(CH_3)).

***tert*-butyl 1-hydroxy-3-(5-iodo-1H-imidazol-4-yl)propan-2-ylcarbamate (65b)**

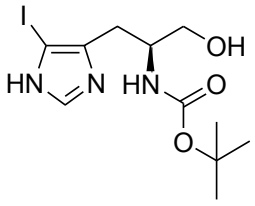

Method A: To a stirring solution of *tert*-butyl 1-hydroxy-3-(1H-imidazol-4-yl)propan-2-ylcarbamate, **64**, (0.1 g, 0.41 mmol) in acetonitrile (2 ml) at room temperature in the dark was added N-iodosuccinimide (0.092 g, 0.41 mmol) in acetonitrile (1 ml). The reaction mixture was stirred for 2 hours and tlc showed a total conversion of the starting material.

The solvent was removed by evaporation to give a yellow waxy residue which was purified by chromatography with methanol-ethyl acetate (1:4) as the mobile phase to give the product as a colourless oil (1.5 mg, 30%). δ H (400 MHz, $CDCl_3$) 7.56 (1 H, s, 2-H), 5.14 (1 H, s, N-H), 3.88 – 3.76 (1 H, m, α-H), 3.71 – 3.57 (2 H, m, CH_2), 2.94 – 2.70 (2 H, m, β-H2), 1.39 (9 H, s, 3(CH_3)).

Method B: Into a stirring solution of thiophenol (0.61 ml, 5.9 mmol) in isopropanol (20 ml) at room temperature, NaH (0.23 g, 5.9 mmol) in isopropanol (2 ml) was added. The reaction mixture was heated up to 35^{o}C and then a solution of *tert*-butyl 1-hydroxy-3-(2,5-diiodo-1H-imidazol-4-yl)propan-2-ylcarbamate, **65a**, (2 g, 5.4 mmol) in isopropanol (5 ml) was added. After 30 minutes the reaction was complete (confirmed by tlc). $NaHCO_3$ saturated solution (50 ml) was added and the aqueous mixture was extracted with DCM (3 x 100 ml), the organic layer washed with water (100 ml) and saturated NaCl solution (100 ml) before dried over $MgSO_4$. The solvent was removed by evaporation to give a yellow waxy residue which was purified by chromatography with methanol-ethyl acetate (1:4) as the mobile phase to give the product as colourless oil (595 mg, 30%).

***tert*-Butyl-5,7,8,9-tetrahydro-5,5-dimethylimidazo[1,5-c][1,3]oxazepin-8-ylcarbamate (66 and 67)**

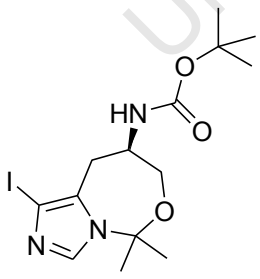

66

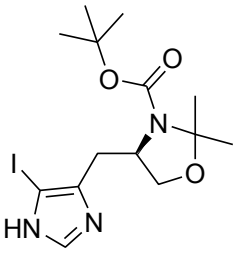

67

Into a stirring solution of *tert*-butyl 1-hydroxy-3-(5-iodo-1H-imidazol-4-yl)propan-2-ylcarbamate, **65**, (0.33 g, 0.9 mmol) in DCM (3 ml), 2.2-dimethoxypropane (3 ml, 24.4 mmol) was added. Para-toluenesulfonic acid (0.034 g, 0.18 mmol) in DCM (2 ml) was

added to the stirring mixture and the mixture was heated to reflux and stirred overnight under nitrogen. The mixture was poured into a saturated $NaHCO_3$ solution (50 ml) and extracted with DCM (3 x 100 ml). The organic phase was washed with water (50 ml), saturated NaCl solution (50 ml), dried over $MgSO_4$ salt and concentrated. Purification by column chromatography using ethyl acetate-petroleum ether (9:1) as eluent afforded two products:

66 as yellow oil (3.66 mg, 26%). δ H (400 MHz, $CDCl_3$) 7.47 (1 H, s, 2-H), 4.59 (1 H, s, N-H), 4.14 – 4.04 (1 H, m, CH), 3.99 (1 H, s, α-H), 3.70 (1 H, dd, J 4.1, 13.0, CH), 3.19 – 2.94 (2 H, m, β-H), 1.77 (3 H, s, CH_3), 1.68 (3 H, s, CH_3), 1.41 (9 H, s, 3(CH_3)). δ C (101 MHz, CDCl3) 136.20, 94.97, 89.89, 67.70, 48.50, 29.79, 28.57, 28.41, 26.58.

67 as yellow solid (70 mg, 19%). δ H (400 MHz, $CDCl_3$) 7.62 (1 H, s, 2-H), 4.09 (1 H, d, J 7.2, α-H), 3.87 (2 H, dd, J 9.4, 14.9, CH_2), 3.05 – 2.80 (2 H, m, β-H2), 1.52 (3 H, s, CH_3), 1.47 (9 H, s, 3(CH_3)), 1.45 (3 H, s, CH_3). δ H (400 MHz, $CDCl_3$) 7.47, 4.59, 4.09, 4.07, 4.06, 3.99, 3.72, 3.71, 3.69, 3.68, 3.10, 3.03, 3.02, 2.99, 2.98, 1.77, 1.68, 1.41.

***tert*-Butyl 1-(methoxycarbonyl)-2-(1-((benzyloxy)methyl)-1H-imidazol-4-yl)ethylcarbamate (68)**

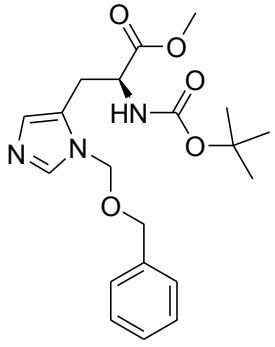

A stirring mixture of 3-Bom-α-N-Boc-His-OH, **44**, (10 g, 26.64 mmol) and K_2CO_3 (4.05 g, 29.3 mmol) in DMF (120 ml) on ice-bath was treated with methyl iodide (1.82 ml, 29.3 mmol). The reaction mixture was stirred overnight at room temperature and then poured into water (500 ml). The aqueous mixture was extracted with DCM (2 x 200 ml).

The organic phase was washed with saturated NaCl solution (200 ml), dried over $MgSO_4$ and concentrated to afford the product as a yellow solid (9.75 g, 94%) which did not require any further purification. δ H (400 MHz, $CDCl_3$) 7.44 (1 H, s, 2-H), 7.36 – 7.24 (5 H, m, phenyl), 6.83 (1 H, s, 4-H), 5.25 (3 H, q, J 11.1, N-H and NCH_2), 4.54 (1 H, s, α-H), 4.41 (2 H, s, OCH_2), 3.68 (3 H, s, OCH_3), 3.11 (2 H, ddd, J 6.3, 15.5, 22.5, β-H), 1.37 (9 H, s, 3(CH_3)).

tert-butyl 3-(1-((benzyloxy)methyl)-1H-imidazol-4-yl)-1-hydroxypropan-2-ylcarbamate (69)

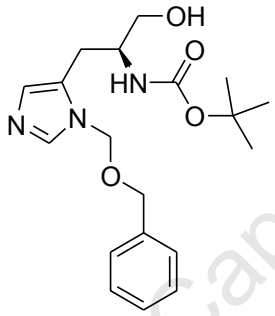

To a stirring suspension of *tert*-butyl 1-(methoxycarbonyl)-2-(1-((benzyloxy)methyl)-1H-imidazol-5-yl)ethylcarbamate, **68**, (1.3 g, 3.1mmol) in THF (15 ml) on ice-NaCl bath, $LiAH_4$ (0.23 g, 6.1 mmol) in THF (3 ml) was slowly added. The reaction mixture was stirred for 15 minutes and the ice-NaCl was removed. After stirring for 2 hours at room temperature, water was slowly added to stop the reaction. The slurry was $MgSO_4$ extracted with DCM (3 x 200 ml) and the organic phase was dried over $MgSO_4$. Removal of the solvent afforded an oily residue which was purified by column chromatography using DCM-methanol (9.5:0.5) as the mobile phase to give the product as a colourless oil (852 mg, 76%). δ H (400 MHz, $CDCl_3$) 7.47 (1 H, s, 2-H), 7.42 – 7.25 (5 H, m, phenyl), 6.88 (1 H, s, 4-H,), 5.32 (2 H, s, NCH_2), 5.09 (1 H, s, N-H), 4.46 (2 H, d, J 6.3, OCH_2), 3.84 (1 H, s, α-H), 3.66 – 3.49 (2 H, m, CH_2), 2.96 – 2.81 (2 H, m, β-H), 1.41 (9 H, s, 3(CH_3)).

***tert*-Butyl 3-(2-methoxypropan-2-yloxy)-1-(1-((benzyloxy)methyl)-1H-imidazol-4-yl)propan-2-ylcarbamate (70)**

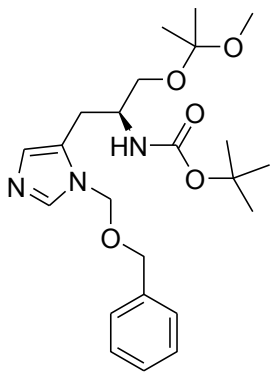

A solution of para-toluenesulfonic acid (0.105 g, 0.55 mmol) in DCM (3 ml) was added into a mixture of *tert*-butyl 3-(1-((benzyloxy)methyl)-1H-imidazol-4-yl)-1-hydroxypropan-2-ylcarbamate, **69**, (1 g, 2.75 mmol) and 2.2-dimethoxypropane (1.7 ml, 13.75 mmol) in DCM (10 ml). The reaction mixture was stirred at room temperature for 3 days and poured into saturated $NaHCO_3$ solution (50 ml). The aqueous mixture was extracted with DCM (3 x 50 ml) and the organic phase was washed with water (100 ml), saturated NaCl solution (100 ml) and dried over $MgSO_4$. The mixture was concentrated and purified by column chromatography using ethyl acetate-petroleum ether (9:1) as a mobile phase. The product was obtained as a colourless oil (0.441 g, 37%). δ H (400 MHz, $CDCl_3$) 7.67 (1 H, s, 2-H), 7.29 (5 H, ddd, J 4.3, 8.3, 25.9, phenyl), 6.85 (1 H, s, 4-H), 5.33 (2 H, s, NCH_2), 4.79 (1 H, s, N-H), 4.48 (2 H, s, OCH_2), 3.84 (1 H, s, α-H), 3.35 (2 H, d, J 4.0, CH_2), 3.13 (3 H, s, OCH3), 2.83 (2 H, dt, J 7.3, 14.5, β-H2), 1.34 (9 H, s, 3(CH_3)), 1.28 (6 H, s, 2(CH_3)).

Histidine methyl ester (35a)

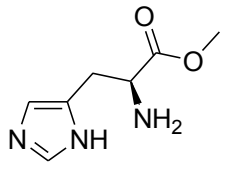

Thionyl chloride (1.59 ml, 26.3 mmol) was added drop-wise into a stirring cold anhydrous methanol (50 ml). Into the solution, L-histidine 1 (3.4 g, 21.91 mmol) was added in four portions to form a suspension. The cold bath was removed and the suspension was refluxed overnight. The mixture was allowed to cool before concentrated to afford a pale yellow paste. Additional methanol (50 ml) was added and the solution was evaporated again to afford a white solid. A hot ethyl acetate (3 x 30 ml) was added to form a suspension which was filtered. The solvent was removed in vacuo and the sample was dried on high vacuum pump to give a pale yellow paste (3.4 g, 76%).

methyl 5,6,7,8-tetrahydro-5-oxoimidazo[1,5-f]pyrimidine-7-carboxylate (36a)

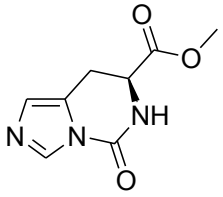

A mixture of histidine methyl ester, **35a**, (0.5 g, 2.96 mmol) and 1.1-carbonyldiimidazole (48 mg, 2.96 mmol) in acetonitrile (20 ml) was stirred at 80^{o}C overnight. The solvent was evaporated to give a yellow oily residue which was dissolved in saturated $NaHCO_3$ solution (50 ml). The aqueous mixture was extracted with ethyl acetate (2 x 100 ml). The organic phase was washed with water (100 ml) and saturated NaCl solution (100 ml) before dried over $MgSO_4$. The mixture was concentrated to give as an oily residue which was purified by column chromatography using methanol-DCM (1:9) as the mobile phase

to give the product as a white solid (468 mg, 81%), mp: 162-163°C. ^{1}H NMR (400 MHz, DMSO) δ 8.56 (s, 1H, N-H), 8.13 (s, 1H, 2-H), 6.85 (s, 1H, 4-H), 4.47 (t, J = 4.7, 1H, N(α)-H), 3.66 (s, 3H, OCH_3), 3.26 (d, J = 4.5, 2H, C-CH_2). ^{13}C NMR (101 MHz, DMSO) δ 172.11, 148.72, 135.03, 126.43, 125.34, 53.40, 52.56, 23.26.

Synthesis of 37a

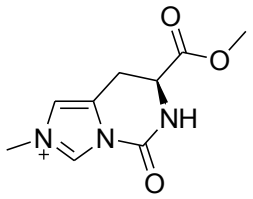

To a stirring suspension of methyl 5,6,7,8-tetrahydro-5-oxoimidazo[1,5-f]pyrimidine-7-carboxylate, **36a**, (0.1 g, 0.51 mmol) in acetonitrile (5 ml) was added methyl iodide (0.1 ml, 1.53 mmol). The reaction mixture was refluxed overnight and then cooled down to room temperature. The yellow crystals precipitated out of the reaction mixture were filtered and the product was recrystallized from acetonitrile to give a yellow solid (79 mg, 74%), mp: 175-176°C. ^{1}H NMR (400 MHz, DMSO) δ 9.77 (s, ^{1}H, 2-H), 9.52 (s, 1H, N-H), 7.64 (s, 1H, 4-H), 4.69 (s, 1H, (α)N-H), 3.92 (s, 3H, N-CH_3), 3.70 (s, 3H, OCH_3), 3.42 (s, 2H, CCH_2). ^{13}C NMR (101 MHz, DMSO) δ 171.11, 145.21, 136.23, 128.77, 121.16, 53.82, 52.03, 37.31, 22.22.

1-methylhistidine (14)

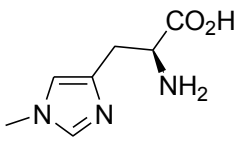

A solution of, **37a**, (0.05 g, 0.24 mmol) in 6 N HCl (5 ml) was stirred at 70°C overnight and the solvent was evaporated *in vacuo* to afford a yellow residue. The crude product was dissolved in 1 mM HCl (2 ml) and applied to an ion-exchange column (Dowex 50X 2-200, H^+ form), 1 ml bed volume. The column was washed with water until the eluent pH was neutral before the product was eluted with 10% NH_4OH solution. Evaporation of the solvent gave a pale yellow crystalline product (22 mg, 55%), mp 245°C. ^{1}H NMR (400 MHz, D_2O) δ 7.42 (s, 1H, 2-H), 6.76 (s, 1H, 4-H), 3.79 (t, J = 6.6, 1H, (α)N-H), 3.41 (s, 3H, NCH_3), 2.79 (qd, J = 6.6, 15.1, 2H, CCH_2). 13C NMR (101 MHz, D_2O) δ 174.02, 138.62, 133.53, 120.27, 53.57, 33.68, 30.07.

Synthesis of 39a

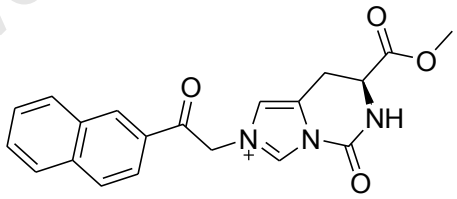

A mixture of methyl 5,6,7,8-tetrahydro-5-oxoimidazo[1,5-f]pyrimidine-7-carboxylate, **36a**, (0.2 g, 1.02 mmol) and 2-bromo-2'-acetonaphthone (0.21 g (1.02 mmol) in acetonitrile (5 ml) was refluxed overnight. The reaction mixture was cooled to room temperature and the formed precipitates were filtered. The crude product was recrystallized from acetonitrile to give the product as white crystals (264 mg, 71%), mp: 193-194°C. M + H: 323.1 (exp), 324.2 (obt). δ H (400 MHz, DMSO) 9.83 (1 H, s, 2-H), 9.65 (1 H, d, J 4.0, N-H), 8.86 (1 H, s, 4-H), 8.32 – 8.02 (4 H, m, aromatic), 7.86 – 7.67

(3 H, m, aromatic), 6.27 (2 H, s, CH_2), 4.76 (1 H, d, J 5.1, α-H), 3.75 (3 H, s, OCH_3), 3.52 (2 H, d, J 3.9, β-H2).

δ C (101 MHz, DMSO) 191.21, 171.17, 145.17, 137.11, 136.36, 132.80, 131.64, 131.31, 130.47, 130.20, 129.64, 128.67, 128.23, 123.93, 121.61, 56.88, 53.83, 52.14, 22.30.

methyl 1-(methoxycarbonyl)-2-(1-(2-(naphthalen-2-yl)-2-oxoethyl)-1H-imidazol-4-yl)ethylcarbamate (40a)

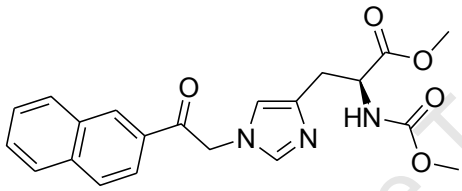

To a solution of, **39a**, (0.1 g, 0.27 mmol) in anhydrous methanol (5 ml) was added diisopropylethylamine (0.1 ml, 0.55 mmol). The resultant reaction mixture was heated to reflux overnight, at that point tlc showed a complete conversion of the starting material. The solvent was removed by evaporation and the residue was dissolved in DCM (20 ml). The solution was washed with water (50 ml), and the saturated NaCl solution (50 ml) before dried over $MgSO_4$. The solution was concentrated and purified by column chromatography using methanol-DCM (0.5:9.5) the mobile phase to afford the product (56 mg, 52%) as white solid, mp: 66-67^oC. ^1H NMR (300 MHz, $CDCl_3$) δ 8.48 (s, 1H, 2-H), 8.13-7.88 (4H, m, aromatic), 7.72-7.58 (3H, m, aromatic), 6.76 (1H, s, 4-H), 6.32 (1H, s, N-H), 5.45 (2H, s, NCH_2), 4.04 (1H, m, α-H), 3.70 (3H, s, $NCOCH_3$), 3.67 (3H, s, OCH_3), 3.22-3.08 (2H, m, β-H2). δ C (75 MHz, $CDCl_3$) 191.36, 172.30, 137.99, 137.59, 136.03, 132.35, 131.47, 129.79, 129.59, 129.24, 129.14, 127.92, 127.31, 123.19, 118.03, 54.03, 52.47, 52.23, 52.14, 30.18.

7,8-dihydroimidazo[1,5-f]pyrimidin-5(6H)-one (36b)

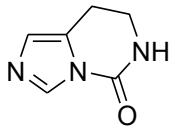

To a suspension of histamine, **35b**, (0.5 g, 4.5 mmol) in acetonitrile (10 ml) was added a solution of 1.1-carbonyldiimidazole (0.73 g, 4.5 mmol) in acetonitrile (10 ml). The reaction mixture was refluxed overnight. The solvent was removed by evaporation and the residue was dissolved in DCM (40 ml) which was then poured in a saturated $NaHCO_3$ solution (60 ml). The extraction of the crude product was done with DCM (3 x 40 ml) and the DCM phase was washed with water (50 ml), saturated NaCl solution (50 ml) and dried over $MgSO_4$ salt. Purification by chromatography with DCM-methanol (9.5:0.5) afforded the product (512 mg, 83%) as white solid, mp 220^{o}C. δ H (400 MHz, DMSO) 8.20 (1 H, s, br, N-H), 8.07 (1 H, s, 2-H), 6.82 (1 H, s, 4-H), 3.42 – 3.36 (2 H, m, NCH_2), 2.91 (2 H, t, J 6.4, CH_2). δ C (101 MHz, DMSO) 149.13, 134.73, 128.06, 125.40, 39.47, 20.04.

Synthesis of 37b

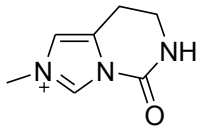

To a suspension of 7,8-dihydroimidazo[1,5-f]pyrimidin-5(6H)-one, **36b**, (0.1 g, 0.73 mmol) in acetonitrile (5 ml) was added methyl iodide (0.14 ml, 2.25 mmol). The resulting suspension was refluxed overnight. The reaction mixture was cooled to room temperature and the formed precipitates were filtered and recrystallized from acetonitrile to afford the product as white crystals (87 mg, 78%); mp: 197^{o}C. ^{1}H NMR (300 MHz,

DMSO) δ 9.63 (s, 1H, 2-H), 8.94 (s, 1H, N-α-H), 7.59 (s, 1H, 4-H), 3.91 (s, 3H, CH_3), 3.49 (td, J = 2.8, 6.5, 2H, N-CH_2), 3.03 (t, J = 6.1, 2H, C-CH_2).

1-methylhistamine (38b)

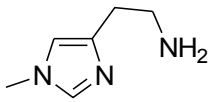

A solution of, **37b**, (0.1 g, 0.657 mmol) in 6 N HCl (5 ml) was stirred overnight at 70°C. The solvent was removed by evaporation; the residue was dissolved in 1 mM HCl (1 ml) and applied to an ion-exchange column (Dowex 50X 2-200, H^+ form). The column was washed with water until the eluent pH was neutral before the product was eluted with 10% NH_4OH solution. Evaporation of the solvent gave a white crystalline product (57 mg, 69%); ^{1}H NMR (300 MHz, CD_3OD) δ 7.48 (s, 1H, 2-H), 6.84 (s, 1H, 4-H), 3.67 (s, 3H, N-CH_3), 3.38 – 3.26 (m, 2H, N(α)-CH_2), 2.67 (t, J = 6.8, 2H, C-CH_2).^{13}C NMR (75 MHz, CD_3OD) δ 140.44, 138.64, 118.84, 40.95, 33.56, 29.63.

Synthesis of 39b

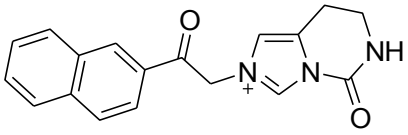

To a solution of 7,8-dihydroimidazo[1,5-f]pyrimidin-5(6H)-one, **36b**, (0.2 g, 1.46 mmol) in acetonitrile (10 ml) was added 2-bromo-2'-acetonaphthone (0.36 g, 1.46 mmol) and the reaction mixture was refluxed overnight, at that point a tlc showed a total conversion of the starting material. The reaction mixture was cooled to room temperature and the

formed precipitates were filtered and recrystallized from acetonitrile to give the product (331 mg, 74%) as white crystals; mp: 192-193^{o}C. ^{1}H NMR (400 MHz, DMSO) δ 9.75 (s, 1H, 2-H), 9.18 (s, 1H, N-H), 8.89 (s, 1H, 4-H), 8.21 (m, 3H, aryl), 7.75 (m, 2H, aryl), 6.30 (s, 2H, N-CH_2), 3.59 (m, 2H, N(α)-CH_2), 3.17 (d, J = 6.4, 2H, C-CH_2).

methyl 2-(1-(2-(naphthalen-2-yl)-2-oxoethyl)-1H-imidazol-4-yl)ethylcarbamate (40b)

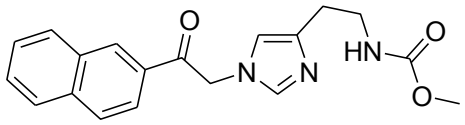

To a solution of, **39b**, (0.2 g, 0.65 mmol) in anhydrous methanol (5 ml) was added diisopropylethylamine (0.228 ml, 1.30 mmol). The resultant reaction mixture was heated to reflux overnight after which tlc showed complete conversion of the starting material. The solvent was removed by evaporation and the residue was dissolved in DCM (20 ml). The solution was washed with water (50 ml), and the saturated NaCl solution (50 ml) before dried over $MgSO_4$. The solution was concentrated and purified by column chromatography using methanol-DCM (0.5:9.5) as the mobile phase to afford the product (105 mg, 48%) as a white solid; mp: 147-149^{o}C. δ H (300 MHz, $CDCl_3$) 8.48 (1 H, s, 2-H), 8.05 – 7.86 (4 H, m, aromatic), 7.63-746 (3 H, dddd, J 1.4, 6.9, 8.2, 14.7, aromatic), 6.75 (1 H, t, J 6.5, 4-H), 5.47 (2 H, s, NCH_2), 3.65 (3 H, s, OCH_3), 3.51 (2 H, dd, J 6.0, 12.2, N(α)CH_2), 2.79 (2 H, t, J 6.4, CH_2).

2-amino-3-(1-((benzyloxy)methyl)-1H-imidazol-4-yl)propanoic acid (45)

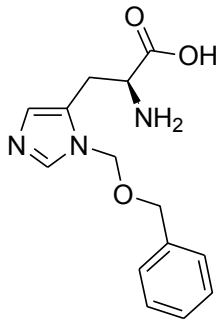

3-Bom-α-N-Boc-His-OH, **44**, (2 g, 5.33 mmol) was added to 20% trifluoroacetic acid in DCM (20 ml). The reaction mixture was stirred for 2 hours at room temperature after

which tlc showed a complete conversion reaction of the starting material. The solvent was removed by evaporation to give a residue which was dissolved in 1mM HCl (5 ml) and applied to an ion-exchange column (Dowex 50X 2-200, H^+ form). The column was washed with water until the eluent pH was neutral before the product was eluted with 10% NH_4OH solution. Evaporation of the solvent gave the product (1.26 g, 86%) as white solid. ^{1}H NMR (400 MHz, DMSO) δ 7.75 (s, 1H, 2-H), 7.40-7.25 (m, 5H, aryl protons), 6.90 (s, 1H, 4-H), 5.55-5.42 (m, 2H, NCH_2), 4.60-4.52 (m, 2H, Ar-CH_2), 3.62 (m, 1H, (α)N-H), 3.31-3.00 (m, 2H, CCH_2). δ C (101 MHz, DMSO) 171.00, 139.22, 138.08, 129.05, 128.93, 128.38, 128.19, 74.41, 70.31, 54.06, 26.57.

tert-Butyl 1-(2-aminoethylcarbamoyl)-2-(1-((benzyloxy)methyl)-1H-imidazol-5-yl)ethylcarbamate (49)

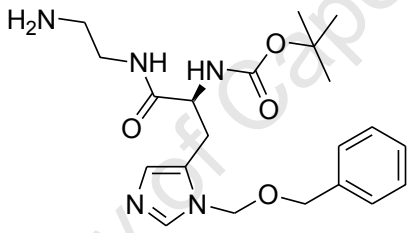

To a solution of 3-Bom-α-N-Boc-His-OH, **44**, (2 g, 5.33 mmol) in THF (20 ml) was added N,N'-carbonyldiimidazole (1.04 g, 6.42 mmol). The mixture was stirred at room temperature until bubbling ceased and the reaction mixture was cooled to -10^{o}C (ice-NaCl bath). Ethylenediamine (1.79 ml, 26.65 mmol) was added. The reaction mixture was stirred vigorously for 30 minutes and the ice bath was removed. After 2 hours the solvent was removed and the residue was purified by flash chromatography using acetone as the mobile phase. The product (1.9 g, 86%) was obtained as yellow oil. M + H: 418.2 (exp), 418.3 (obt). ^{1}H NMR (400 MHz, $CDCl_3$) δ 7.50 (s, 1H, 2-H), 7.41 – 7.29 (m, 5H, aromatic), 6.89 (s, 1H, 4-H), 5.34 (dd, J = 10.9, 23.1, 2H, NCH_2), 4.53 (d, J = 11.9, 2H, aryl-CH_2), 4.38 (s, 1H, (α)N-H), 3.17 (m, 2H, CCH_2), 3.09 (d, J = 7.1, 2H, amide-CH_2), 2.65 (d, J = 12.2, 2H, amine-CH_2), 1.42 (d, J = 5.6, 9H, $C(CH_3)_3$).^{13}C NMR (75 MHz,

$CDCl_3$) δ 170.85, 138.35, 135.94, 129.39, 128.72, 128.40, 128.09, 127.28, 73.11, 70.11, 54.10, 42.10, 41.04, 30.84, 28.26, 27.10.

tert-Butyl 1-(2-aminoethylcarbamoyl)-2-(1H-imidazol-5-yl)ethylcarbamate (50)

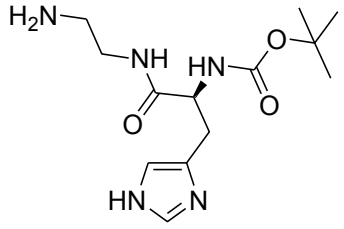

Into a stirring solution of _tert_-butyl 1-(2-aminoethylcarbamoyl)-2-(1-((benzyloxy)methyl)-1H-imidazol-5-yl)ethylcarbamate, **49**, (0.2 g, 0.48 mmol) in anhydrous methanol (1 ml), 10% Pd-C (0.2 g) in anhydrous methanol (2ml) was added. To the stirring suspension hydrazinium monoformate (0.2 ml, 2.3 mmol) was added. The mixture was stirred overnight. The mixture was then filtered over celite and washed with methanol (10 ml). Evaporation of the solvent afforded a yellow residue which was dissolved in ethyl acetate (20 ml) and washed with saturated NaCl solution (50 ml). The organic solvent was dried over $MgSO_4$ and the solvent was removed. The residue was dissolved in 1 mM HCl (2 ml) and transferred onto ion exchange column (Dowex 50X 2-200, H^+ form). The column was washed with water until the eluent pH was neutral before the product was eluted with 10% NH_4OH solution. Evaporation of the solvent afforded the product (60 g, 42%) as a yellow oil; ^{1}H NMR (400 MHz, CD_3OD) δ 7.58 (s, 1H, 2-H), 6.84 (s, 1H, 4-H), 4.25 (s, 1H, (α)N-H), 3.30 (d, J = 1.7, 2H, amide-CH_2), 2.95 (d, J = 57.1, 2H, CCH_2), 2.42 (t, J = 6.7, 2H, amine-CH_2), 1.40 (s, 9H, $C(CH_3)_3$). ^{13}C NMR (101 MHz, CD_3OD) δ 126.80, 49.53, 46.77, 35.91, 28.41, 21.21, 19.14.

2-amino-N-(2-aminoethyl)-3-(1-((benzyloxy)methyl)-1H-imidazol-5-yl)propanamide (17)

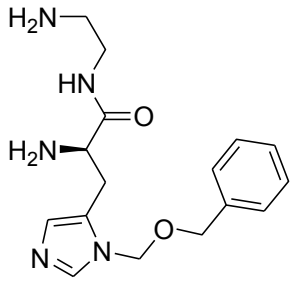

tert-Butyl 1-(2-aminoethylcarbamoyl)-2-(1-((benzyloxy)methyl)-1H-imidazol-5-yl) ethylcarbamate, **49**, (0.5 g, 1.2 mmol) was dissolved in 20% trifluoroacetic acid in DCM (10 ml). After 2 hours of stirring the solvent was removed by evaporation and the residue was loaded onto a silica column. The column was washed with acetone and then eluted with a mixture of methanol-water (4:1). The solvent was removed to give a residue which was dissolved in 1 mM HCl (5ml) and applied to an ion-exchange column (Dowex 50X 2-200, H^+ form). The column was washed with water until the eluent pH was neutral before the product was eluted with 10% NH_4OH solution. Evaporation of the solvent afforded the product (278 mg, 73%) as yellow oil. M + H: 318.2 (exp), 318.2 (obt). ^1H NMR (300 MHz, cd3od) δ 7.73 (s, 1H, 2-H), 7.39 – 7.22 (m, 5H, aryl protons), 6.87 (s, 1H, 4-H), 5.52 (dt, J = 10.7, 21.3, 2H, NCH_2), 4.49 (s, 2H, Aryl-CH_2), 3.88 (dd, J = 4.0, 7.8, 1H, (α)N-H), 3.32 – 3.27 (m, 2H, amide-CH_2), 3.20 (dt, J = 4.9, 17.0, 2H, CCH_2), 2.77 (dd, J = 8.4, 15.6, 2H, amine-CH_2). δ C (75 MHz, CD_3OD) 176.09, 139.51, 129.56, 129.52, 129.04, 128.99, 128.83, 128.79, 78.04, 75.29, 71.34, 59.02, 43.06, 41.39, 26.41.

2-amino-N-(2-aminoethyl)-3-(1H-imidazol-4-yl)propanamide (16)

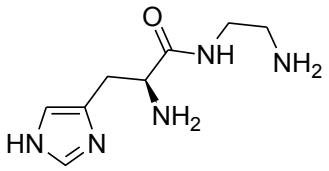

A solution of *tert*-butyl 1-(2-aminoethylcarbamoyl)-2-(1H-imidazol-5-yl)ethylcarbamate, **50**, (0.2 g, 0.67 mmol) in 20% trifluroacetic acid in DCM (5 ml) was stirred at room temperature for 2 hours. The solvent was evaporated and the crude residue dissolved in 1 mM HCl (2ml) and transferred onto ion exchange column (Dowex 50 WX 2-200, H^+ form). The column was washed with water until the eluent pH was neutral before the product was eluted with 10% NH_4OH solution. The column was washed with water until the eluent pH was neutral before the product was eluted with 10% NH_4OH solution. Evaporation of the solvent afforded the product (69 mg, 52%) as yellow oil; ^1H NMR (400 MHz, D_2O) δ 7.41 (s, 1H, 2-H), 6.66 (s, 1H, 4-H), 3.35 (d, J = 6.6, 1H, (α)N-H), 3.12 (d, J = 8.9, 2H, amide-CH2), 2.66 (t, J = 20.8, 2H, CCH_2), 2.45 (dd, J = 11.5, 18.0, 1H, amide-CH_2).

Alternatively, **16** could be synthesized from **17**. Thus, into a stirring solution of 2-amino-N-(2-aminoethyl)-3-(1-((benzyloxy)methyl)-1H-imidazol-5-yl)propanamide, **17**, (0.15 g, 0.47 mmol) in anhydrous methanol (1 ml), 10% Pd-C (0.2 g) in anhydrous methanol (2 ml) was added. To the stirring suspension hydrazinium monoformate (0.2 ml, 2.3 mmol) was added. The mixture was stirred overnight, then filtered over celite and washed with methanol (10 ml). The residue was dissolved in 1 mM HCl (2 ml) and transferred onto ion exchange column (Dowex 50X 2-200, H^+ form). The column was washed with water until the eluent pH was neutral before the product was eluted with 10% NH_4OH solution. The column was washed with water until the eluent pH was neutral before the product was eluted with 10% NH_4OH solution. Evaporation of the solvent afforded the product (35 mg, 38%) as yellow oil.

4,5-diiodo-1H-imidazole (52)

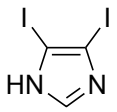

Hexane (75 ml) was added into a solution of imidazole, **50**, (1g, 14.5 mmol) in 0.04N NaOH (300 ml) and stirred vigorously. The mixture was cooled to 0^{o}C before a solution of iodine (3.72 g, 14.5 mmol) in hexane (300 ml) was added. 0.2 N NaOH (300 ml) was added drop-wise over 1.2 hours and the temperature was raised to about 8^{o}C. The reaction mixture was neutralized to pH 7 using 4N HCl and refrigerated overnight to form precipitates. The crystalline material was collected by filtration and recrystallized from ethanol-water (4:1) mixture to give the product (3.1 g, 67%) as white crystals; mp: 196-196^{o}C. δ H (300 MHz, DMSO) 7.77 (1 H, s, 2-H).

1-((benzyloxy)methyl)-4,5-diiodo-1H-imidazole (53)

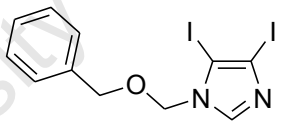

To a stirring solution of 4,5-diiodo-1H-imidazole, **52**, (0.5 g, 1.56 mmol) in anhydrous DMF (10 ml) under nitrogen, K_2CO_3 (4.3 g, access) was added to form a suspension, and to this benzyl chloromethyl ether (0.22 ml, 1.56 mmol) was added drop-wise. The mixture was stirred overnight at room temperature under nitrogen. The suspension was filtered and the filtrates were dissolved into water (100 ml). The solution was extracted with DCM (3 x 50 ml) and dried over $MgSO_4$. The solvent was reduced to 20ml before silica (5 g) was added. The dried silica was transferred onto a packed column and the column was eluted with ethyl acetate-petroleum ether mixture (3:7) and the product (475 mg, 72%) was obtained as pale yellow solid; mp: 89-90^{o}C. δ H (400 MHz, $CDCl_3$) 7.65 (1 H, s, 2-H), 7.37 – 7.24 (5 H, m, phenyl), 5.32 (2 H, s, NCH_2), 4.47 (2 H, s, OCH_2).

1-((benzyloxy)methyl)-4-iodo-1H-imidazole-5-carbaldehyde (55)

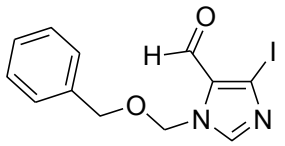

Into a solution of 1-((benzyloxy)methyl)-4,5-diiodo-1H-imidazole 25 (0.2 g, 0.45 mmol) in THF (5ml) at -78^{o}C under nitrogen, nBuLi (0.29 ml, 0.5 mmol) was slowly added. The reaction mixture was stirred for 10 min before DMF (1ml) was added. The mixture was allowed to warm to room temperature before it was quenched with saturated NH_4Cl solution (10 ml). The aqueous mixture was extracted with ethyl acetate (2 x 50 ml) and the organic phase was washed with water (50 ml) and saturated NaCl solution (50 ml) before dried over $MgSO_4$. Removal of the solvent afforded a yellow residue which was purified by chromatography to give the product (105 mg, 68%) as yellow oil; δ H (300 MHz, $CDCl_3$) 9.75 (1 H, dd, J 1.0, 2.1), 7.41 (1 H, d, J 0.9), 7.39 – 7.19 (8 H, m), 5.86 – 5.78 (3 H, m), 4.57 (2 H, s). δ C (75 MHz, $CDCl_3$) 181.19, 136.00, 130.89, 129.13, 128.62, 128.40, 127.98, 127.82, 85.49, 75.73, 71.75.

REFERENCES

Allen, C.L. Goulding, D. and Field, M.C. (2003) Clathrin-mediated endocytosis is essential in *Trypanosoma brucei*. EMBO J. 22:4991–5002.

Ariyanayagam, M.R. and Fairlamb, A.H. (2001) Ovothiol and trypanothione as antioxidants in trypanosomatids. Mol. Biochem. Parasitol. 115: 189–198.

Arnoštová, H. Kučerová, Z. Tišlerová, I. Trnka, T. Tichá, M. (2001) Affinity chromatography of porcine pepsin on different types of immobilized 3,5-diiodo-L-tyrosine. Journal of Chromatography A. 911 (2): 211-216.

Arrick, B.A. Griffith, O.W. and Cerami, A. (1981) Inhibition of glutathione synthesis as a chemotherapeutic strategy for trypanosomiasis. J. Exp. Med. 153:720–725.

Bailly, F. Zoete, V. Vamecq, J. Catteau, J.P. Jean-Luc Bernie, J.L. (2000)
Antioxidant actions of ovothiol-derived 4-mercaptoimidazoles: glutathione peroxidase activity and protection against peroxynitrite-induced damage. FEBS Letters 486: 19- 22.

Bajwa, J.S. Chen, G.P. Prasad, K. Repic, O. and Blacklock, T.J. (2006) Deprotection of N-tosylated indoles and related structures using cesium carbonate. Tetrahedron Lett. 47(36): 6425-6427.

Bakhiet, M. Olsson, T. Edlund, C. Hojeberg, B. Holmberg, K. Lorentzen, J. and Kristensson, K. (1993) A Trypanosoma brucei brucei-derived factor that triggers CD8+ lymphocytes to interferon-gamma secretion: purification, characterization and protective effects in vivo by treatment with a monoclonal antibody against the factor. Scand. *J. Immunol.* 37:165- 178.

Balaña-Fouce, R. Reguera, R.M. Cubrìa, J.C. and Ordóñez, D. (1998) The Pharmacology of Leishmaniasis. Gen. Pharmac. 30(4): 435–443.

Basu, M.J. Mookerjee, A. Banerjee, R. Saha, M. Singh, S. Naskar, K. Tripathy, G. Sinha, K.P. Pandey, K. Sundar, S. Bimal, S. Das, K.P. Choudhuri, K.S. and Roy, S. (2008) Inhibition of ABC Transporters Abolishes Antimony Resistance in Leishmania Infection. ANTIMICROBIAL AGENTS AND CHEMOTHERAPY. 1080–1093.

Bellina, F. and Rossi, R. (2010) Regioselective Functionalization of the Imidazole Ring via Transition Metal-Catalyzed C-N and C-C Bond Forming Reactions. Adv. Synth. Catal. 2010, 352, 1223 – 1276.

Bisser, S. N'Siesi, F.X. Lejon, V. Preux, P.M. Van Nieuwenhove, S. Bilenge, C.M. M. and Büscher, P. (2007) Equivalence Trial of Melarsoprol and Nifurtimox Monotherapy and Combination Therapy for the Treatment of Second-Stage Trypanosoma brucei gambiense Sleeping Sickness. *J Infect Dis.* 195: 322–329.

Blum, J. and Burri, C. (2002) Treatment of late stage sleeping sickness caused by *T. b. gambiense*: a new approach to the use of an old drug. SWISS MED WKLY. 132: 51–56.

Boger, D.L. and Yohannes, D. (1988) Studies on the Total Synthesis of Bouvardin and Deoxybouvardin: Cyclic Hexapeptide Cyclization Studies and Preparation of Key Partial Structures. J. Org. Chem. 53: 487-499.

Brak, K. Doyle, S.P. McKerrow, H.J. and Ellman, A.J. (2008) Identification of a New Class of Nonpeptidic Inhibitors of Cruzain. J. Am. Chem. Soc.130: 6404–6410.

Bruijnincx, A.C.P. van Koten, G. and Klein Gebbink, J.M.R. (2008) Mononuclear non-heme iron enzymes with the 2-His-1-carboxylate facial triad: recent developments in enzymology and modeling studies. Chem. Soc. Rev. 37: 2716–2744.

Bushnell, A.C.E. Fortowsky, B.G. and Gauld, W.J. (2012) Model-Oxo Species and the Oxidation of Imidazole: Insights into the Mechanism of OvoA and EgtB? Inorganic Chemistry. 51: 13351 – 13356.

Callens, M. and Hannaert, V. (1995) The rational design of trypanocidal drugs: selective inhibition of the glyceraldehyde-3-phosphate dehydrogenase in Trypanosomadidae. Ann Trop. Med. Parasitol. 89: 23 – 30.

Carrillo, C. Cejas, S. González, N.S. and Algranati, I.D. (1999) Trypanosoma cruzi epimastigotes lack ornithine decarboxylase but can express a foreign gene encoding this enzyme. FEBS Lett. 454: 192–196.

Carver, D.S. Lindell, S.D. and Saville-Stones, E.A. (1997) Polyfunctionalisation of Imidazole via Sequential Imidazolyl Anion Formation. Tetrahedron. 53: 14481 – 14496.

Cheah, K.I. and Halliwell, B. (2012) Ergothioneine, antioxidant potential, physiological function and role in disease. Biochemica et Biophysica Act. 1822: 784 – 793.

Chivikas, C.J. and Hodges, J.C. (1987) Phenacyl-Directed Alkylation of Imidazoles: A New Regiospecific Synthesis Qf 3-Substituted L-Histidines. J. Org. Chem. 52: 3591-3594.

Comini, M. Menge, U. Flohe, L. (2003) Biosynthesis of trypanothione in Trypanosoma brucei brucei. Biol. Chem.. 384: 653–6.

Comini, M.A. Guerrero, S.A. Haile, S. Menge, U. Lunsdorf, H. and Flohe, L. (2004) Validation of Trypanosoma brucei trypanothione synthetase as drug target. Free Radical Biol. Med. 36: 1289–1302.

Costas, M. Mehn, M.P. Jensen, M.P. and Que, L. Jr. (2004) Dioxygen activation at mononuclear nonheme iron active sites: enzymes, models, and intermediates. Chem. Rev. 104: 939–986.

Coura, R.J. and de Castro, L.S. (2002) A Critical Review on Chagas Disease Chemotherapy. Mem Inst Oswaldo Cruz, Rio de Janeiro. 97(1): 3-24.

Cox, G.E.F. (2002) History of Human Parasitology. Clin. Microbio. Rev. 15(4): 595–612.

Crich, D. and Banerjee, A. (2006) Expedient Synthesis of threo-β Hydroxy-l-amino Acid Derivatives: Phenylalanine, Tyrosine, Histidine, and Tryptophan. J. Org. Chem. 71 (18): 7106-7109.

Dawson, R.M.C. *et al.,* (1959) Data for Biochemical Research, Oxford, Clarendon Press.

Denisov, I.G. Makris, T.T. Sligar, S.G. and Schlichting, I. (2005) Structure and Chemistry of Cytochrome P450. Chem. Rev. 105: 2253–2277.

Desjeux, P. (2001) The increase in risk factors for leishmaniasis worldwide (2001) *Transactions of the Royal Society of Tropical Medicine and Hygiene*. 95 (3): 239-243.

Droge, W. (2002) Free radicals in the physiological control of cell function. Physiol. Rev. 82: 47–95.

Duleu, S. Vincendeau, P. Courtois, P. Semballa, S. Lagroye, I. Daulouede, S. Boucher, J.L. Wilson, K.T. Veyret, B. and Gobert, A.P. (2004) Mouse strain susceptibility to trypanosome infection: an arginase-dependent effect, *J. Immunol.* 172: 6298- 6303.

Eichler, J.F. Cramer, J. C. Kirk, K.L. Bann, J.G. (2005) Biosynthetic incorporation of fluorohistidine into proteins in E. coli: A new probe of macromolecular structure. Chem. Bio. Chem. 6(12): 2170-2173.

El Kouni, H.M. (2003) Potential chemotherapeutic targets in the purine metabolism of parasites. Pharmacology & Therapeutics. 99: 283– 309.

Faundez, M. Pino, L. Letelier, P. Ortiz, C. Lopez, R. Seguel, C. Ferreira, J. Pavani, M. Morello, A. Maya, J.D. (2005) Buthionine sulfoximine increases the toxicity

of nifurtimox and benznidazole to Trypanosoma cruzi. Antimicrob. Agents Chemother. 49:126–130.

Flashman, E. Davies, L.S. YEOH, K.K. and Schofield, J.C. (2010) Investigating the dependence of the hypoxia-inducible factor hydroxylases (factor inhibiting HIF and prolyl hydroxylase domain 2) on ascorbate and other reducing agents. Biochem. J. 427: 135-142.

Foerder, A.C. and Shapiro, M.B. (1977) Release of ovoperoxidase from sea urchin eggs hardens the fertilization membrane with tyrosine crosslinks. Proc. Natl. Acad. Sci. USA. 74(10): 4214-4218.

Fonseca, G.S. Romáo, R.T.P. Figueiredo, F. Morais, H.R. Lima, C.H. Ferreira, H. S. and Cunha, Q.F. (2003) TNF-α mediates the induction of nitric oxide synthase in macrophages but not in neutrophils in experimental cutaneous leishmaniasis. Eur. J. Immunol. 33: 2297–2306.

Frézard, F. Demicheli, C. and Ribeiro, R.R. (2009) Pentavalent Antimonials: New Perspectives for Old Drugs. Molecules. 14: 2317-2336.

Garin, W.J.F. Meneceur, P. Pratlong, F. Dedet, J.P. Derouin, F. and Lorenzo, F. (2005) A2 gene of Old World cutaneous Leishmania is a single highly conserved functional gene BMC Infectious Diseases. 5:18.

Ghedin, E. Zhang, W.W. Charest, H. Sundar, S. Kenney, R.T. and Matlashewski, G. (1997) Antibody response against a Leishmania donovani amastigote-stage-specific protein in patients with visceral leishmaniasis. Clin. Diagn. Lab. Immunol. 4: 530- 535.

Ghoda, L. Phillips, M.A. Bass, K.E. Wang, C.C. and Coffino, P. (1990) Trypanosome ornithine decarboxylase is stable because it lacks sequences found in the carboxyl terminus of the mouse enzyme which target the latter for intracellular degradation. J. Biol. Chem. 265:11823–11826.

Giralt, E. Ludevid, M. Albericio, F. and Bassedas, M. (1979) Acid-Base Properties of 4-Nitro-L-histidine and Related Compounds. Bioorganic chemistry. 8: 659-67.

Giralt, E. Pons, M. and Andreu, D. (1985) Use of Histidine pK, Changes to StudyPeptide-DNA Interactions. Bioorganic chemistry. 13: 171 – 178.

Gobert, A.P. Daulouede, S. Lepoivre, M. Boucher, J.L. Bouteille, B. Buguet, A. Cespuglio, R. Veyret, B. and Vincendeau, P. (2000) L-arginine availability modulates local nitric oxide production and parasite killing in experimental trypanosomiaisis. *Infect. Immun.* 68: 4653- 4657.

Gowda, C.D. and Mahesh, B. (2002) New hydrogen donor: a facile method for the removal of hydrogenolyzable protecting groups in peptide synthesis. Protein and Peptide Letters. 9(3): 225-230.

Goyeneche-Patino, A.D. Valderrama, L. Walker, J. and Saravia, G.N. (2008) Antimony Resistance and Trypanothione in Experimentally Selected and Clinical Strains of Leishmania panamensis. Antimicrobial Agents and Chemotherapy. 52(12): 4503–4506.

Groziak, M.P. and Wei, L. (1991) Regioselective Formation of Imidazol-2-yllithium, Imidazol-4-yllithium, and Imidazol-8- yllit hium Species. J. Org. Chem. 56: 4296-4300.

Guhl, F. Jaramillo, C. Yockteng, R. Vallejo, G.A. and Cardenas-Arroyo, F. (1997) Trypanosoma cruzi DNA in human mummies. *Lancet.* 349: 1370.

Guido, V.C.R. Oliva, G. Montanari, A.C. and Andricopulo, D.A. (2008) Structural Basis for Selective Inhibition of Trypanosomatid Glyceraldehyde-3-Phosphate Dehydrogenase: Molecular Docking and 3D QSAR Studies. J. Chem. Inf. Model. 48: 918–929.

Hand, E.C. Taylor, J.N. and John, F. Honek, F.J. (2005) Ab initio studies of the properties of intracellular thiols ergothioneine and ovothiols. Bioorganic & Medicinal Chemistry Letters. 15: 1357–1360.

Harth, G. Andrews, N. Mills, A.A. Engel, J.C. Smith, R. and McKerrow, J.H. (1993) Mol. Biochem. Parasitol. 58: 17–24.

Heby, O. Persson, L. and Rentala, M. (2007) Targeting the polyamine biosynthetic enzymes: a promising approach to therapy of African sleeping sickness, Chagas' disease, and leishmaniasis. Amino Acids. 33: 359–366.

Heby, O. Roberts, C.S. and Ullman, B. (2003) Polyamine biosynthetic enzymes as drug targets in parasitic protozoa. Biochemical Society Transactions. 31. part 2: 415- 149.

Heinzel, F.P. Schoenhaut, D.S. Rerko, R.M. Rosser, L.E. and Gately, M.K. (1993) Recombinant interleukin 12 cures mice infected with Leishmania major. J. Exp. Med. 177: 1505–1512.

Holler, P.T. and Hopkins, B.P. (1990) Ovothiols as Free-Radical Scavengers and the Mechanism of Ovothiol-Promoted NAD(P)H-O_2 Oxidoreductase Activity. Biochemistry. 29(7): 1953-1961.

Holler, P.T. and Hopkins, B.P. (1988) Ovothiols as Biological Antioxidants. The Thiol Groups of Ovothiol and Glutathione Are Chemically Distinct. J. Am. Chem. SOC. 110: 4837-4838.

Holzmuller, P. Biron, D.G. Courtois, P. Koffi, M. Bras-Gonçalves, R. Dauloue`de, S. Solano, P. Cuny, G. Vincendeau, P. and Jamonneau, V. (2008) Virulence and pathogenicity patterns of Trypanosoma brucei gambiense field isolates in experimentally infected mouse: differences in host immune response modulation by secretome and proteomics. *Microbes and Infection.* 10: 79- 86.

Hou, D. Reibenspies, J.H. and Burgess, K. (2001) New, Optically Active Phosphine Oxazoline (JM-Phos) Ligands: Syntheses and Applications in Allylation Reactions. J. Org. Chem. 66: 206-215.

Howard, R.J. Andrutis, A.T. Leech, J.H. Ellis, W.Y. Cohen, L.A. and Kirk, L.K. (1986) Inhibitory effects of histidine analogues on growth and protein synthesis by Plasmodium falciparum in vitro. Biochemical Pharmacology. 35(9): 1589-1596.

Huynh, T.T. Huynh, T.V. Harmon, A.M. and Phillips, A.M. (2003) Gene knockdown of gammaglutamylcysteine synthetase by RNAi in the parasitic protozoa Trypanosoma brucei demonstrates that it is an essential enzyme. J. Biol. Chem. 278: 39794–39800.

Iddon, B. Khan, N. and Lim, B.L. (1987) Azoles. Part 4.' Nucleophilic Substitution Reactions of Halogenoimidazoles. J. Chem. Soc. Perkin Trans 1: Org. Bio-Org. Chem. (1972-1999)7: 1437-43.

Irigoín, F. Cibils, L. Comini, A.M. Wilkinson, R.S. Flohé, L. and Radi, R. (2008) Insights into the redox biology of Trypanosoma cruzi: Trypanothione metabolism and oxidant detoxification. Free Radical Biology & Medicine.10. 4C: 4.

Ishikawa, Y. Israel, S.E. and Melville, D.B. (1974) Participation of an intermediate sulfoxide in the enzymatic thiolation of the imidazole ring of hercynine to form ergothioneine. J. Biol. Chem. 249: 4420- 4427.

Iten, M. Matovu, E. Brun, R. and Kaminsky, R. (1995) Innate lack of susceptibility of Ugandan Trypanosoma brucei rhodesiense to DL-alpha-difluoromethylornithine (DFMO). Trop. Med. Parasitol. 46: 190–194.

Jain, R. and Cohen, L.A. (1996) Regiospecific Alkylation of Histidine and Histamine at N-1 (τ) Tetrahedron. 5(15): 5363-5370.

Jain, R. Avramovitch, B. and Cohen, L.A. (1998) Synthesis of Ring-Halogenated Histidines and Histamines. Tetrahedron. 54: 3235-3242.

Kennedy, G.E.P. (2006) Diagnostic and neuropathogenesis issues in human African trypanosomiasis. International *Journal for Parasitology.* 36: 505–512.

Kennedy, G.E.P. (2008) Diagnosing central nervous system trypanosomiasis: two stage or not to stage? Transactions of the Royal Society of Tropical Medicine and Hygiene. 102: 306—307.

Khabnadideh, S. Pez, D. Musso, A. Brun, R. Pérez, M.R.L. González-Pacanowska, D. and Gilbert, H.I. (2005) Design, synthesis and evaluation of 2,4 diaminoquinazolines as inhibitors of trypanosomal and leishmanial dihydrofolate reductase. Bioorg. Med. Chem. 13: 2637–2649.

Kise, N. Urai, T. Yoshida, J.I. (1998) Formation and reaction of 2-metalated N-Boc-4,4-dimethyl-1,3- oxazolidines in the presence of (-)-sparteine: New chiral formyl anion equivalents. Tetrahedron As. 9(17): 3125-3128.

Krauth-Siegel, R.L. and Comini, M.A. (2008) Redox control in trypanosomatids, parasitic protozoa with trypanothione-based thiol metabolism. Biochimica et Biophysica Acta. 1780: 1236–1248.

Kumar, A. Ghilagaber, S. Knight, J. and Wyatt, P.B. (2002) The homologation of histidine. Tetrahedron Lett. 43: 6991–6994.

Laemmli, U.K. (1970) Cleavage of Structural Proteins during the Assembly of the Head of Bacteriophage T4. Nature. 227: 680-685.

Lake, J.A. De La Cruz, V.F. Ferreiraf, P.C.G. Morels, C. and Simpson, L. (1988) Evolution of parasitism: Kinetoplastid protozoan history reconstructed from mitochondrial rRNA gene sequences *Proc. Natl. Acad. Sci.* 85: 4779- 4783.

Lejon, V. Legros, D. Richer, M. Ruiz, J.A. Jamonneau, V. Truc, P. Doua, F. Dje, N. N'Siesi, F.X. and Bisser, S. et al. (2002) IgM quantification in the cerebrospinal fluid of sleeping sickness patients by a latex card agglutination test. Trop. Med. Int. Health 7: 685—692.

Lejon, V. Reiber, H. Legros, D. Dje, N. Magnus, E. Wouters, I. Sindic, C.J. and Büscher, P. (2003) Intrathecal immune response pattern for improved diagnosis of central nervous system involvement in trypanosomiasis. J. Infect. Dis. 187: 1475—1483.

López-Antuñano, J.F. Rangel-Flores, H. and Ramo, C. (2000) Diagnosis of Chagas' Disease. Revista Latinoamericana de Microbiología. 42: 121-129.

Lourie, E.M. (1942) Treatment of sleeping sickness in Sierra Leone. Ann. Trop. Med. Parasitol. 36: 113–131.

Mantovani, A. (2006) Macrophage diversity and polarization: in vivo veritas. Blood. 108: 408- 409.

Mathers, C.D. Ezzati, M. and Lopez, A.D. (2007) Measuring the burden of neglected tropical diseases: the global burden of disease framework. Public Library of Science Neglected Tropical Diseases. 1:e114.

McKerrow, J.H. Engel, J.C. and Caffrey, C.R. (1999) Biorg. Med. Chem. 7: 639–644.

Melville, D.B. Genghof, D.S. Inamine, E. and Kovalenko, V. (1956) Ergothioneine in microorganisms, J. Biol. Chem. 223: 9 – 17.

Melville, D.B. Eich, S. Ludwig, M.L. (1957) The biosynthesis of ergothionine. J. Biol. Chem. 224(2):871-7.

Michels, M.A.P. Bringaud, F. Herman, M. and Hannaert, V. (2006) Metabolic functions of glycosomes in trypanosomatids. Biochimica et Biophysica Acta. 1763: 1463–1477.

Morgan, G.W. Allen, C.L. Jeffries, T.R. Hollinshead, M. and Field, M.C. (2001) Developmental and morphological regulation of clathrin-mediated endocytosis in *Trypanosoma brucei*. J. Cell Sci. 114:2605–2615.

Montrichard, F. Le Guen, F. Laval-Martin, L.D. Davioud-Charvet, E. (1999) Evidence for the coexistence of glutathione reductase and trypanothione reductase in the nontrypanosomatid Euglenozoa: Euglena gracilis Z. FEBS Lett. 442: 29–33.

Moutiez, M. Meziane-Cherie, D. Aumercier, M. Sergheraert, C. and Tartar, A. (1994) Compared reactivities of trypanothione and glutathione in conjugation reactions. Chem. Pharm. Bull. 42: 2641–2644

Naidu, M.S.R. and Bensusan, H.B. (1968) Reinvestigation of the Orientation of Halogen Substitution in Imidazoles by Nuclear Magnetic Resonance Spectroscopy. J. Org. Chem. 53: 1307.

Narayanan, S. Vangapandu, S. and Jain, R. (2001) Regiospecific Synthesis of 2,3-Disubstituted-L-Histidines and Histamines. Biorganic & Medical Chemistry Lettrs. 11: 1133-1136.

Nguewa, A.P. Fuertesb, A.M. Cepeda, V. Iborra, S. Carrion, J. Valladares, B. Alonso, C. and Perez, M.J. (2005) Pentamidine Is an Antiparasitic and Apoptotic Drug That Selectively Modifies Ubiquitin. Chemistry & Biodiversity. 2: 1387- 1400.

Nok, J.A. (2003) Arsenicals (melarsoprol), pentamidine and suramin in the treatment of human African trypanosomiasis. Parasitol Res. 90: 71–79.

Nowicki, W.M. Tulloch, B.L. Worrall, L. McNae, W.I. Hannaert, V. Michels, M.A.P. Fothergill-Gilmore, A.L. Walkinshaw, D.M. and Turner, J.N. (2008) Design, synthesis and trypanocidal activity of lead compounds based on inhibitors of parasite glycolysis. Bioorganic & Medicinal Chemistry. 16: 5050–5061.

O'Beirne, C. Lowry, C.M. and Voorheis, H.P. (1998) Both IgM and IgG anti-VSG antibodies initiate a cycle of aggregation-disaggregation of bloodstream forms of *Trypanosoma brucei* without damage to the parasite. *Mol. Biochem. Parasitol.* 91: 165-193.

Oli, M.W. Cotlin, L.F. Shiflett, A.M. and Hajduk, S.L. (2006) Serum Resistance-Associated Protein Blocks Lysosomal Targeting of Trypanosome Lytic Factor in *Trypanosoma brucei*. Eukaryotic cell. 5(1): 132–139.

Oza, S.L. Tetaud, E. Ariyanayagam, M.R. Warnon, S.S. and Fairlamb, A.H. (2002) A single enzyme catalyses formation of trypanothione from glutathione and spermidine in *Trypanosoma cruzi*. J. Biol. Chem. 277: 35853–61.

Paintner, F.F. Allmendinger, L. Bauschke, G. and Klemann, P. (2005) Highly Efficient Approach to Orthogonally Protected (2S,4R)- and (2S,4S)-4-Hydroxyornithine. Org. Lett. 7(7): 1423-1426.

Paton, L.J. Rossan, R.N. Escajadillo, A. Matsumoto, Y. Lee, A. T. Labroo, V.M. Kirk, K. L. Cohen, L. A. Aikawa, M. and Howard, R.J. (1988) In Vitro and In Vivo Studies of the Effects of Halogenated Histidine Analogs on Plasmodium falciparum. Antimicrob. Agents Chemother. 32: 1655-1695.

Pays, E. and Vanhollebeke, B. (2008) Mutual self-defence: the trypanolytic factor story. Microbes and Infection. 10: 985- 989.

Peer, M. de Jong, J.C. Kiefer, M. Langer, T. Rieck, H. Schell, H. Sennhenn, P. Sprinz, J. Steinhagen, H. Wiese, B. and Helmchen, G. (1996) Preparation of Chiral Phosphorus, Sulfur and Selenium Containing 2-Aryloxazolines. Tetrahedron. 52(21): 7547-7583.

Pepin, J. and Milord, F. (1994) The treatment of human African trypanosomiasis. Adv. Parasitol. 33: 1–47.

Pérez-Morga, D. Vanhollebeke, B. Paturiaux-Hanocq, F. Nolan, D.P. Lins, L. Homblé, F. Vanhamme, L. Tebabi, P. Pays, A. Poelvoorde, P. Jacquet, A. Brasseur, R. and Pays, E. (2005) Apolipoprotein L-I promotes trypanosome lysis by forming pores in lysosomal membranes. Science. 309: 469- 472.

Perrin, D.D. and Armarego, W.L.F. (1988) Purification of Laboratpry Chemicals; Pergamon Press: Oxford.

Piedrafita, D. Proudfoot, L. Nikolaev, A.V. Xu, D. Sands, W. Feng, G.J. Thomas, E. Brewer, J. Michael, A.J. Ferguson, M.A.J. Alexander, J. and Liew, F.Y. (1999) Regulation of macrophage IL-12 synthesis by Leishmania phosphoglycans. Eur J Immunol. 29: 235- 244.

Plewes, K.A. Barr, S.D. and Gedamu, L. (2003) Iron superoxide dismutases targeted to the glycosomes of Leishmania chagasi are important for survival. Infect. Immun. 71:5910–5920.

Roberts, C.W. McLeod, R. Rice, D.W. Ginger, M. Chance, M.L. and Goad, L.J. (2003) Fatty acid and sterol metabolism: potential antimicrobial targets in apicomplexan and trypanosomatid parasitic protozoa. Molecular & Biochemical Parasitology. 126: 129–142.

Röhl, I. Schneider, B. Schmidt, B. and Zeeck, E. (1999) Ovothiol A: the egg release pheromone of the marine polychate Platynereis dumerilii. Annelida: Polychaeta. Z Naturforsch. 54: 1145–1147.

Rosenblatt, E.J. (2009) Laboratory Diagnosis of Infections Due to Blood and Tissue Parasites. CID. 49 (7):1103 – 1108.

Ross, R. (1903) "Further notes on Leishman's bodies". *Ibid.*: ii: 1401

Rothhammer, F. Marvin, J. Allison, M.J. Núñez, L. Standen, V. and Arriaza, B. (1985) Chagas disease in pre-Colombian South America. *Am. J. Phys. Anthropol.* 68:355–356.

Sao Emani, C. Williams, J.M. Wiid, J.I. Hiten, F.N. Viljoen, J.A. Pietersen, D.R. van Helden, D.P. and Baker, B. (2013) Ergothioneine is a secreted antioxidant in Mycobacterium smegmatis. Antimicrob. Agents Chemother. 57(7): 3202-7

Schröter, S. Stock, C. and Bach, T. (2005) Regioselective cross-coupling reactions of multiple halogenated nitrogen-, oxygen-, and sulfur-containing heterocycles. Tetrahedron 61: 2245–2267.

Scott, P. Natovitz, P. Coffman, R.L. Pearce, E. and Sher, A. (1988) Immunoregulation of cutaneous leishmaniasis. T cell lines that transfer protective immunity or exacerbation belong to different T helper subsets and respond to distinct parasite antigens. J. Exp. Med. 168: 1675–1684.

Seebeck, P.F. (2010) In vitro reconstitution of Mycobacterial ergothioneine biosynthesis. J. Am. Chem. Soc. 132: 6632 – 6633.

Selman-Reimer, S. Duhe, R.J. Stockman, B.J. and Selman, B.R. (1991) L-1-N-Methyl-4-mercaptohistidine disulfide, a potential endogenous regulator in the redox control of chloroplast coupling factor 1 in Dunaliella. J. Biol. Chem. 266: 182–188.

Shames, S.L. Fairlamb, A.H. Cerami, A. Walsh, C.T. (1986) Purification and characterization of trypanothione reductase from *Crithidia fasciculata*, a newly discovered member of the family of disulfide-containing flavoprotein reductases. Biochemistry. 25: 3519-3526.

Shapiro, M.B. (1991) The Control of Oxidant Stress at Fertilization. Science. 252: 533-536.

Singh, N. (2006) Drug resistance mechanisms in clinical isolates of *Leishmania Donovani.* Indian J. Med. Res. 123: 411-422.

Smith, K. Nadeau, K. Walsh, C. Fairlamb, A.H. (1992) Purification of glutathionylspermidine and trypanothione synthetases from *Crithidia fasciculata*. Protein Sci. 1:874–83.

Soto, J. Arana, A.B. Toledo, J. Rizzo, N. Vega, C.J. Diaz, A. Luz, M. Gutierrez, P. Arboleda, P. Berman, D.J. Junge, K. Engel, J. and Sindermann, H. (2004) Miltefosine for new world cutaneous leishmaniasis. Clin. Infect. Dis. 38:1266–1272.

Souza, D. H. Garratt, R.C. Araújo, A.P. Guimarães, B.G. Jesus, W.D. Michels, P.A. Hannaert, V. and Oliva, G. (1998) Trypanosoma cruzi glycosomal glyceraldehyde-3-phosphate dehydrogenase: structure, catalytic mechanism and targeted inhibitor design. FEBS Lett. 424: 131-135.

Sprout, C.M. Richmond, M.L. and Seto, C.T. (2005) A Positional Scanning Approach to the Discovery of Dipeptide-Based Catalysts for the Enantioselective Addition of Vinylzinc Reagents to Aldehydes. J. Org. Chem. 70 (18): 7408-7417.

Steenkamp, D.J. (2002) Trypanosomal Antioxidants and Emerging Aspects of Redox Regulation in the Trypanosomatids. Antioxidants & Redox Signaling. 4(1): 105- 121.

Steenkamp, J.D. and Spies, C.S.H. (1994) Identification of a major low-molecular-mass thiol of the try panosomatid *Crithidia fasciculata* as ovothiol A Facile isolation and structural analysis of the bimane derivative. Eur. J. Biochem. 223: 43-50.

Steenkamp, J.D. (1993) Simple methods for the detection and quantification of thiols from *Crithidia fasciculata* and for the isolation of trypanothione. Biochem. J. 292: 295-301.

Steverding, D. (2008) The history of African trypanosomiasis. Parasites & Vectors. 1: 1-8.

Stich, A. Abel, M.P. and Krishna, S. (2002) Human African trypanosomiasis. BMJ. 325: 203-206.

Stuart, K. Brun, R. Croft, S. Fairlamb, A. Gürtler, E.R. McKerrow, J. Reed, S. and Tarleton, R. (2008) Kinetoplastids: related protozoan pathogens, different diseases. J. Clin. Invest. 118:1301–1310.

Sundar, S and Rai, M. (2002) Laboratory Diagnosis of Visceral Leishmaniasis. Clin. and diagn. Lab. Immuno. 9(5): 951–958.

Sypek, J.P. Chung, C.L. Mayor, S.E.H. Subramanyan, J. M. Goldman, S.J. Sieburgh, D.S. Wolf, S.F. and Schaub, R.G. (1993) Resolution of cutaneous leishmaniasis: interleukin 12 initiates a protective T helper type 1 immune response. J. Exp. Med. 177: 1797–1802.

Ta, P. Buchmeier, N. Newton, L.G. Rawat, M and Fahey, C.R. (2011) Organic Hydroperoxide Resistance Protein and Ergothioneine Compensate for Loss of Mycothiol in *Mycobacterium smegmatis* Mutants. J. Bacteriol. 139 (8): 1981-1990

Tabor, C.W. and Tabor, H. (1984). Polyamines. Annu. Rev. Biochem. 53:749–790.

Temperton, N.J. Wilkinson, S.R. Meyer, D.J. Kelly, J.M. (1998) Overexpression of superoxide dismutase in Trypanosoma cruzi results in increased sensitivity to the trypanocidal agents gentian violet and benznidazole. Mol. Biochem. Parasitol. 96:167–176.

Tanret, C. (1909) Sur une base nouvelle retiree du seigle ergote, l'ergothioneine, Compt.Rend. 149: 222–224

Thrower, S.J. Blalock, R. 3rd. and Klinman, P.J. (2001) Steady-kinetics of substrate binding and iron release in tomato ACC oxidase. Biochemistry. 40: 9717-9724.

Tolbert, T.J. and Wong, C. (2000) Intein-Mediated Synthesis of Proteins Containing Carbohydrates and Other Molecular Probes. J. Am. Chem. Soc. 122(23): 5421-5428.

Torrence, D.F. Friedmann, R.M. Kirk, K.L. Cohen, L.A. and Creveling, C.R. (1979) 2-fluorohistidine—Effects on protein synthesis in cell-free systems and in mouse L cells. Biochem. Pharmacol. 28:1565-1567.

Turner, E. Klevit, R. Hager, J.L. and Shapiro, M.B. (1987) Ovothiols, a Family of Redox-Active Mercaptohistidine Compounds from Marine Invertebrate Eggs. Biochemistry. 26: 4028-4036.

Turner, E. Klevit, R. Hopkins, B.P. and Shapiro, M.B. (1986) Ovothiol: A Novel Thiohistidine Compound from Sea Urchin Eggs That Confers NAD(P)H-02 Oxidoreductase Activity on Ovoperoxidase. The Journal of Biological Chemistry. 261(28): 13056- 13063.

Turner, E. Somers, E.C. and Shapiro, M.B. (1985) The Relationship between a Novel NAD(P)H Oxidase Activity of Ovoperoxidase and the CN--resistant Respiratory Burst That Follows Fertilization of Sea Urchin Eggs. The Journal of Biological Chemistry. 260(24): 13163-13171.

Urbina, J.A. Concepcion, J.L. Rangel, S. Visbal, G. and Lira, R. (2002) Squalene synthase as a chemotherapeutic target in Trypanosoma cruzi and Leishmania mexicana. Molecular & Biochemical Parasitology. 125: 35- 45.

Urbina1, A.J. and Docampo, R. (2003) Specific chemotherapy of Chagas disease: controversies and advances. TRENDS in Parasitology. 19(11): 495- 501.

Vanhamme, L. Paturiaus-Hanocq, F. Poelvoorde, P. Nolan, D.P. Lins, L. Van Den Abbeele, J. Pays, A. Tebabi, P. Van Xong, H. Jacquet, A. Moguilevsky, N. Dieu, M. Kane, J.P. de Baetselier, P. Brasseur, R. and Pays, E. (2003) Apolipoprotein L-I is the trypanosome lytic factor of human serum. Nature. 422: 83–87.

Van Lear, K. Hamilton, J.C. and Messens, J. (2013) Low-Molecular-Weight Thiols in Thiol-Disulfide Exchange. Antioxidants & Redox Signaling. 18(13): 1642 – 1653.

Vanhollebeke, B. Demuylder, G. Nielsen, M.J. Pays, A. Tebabi, P. Dieu, M. Raes, M. Moestrup, S.K. and Pays, E. (2008) An haptoglobin-hemoglobin receptor conveys innate immunity to Trypanosoma brucei in humans. Science. 320: 677- 681.

Vaz, E. Fernandez-Suarez, M. and Muñoz, L. (2003) Determination of the absolute stereochemistry of Etzionin. Tetrahedron. 14: 1935–1942.

Vogt, N.R. Spies, C.S.H. and Steenkamp, J.D. (2001) The biosynthesis of ovothiol A (N 1-methyl-4-mercaptohistidine) Identification of S-(4'-L-histidyl)-L-cysteine sulfoxide as an intermediate and the products of the sulfoxide lyase reaction. Eur. J. Biochem. 268: 5229- 5241.

Vogt, R.N. and Steenkamp, D.J. (2003) The metabolism of S-nitrosothiols in the trypanosomatids: the role of ovothiol A and trypanothione. Biochem. J. 371: 49 – 59.

Vogt, R.N. Spies, H.S.C. and Steenkamp, D.J. (2001) The biosynthesis of ovothiol A (N 1-methyl-4-mercaptohistidine). Eur. J. Biochem. 268: 5229-5241.

Wamalasena, S.D. Cramer, C.J. Janowiak, E.R. Juris, J.S. Meinyk, A.R. Anderson, E.D. Kirk, L.K. Collier, J.R. and Bann, G.J. (2007) Biochemistry. 46: 14928- 14936.

Weaver, H.K. and Rabenstein, L.D. (1995) Thiol/disulfide exchange reactions of ovothiol A with glutathione. J. Org. Chem. 60: 1904–1907.

Webster, P. and Griffiths, G. (1994) A novel method mean cell volume estimation. *J. Microsc.* 174: 85-92.

Webster, P. and Shapiro, S.Z. (1990) *Trypanosoma brucei*: a membraneassociated protein in coated endocytic vesicles. *Exp. Parasitol.* 70: 154- 163.

Who report on Cutaneous Leishmaniasis: http://whqlibdoc.who.int/hq/2007/WHO_CDS_NTD_IDM_2007.3_eng.pdf World Health Organization. Tech. Rep. Ser., 2002, 905, 1. Chagas disease epidemiology

Williams, B.I. (1996) African trypanosomiasis. In: The Wellcome Trust Illus- trated History of Tropical Diseases (ed. Cox FEAG), pp. 178–91.

World Health Organization. (2006) Human African trypanosomiasis (sleeping sickness): epidemiological update. Weekly Epidemiological Record. 81:71-80.

Wyllie, S. Oza, S.L. Patterson, S. Spinks, D. Thompson, S. and Fairlamb, A.H. (2009) Dissecting the essentiality of the bifunctional trypanothione synthetase-amidase in Trypanosoma brucei using chemical and genetic methods. Molecular Microbiology.1365-2958.

Xong, H.V. Vanhamme, L. Chamekh, M. Chimfwembe, C.E. Van Den Abbeele, J. Pays, A. Van Meirvenne, N. Hamers R, De Baetselier P, and Pays, E. (1998) A VSG expression site-associated gene confers resistance to human serum in Trypanosoma rhodesiense. Cell. 95:839–846.

Yeh, H.J.C. Kirk, K.L. Cohen, L.A. and Cohen, J.S. (1975) Fluorine-19 and proton nuclear magnetic resonance studies of ring-fluorinated imidazoles and histidines. Journal of the Chemical Society, Perkin Transactions 2: Physical Organic Chemistry. 9: 928-34.

Zhang, W.W. and Matlashewski, G. (2001) Characterization of the A2- A2rel gene cluster in Leishmania donovani: involvement of A2 in visceralization during infection. Molecular Microbiology. 39(4): 935- 948.

Zhang, W.W. and Matlashewski, G. (1997) Loss of virulence in Leishmania donovani deficient in an amastigote-specific protein,A2. Proc Natl. Acad. Sci. USA. 94: 8807-8811.

Zhang, W.W. Charest, H. Ghedin, E. and Matlashewski, G. (1996) Identification and overexpression of the A2 amastigote-specific protein in Leishmania donovani. Mol. Biochem. Parasitol. 78: 79- 90.

Zuccotto, F. Brun, R. Gonzalez, P.D. Ruiz, P.L.M and Gilbert, I.H. (1999) The structure-based design and synthesis of selective inhibitors of Trypanosoma cruzi dihydrofolate reductase. Bioorg. Med. Chem. Lett. 9: 1463-1468.

APPENDIX:

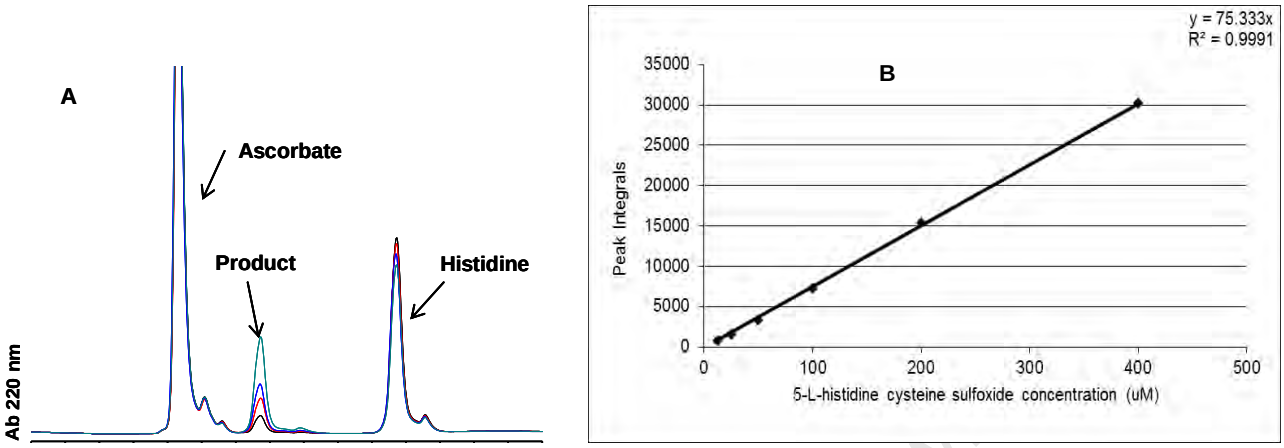

Figure S1: Analysis of OvoA reaction mixture. HPLC chromatograms showing increasing 5-histidyl cysteine sulfoxide peak at 3.2 minutes (A) and calibration curve from which product concentrations were determined. 2000 µM cysteine, 2.89 µM OvoA and increasing concentrations of histidine (12.5 – 400 µM) were used in a standard reaction as described in section 3.2.2. For B, the reactions were allowed to proceed until all histidine was consumed as monitored by HLPC (20 µL injection volume). Absorbances of completed reactions were plotted against the histidine concentrations (with histidine concentrations equal to 5-L-histidyl sulfoxide sulfoxide concentrations). Data plotted here were averages of three determinants.

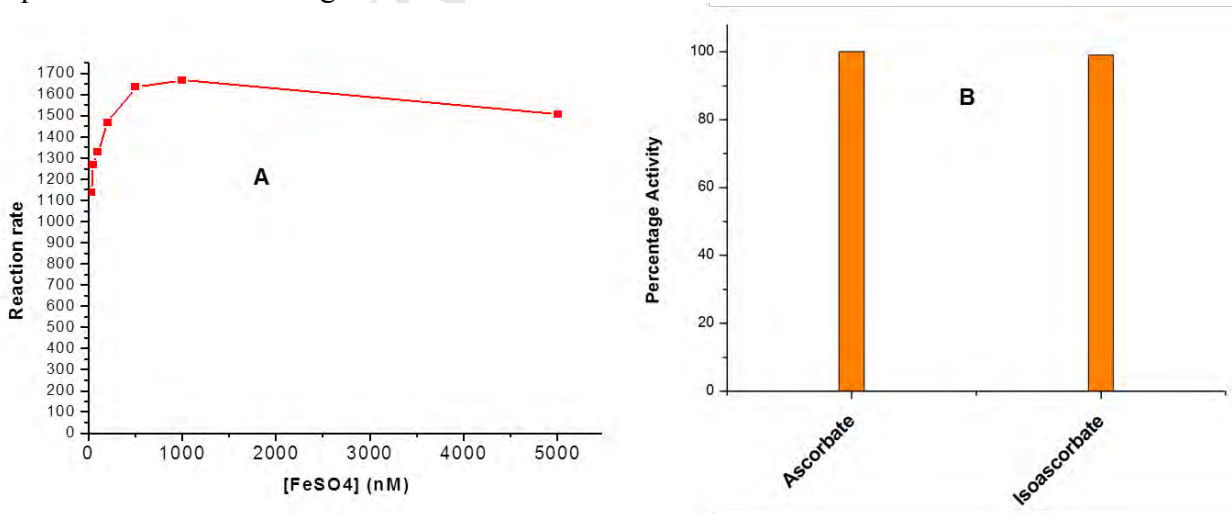

Figure S2: Effect of iron concentration on OvoA reaction (A) and activation of OvoA by ascorbate and isoascorbate (B). Reaction conditions were similar to those described on figure 3.3. For A, iron concentrations of 20, 62.5, 125, 250, 500, 1000 and 5000 nM were used. For B 2 mM ascorbate and isoascorbate each was used.

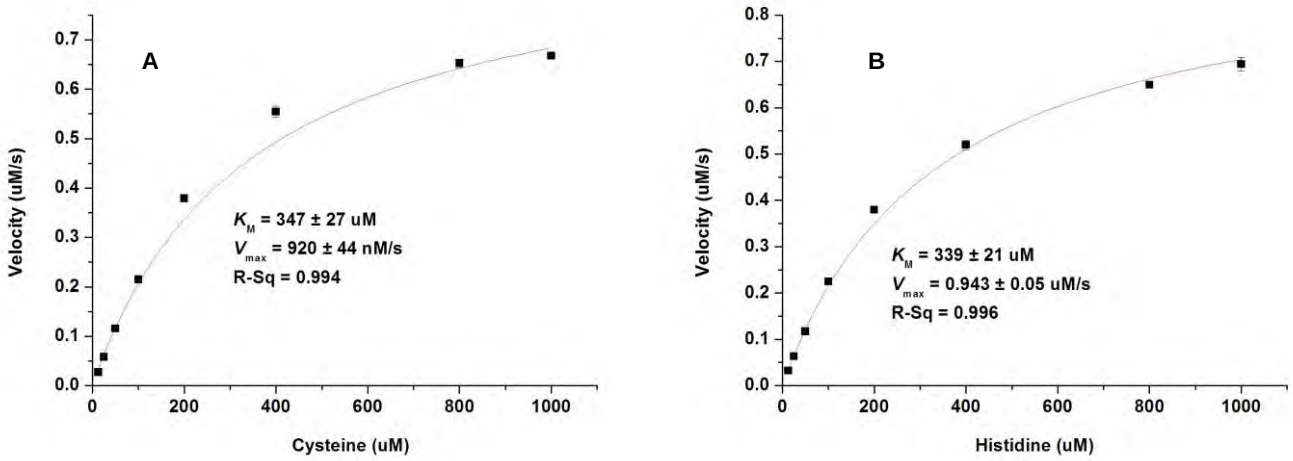

Figure S3: Michaelis-Menten graphs of OvoA with cysteine substrate (A) and histidine substrate (B). The standard reaction mixtures contained 20 mM Tris pH 8.0, 20 mM NaCl, 2 mM TCEP, 2 mM ascorbate and 1 µM $FeSO_4$ in a final volume of 250 µL at 26°C. For cysteine kinetics (A), 800 µM histidine, cysteine (12.5 – 1000 µM), 294 nM OvoA were used. For histidine kinetics (B), 800 µM cysteine, histidine (12.5 – 1000 µM), 289 nM OvoA were used. At 2, 4, 8 and 16 minutes, 30 µL aliquots of the reactions were quenched by addition of 15 µL 1 M phosphoric acid and analyzed for formation of 5-D-histidyl cysteine sulfoxide using HPLC method 1. Data plotted here were averages of two determinants.

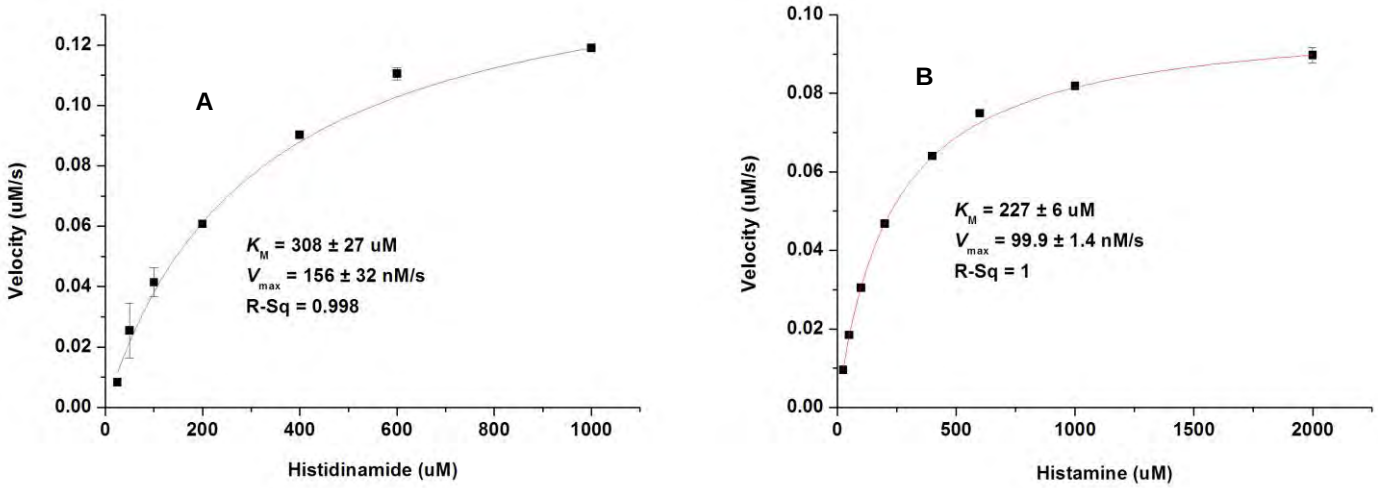

Figure S3: Michaelis-Menten graphs of OvoA with histidinamide substrate (A) and histamine substrate (B). 250 µL reaction mixtures contained 20 mM Tris pH 8.0, 20 mM NaCl, 2 mM TCEP, 2 mM ascorbate, 1µM $FeSO_4$ and 800 uM cysteine at 26°C. For histidinamide kinetics (A) 25 – 2000uM histidinamide and 371 nM OvoA were used. , For histamine kinetics 25 – 2000 µM histamine and 377 nM OvoA were used. At 2, 4, 8 and 16 minutes, 30 µL aliquots of the reactions were quenched by addition of 15 µL 1 M phosphoric acid and analyzed by HPLC method 1. Data plotted here were averages of two determinants

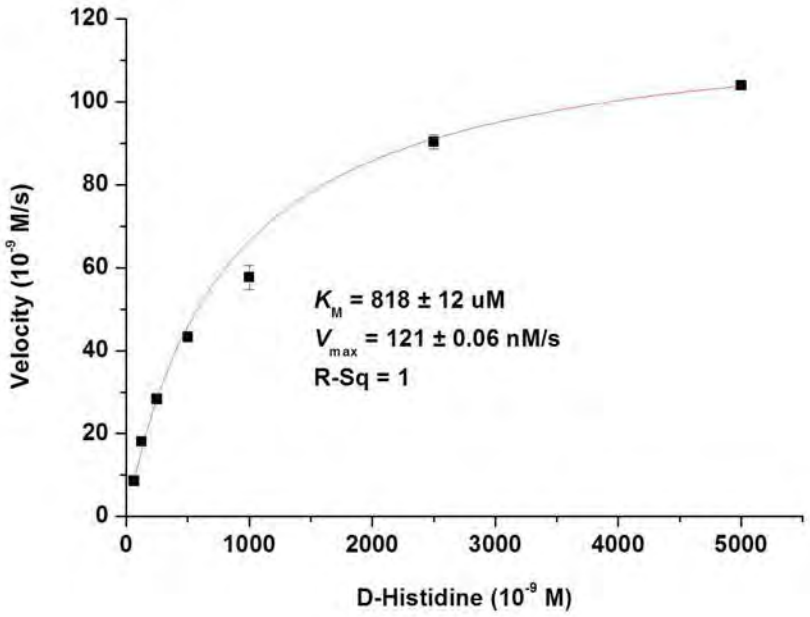

Figure S3: Michaelis-Menten graphs of OvoA with D-histidine substrate. Reaction mixtures containing 20 mM Tris pH 8.0, 20 mM NaCl, 2 mM TCEP, 2 mM ascorbate, 1 µM $FeSO_4$, 800 µM cysteine, D-histidine (62.5 – 5000 µM), 346 nM OvoA in final volume of 250 µL were incubated at 26°C. At 2, 4, 8 and 16 minutes, 30 ul aliquots of the reactions were quenched by addition of 15 µL 1 M phosphoric acid and analyzed for formation of 5-D-histidyl cysteine sulfoxide using HPLC method 1. Data plotted here were averages of two determinants.

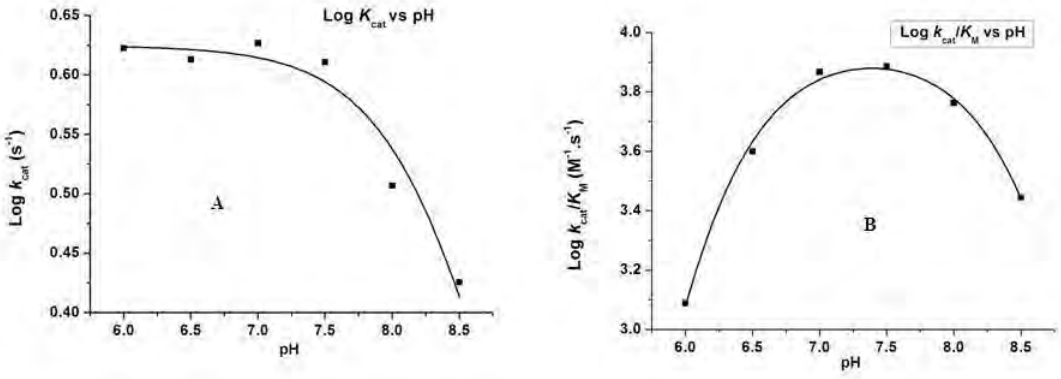

Figure S4: Effect of pH on histidine specificity and kinetic constant. 250 µL reaction mixtures at 26°C contained 800 µM cysteine, histidine (12.5 – 1000 µM), 2 mM TCEP, 2 mM ascorbate, 1 µM $FeSO_4$, 20 mM NaCl, 283 nM OvoA in 50 mM Britton-Robinson buffer at different pHs (6 – 8.5). At points 1, 2, 4 and 8 minutes, 40 µL samples were quenched with 20 µL 1 M phosphoric acid solution and analyzed by HPLC using method 1. (A): k_{cat} vs pH, (B): k_{cat}/K_M vs pH, (C): log k_{cat} vs pH and (D): log k_{cat}/K_M vs pH.